Response to all reviewers
Climate and impact attribution of compound flooding induced by tropical cyclone Idai in Mozambique

We thank all three anonymous reviewers for their elaborate comments and suggestions on how to improve the manuscript. We address each point raised by the reviewers below (in blue). Line numbers refer to the revised documents (manuscript or supplement) with tracked changes, that are attached in this document after the point-by-point responses.

Given the alignment of the comments of all three reviewers, we would like to clarify the scope of the paper, and justify the validity of our approach. The aim of the paper is to showcase the applicability of a storyline attribution framework for tropical cyclones using global data only, thereby exploring an approach that could be implemented operationally, particularly in data-scarce contexts such as Mozambique. In this novel storyline attribution framework, we make significant steps for climate and impact attribution of compound flooding from tropical cyclones. We have clarified in the revised version of the manuscript that this framework provides a *conditional* attribution assessment of the observed event under a range of *plausible* climate trends. This framework focuses on changes in TC flood drivers for which there is robust scientific evidence.

For the attribution experiments within our paper, we utilize well established storyline attribution principles (Lloyd and Shepherd, 2021; Shepherd, 2016; Sillmann et al., 2021). For event-based attribution of tropical cyclones (TCs), assumptions and benchmark choices are necessary. For instance, keeping the original TC track reduces the number of degrees of freedom in choosing counterfactual scenarios necessary for practical application of the attribution approach, which is a typical example of a conditional attribution assessment (Mester et al., 2023; Strauss et al., 2021). Constructing counterfactuals per definition violates consistencies as it puts an event into a different environment, which implies assuming an infinite number of unchanged impacts that could have unfolded differently in the real world. A conditional attribution experiment should be considered a thought experiment, not a physical reconstruction where all physical forces and budgets are closed. Consequently, counterfactual scenarios are designed to study plausible what-if scenarios of the effect of climate change on the event (Lloyd and Shepherd, 2020). Such what-if scenarios are especially relevant for low-likelihood high-impact events, such as tropical cyclones (Sillmann et al., 2021). Inherently, our experimental setup relies on assumptions, which are kept constant between scenarios. We argue that some of the sensitivity experiments requested by the reviewers go beyond the essential reasoning of the intent of a storyline attribution experiment. Including uncertainties in all modelling parameters will blow-up uncertainty levels that will bury useful information, especially for data-scarce regions with many unknowns (where some uncertainty might not even be quantifiable), as is the case for Mozambique. We rely on the best available global datasets to allow global applicability of our framework, also in data-scarce environments, and use state-of-the-art or conservative estimates for model parameter uncertainty.

We agree with the reviewers' suggestions to include uncertainty quantification of the effect of climate change on the flood drivers and have therefore provided our results as a range of plausible values for the conditional attribution statement. We have included additional counterfactual scenarios with plausible values for the climate trend in the flood drivers of tropical cyclone Idai (see Table 1 and updated section 2.3.2 in manuscript) based on best available literature. We now present the results including a low, medium, and high plausible climate trends for different driver combinations (22 combinations; see Table below):

- **Low, medium and high counterfactual values for TC rainfall (-4%, -8% and -16%)**, following Clausius Clapeyron for the medium counterfactual scenario (-8%; Knutson et al., 2020), the super-Clausius Clapeyron principle for the high counterfactual scenario (-16%; Guzman and Jiang, 2021; Liu et al., 2019; Patricola and Wehner, 2018) and a plausible TC

rainfall reduction by negative ocean-atmosphere feedback for the low counterfactual scenario (-4%; Tu et al., 2022).

- **Low, medium and high counterfactual values for TC wind speed (-1%, -5%, and -10%)**, according to the findings from Knutson et al. (2020) for the low and medium counterfactual scenarios (-1%, -5%), as suggested by reviewer 1. The high counterfactual scenario (-10%) is based on the TC wind speed trend from IBTrACS for the southern Indian Ocean from Mester et al. (2023).
- **Low, medium and high counterfactual values for SLR (-0.05 m, -0.10 m, and -0.15 m)**. Our best-estimate SLR is based on Treu et al. (2024) and is the mean of all stations along the coast of Mozambique, within our D-Flow FM domain, resulting in a plausible -0.10 m value for the medium counterfactual scenario. We add a plausible low and high counterfactual SLR scenario of ±0.05 m based on Strauss et al. (2021), resulting in -0.05 m and -0.15 m. For our best-estimate SLR analysis, we have switched from the geocentric water level to the water level dataset of Treu et al., which includes vertical land movement, as it is considered to be more plausible data for the effect of SLR on flooding.

NR	RUN NAME	RAIN [%]	WIND [%]	SLR [m]
1	Factual	0	0	0
2	CF_all_low	-4	-1	-0.05
3	CF_all_medium	-8	-5	-0.10
4	CF_all_high	-16	-10	-0.15
5	CF_rain_low	-4	0	0
6	CF_rain_medium	-8	0	0
7	CF_rain_high	-16	0	0
8	CF_wind_low	0	-1	0
9	CF_wind_medium	0	-5	0
10	CF_wind_high	0	-10	0
11	CF_SLR_low	0	0	-0.05
12	CF_SLR_medium	0	0	-0.10
13	CF_SLR_high	0	0	-0.15
14	CF_rainwind_low	-4	-1	0
15	CF_rainwind_medium	-8	-5	0
16	CF_rainwind_high	-16	-10	0
17	CF_rainSLR_low	-4	0	-0.05
18	CF_rainSLR_medium	-8	0	-0.10
19	CF_rainSLR_high	-16	0	-0.15
20	CF_windSLR_low	0	-1	-0.05
21	CF_windSLR_medium	0	-5	-0.10
22	CF_windSLR_high	0	-10	-0.15

Also worth noting is that we removed Table S2 from the supplement, as Table 2 in the manuscript is now updated to include a range of plausible counterfactual values for the considered scenarios. Moreover, we have updated the land cover dataset to Vito 2019 compared to the earlier used Vito 2015 for consistency but this had a negligible impact on the factual flooding values.

Reply to reviewer 1

This manuscript addresses an important gap in attribution science by developing a storyline framework for tropical cyclone-induced compound flooding in data-sparse regions. The authors demonstrate technical sophistication in coupling multiple state-of-the-art models (SFINCS, wflow, D-Flow FM) to resolve all flood drivers dynamically. The application to TC Idai in Mozambique is particularly valuable given the underrepresentation of African cyclones in attribution literature. The work makes meaningful contributions to understanding how climate signals propagate from hazard to impact through nonlinear damage relationships.

However, the manuscript requires strengthening in several critical areas before publication. The counterfactual design lacks sufficient scientific justification for key parameter choices, the validation strategy needs refinement given data limitations, and the uncertainty quantification is inadequate for the compounding uncertainties inherent in this multi-model framework.

We thank the reviewer for the detailed comments and feedback they have provided. As explained in the general response section, quantifying all uncertainties and propagating these through the whole framework is not in the scope of our study and would also reduce the framework's applicability for possible future operational applications in data-scarce regions. We have made significant revisions to the manuscript to ensure that the results are interpreted within their limitations, presenting plausible and informative attribution statements that advance current attribution science. We agree that the description of those inherent uncertainties, limitations and inconsistencies lacked in the submitted manuscript, which has now been revised.

Major Comments

1. Counterfactual Design and Scientific Justification

The manuscript's attribution conclusions depend entirely on robust counterfactual scenarios, yet the justification for key parameters is insufficient:

For all of the points below, Sections 2.3.3 and S1.6 have been updated in the revised manuscript and supplementary material. We have included uncertainty bounds in Fig. 5 and Table 2 of the manuscript. The earlier described medium counterfactual scenarios are used for Fig. 4 and 6. We have also added more emphasis on the plausibility of these values, to better convey our confidence in the conditional attribution assessment. Since Fig. 5 only shows relative changes, we added a figure below for reference showing the uncertainty bounds of the different plausible climate trends on the absolute values for flood extent, flood volume and flood damage.

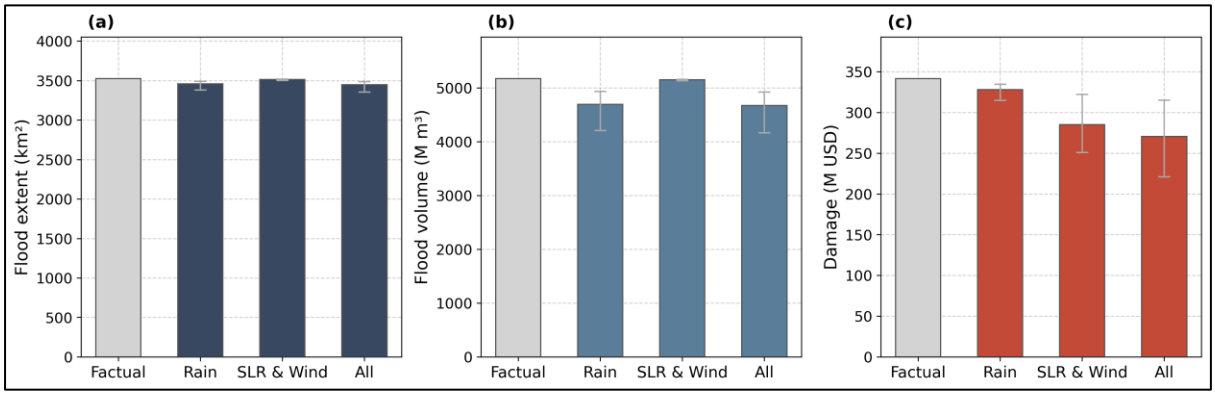

- **Rainfall reduction** (8%): While the Clausius-Clapeyron relationship is cited, the manuscript should explicitly demonstrate this calculation rather than only asserting it. Recent literature supports 8% reductions for ~1.1°C warming, but this warrants a dedicated methods subsection showing this applied to the case here and a discussion of uncertainties in this approach, particularly for tropical cyclones, where dynamic effects may deviate from thermodynamic expectations.

Following the suggestion of the reviewer, we have added additional counterfactual rainfall scenarios of -4% (lower than Clausius–Clapeyron due to possible enhanced cooling from slower TC translation speeds in a warmer climate; Tu et al., 2022) and -16% (super Clausius–Clapeyron; Guzman and Jiang, 2021; Liu et al., 2019; Patricola and Wehner, 2018), and added scientific support for these values in L195-202. We have also explicitly added the Clausius–Clapeyron relationship used for the calculation of the counterfactual rainfall values in the method Section 2.3.2 in L197. Lines L195-202 are presented below for convenience:

"*The plausible climate trend of TC rainfall, maximum wind speed and SLR is based on best available literature and global datasets. For the climate change effect on TC rainfall, some studies find that the trend is in line with the Clausius– Clapeyron relationship (7 %/°C of warming; Knutson et al., 2020), while other studies show trends higher than Clausius–Clapeyron (Guzman and Jiang, 2021; Liu et al., 2019a; Patricola and Wehner, 2018), referred to as super Clausius–Clapeyron (14 %/°C of warming), and lower due to enhanced cooling from slower TC translation speeds in a warmer climate (Tu et al., 2022). As Idai took place in a ~1.1 °C warmer world, we adopt plausible reductions of rainfall of 4 %, 8 % and 16 % for the low, medium and high counterfactual scenarios, respectively.* "

- **Wind speed reduction** (10%): This is more problematic. Knutson et al. (2020) report median projections of 1-10% intensity increases for 2°C warming, suggesting 0.5-5% for current ~1.1°C warming. A 10% reduction appears to overestimate the counterfactual change, potentially inflating the attributed impact from wind-driven processes. The manuscript cites Mester et al. (2023), who used regional observed trends, but doesn't establish why this particular value is appropriate.

Following the suggestion of the reviewer, we have added additional counterfactual wind speed scenarios of -1% and -5%, both based on Knutson et al. (2020) and rounding to integers (L202-206), to capture uncertainty in the climate change effect on TC wind speed:

"*For the climate change effect on TC maximum wind speeds, we use plausible reductions of a 1%, 5% and 10 % for the low, medium and high counterfactual scenarios, respectively. The low and medium scenarios are based on the likely range of 1–5 % per °C of warming for the Southern Indian ocean from climate models (Knutson et al., 2020), and the high scenario of a 10 % wind speed reduction is based on regional trends from observed TCs (Mester et al., 2023).*"

- **Sea level rise component**: The methodology for SLR estimation needs clarification:
    - Authors use the Treu et al. (2024) dataset but this contains systematic biases. The manuscript must explicitly address whether such biases affect factual and counterfactual equally (canceling in differences) or differently (amplifying attribution error)

To capture uncertainty in the climate change effect on SLR, we have added two additional counterfactual SLR scenarios. As mentioned in the general response section, we have switched from the geocentric water level to the water level dataset from Treu et al. (2024), which includes vertical land

movement. This is also incorporated in our correction for the vertical datum of the bathymetry (see Section 1.6). Analyzing the water level dataset from Treu et al. (2024) for the stations in Mozambique within our D-Flow FM domain leads to a mean SLR of +0.10 m at the time of Idai since 1901 (see updated Sections 2.3.2 and S1.6). For our medium counterfactual scenario, we remove this best estimate of SLR (-0.10 m). For the low and high counterfactual scenarios, we take ±0.05 m from the medium counterfactual SLR scenario based on Strauss et al. (2021), which results in values of -0.05 m and -0.15 m for the low and high scenarios (L204-210):

"*For the climate change effect on SLR, we use plausible reductions of 5, 10 and 15 cm for the low, medium and high counterfactual scenario, respectively. The medium scenario is based on the dataset by Treu et al. (2024), used to estimate the SLR between the time of the event and pre-industrial levels, and the low and high scenarios are based on uncertainty bounds from Strauss et al. (2021)*"

The dataset of True et al. (2024) is derived by combining different state-of-the-art global datasets. While there may be biases (as with any dataset), we now include additional counterfactual scenarios to account for uncertainty in our attribution results (see Table 2 in the revised manuscript). As such, we consider the dataset by Treu et al. (2024) to be suitable for the type of application that we present here.

- Figure S10 shows only 2015 data, yet the authors extrapolate to 2019, assuming linear trends.

Instead of extrapolating the 2015 SLR data from Treu et al. (2024), we have now extrapolated the data based on 30 years of data and used both linear and LOWESS extrapolation, see figure below. The difference between these extrapolation methods is minimal (1.6%), but the LOWESS-based extrapolation fits slightly better and is therefore adopted (updated figure S10 in Supplement).

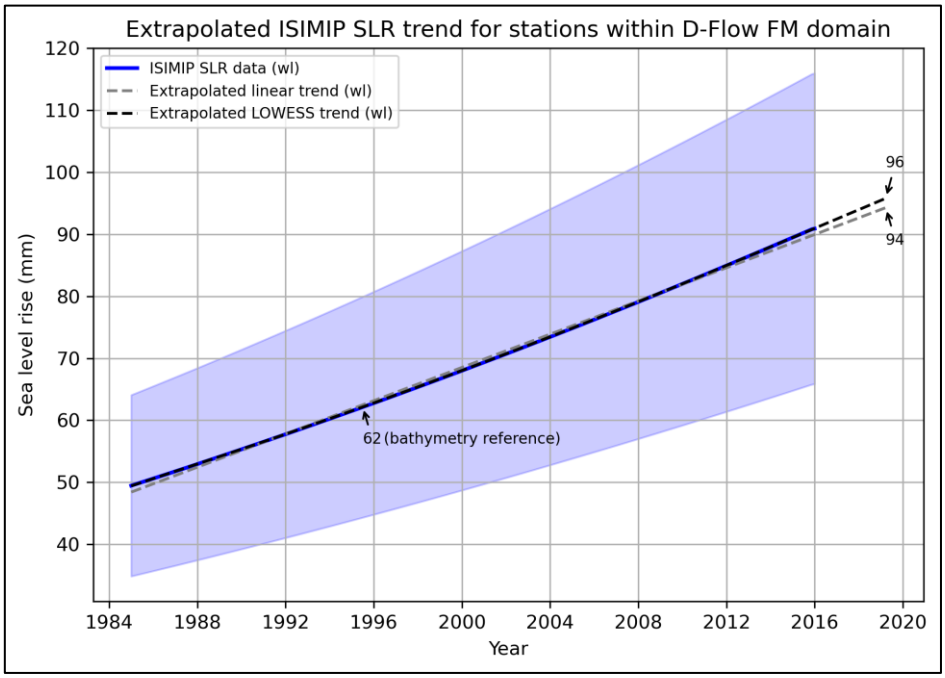

- Long-term tide gauge observations from the region should be incorporated to validate the 14 cm estimate

There is no tide gauge data available along the coast of Mozambique, but we did a trend analysis for the nearest tide gauge station with sufficient data, located in Durban, South Africa, using Permanent Service for Mean Sea Level (PSMSL) data (Holgate et al., 2013; Permanent Service for Mean Sea Level

(PSMSL), 2026). Similar to the long-term SLR data from True et al., we have fitted a LOWESS trend to the tide gauge data:

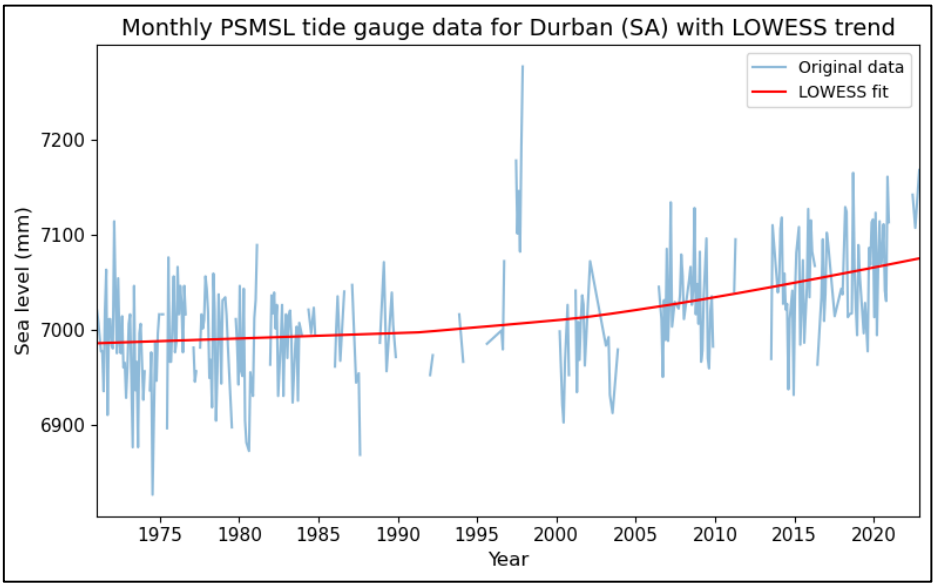

For our comparison, we assume equal SLR of the tide gauge data as at the start of the 30-year timeseries from Treu et al. (2024). Comparing the SLR at the time of event, we find the tide gauge data to result in a SLR of 119 mm compared to our SLR estimate of 96 mm. The tide gauge SLR value of 119 mm falls within the additionally included plausible range for SLR (150 mm).

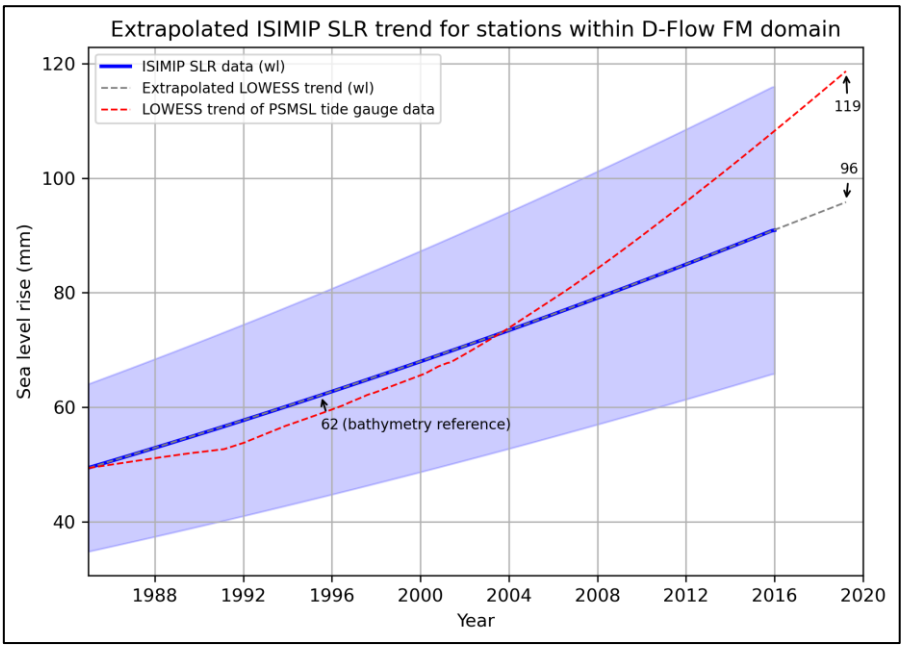

- Bankfull discharge assumption: The 2-year return period assumption for bankfull discharge should scale between scenarios. If climate change increases discharge, the effective channel capacity may differ between factual and counterfactual. Holding this constant creates an inconsistent comparison -the counterfactual world would have had different equilibrium channel geometries. This deserves explicit discussion or sensitivity testing.

We thank the reviewer for the comment about possible realistic changes of climate change on river bathymetry due to increased precipitation, but argue that this is beyond the scope of this study. As

explained in the general response section, we assume similar river bathymetry for the purpose of this storyline attribution assessment. We have made this assumption explicit in L192-193: "*We assume no change of non-flood drivers, such as exposure and vulnerability.*" and L225-226: "*The attributable change is conditional on the considered counterfactual flood drivers, and on the assumptions made in the model schematizations and input datasets.* "

2. Methodological Concerns

- **Model simulation duration**: How long were the simulations run? The manuscript doesn't specify the total simulation period or spin-up time. For compound flood modeling, the synchronization of multiple drivers is critical. Eilander et al. (2023) found surge peaked 3-5 days before discharge for TC Idai, producing limited compound interaction. Does this framework capture such timing effects?

Yes, we do capture timing effects, see Fig. S13b-c. The total simulation period was mentioned in line 91 *"(9 to 25 March 2019)*") but has been made more explicit in the revised version of the manuscript *"(simulated for 9 to 25 March 2019)*" (L93). We refer to the next response for comments on the spin-up time.

- **Boundary condition consistency**: How are the multiple drivers synchronized temporally across model domains? The wflow warm-up (365 days) is mentioned, but what about SFINCS, D-Flow FM initialization? Are antecedent soil moisture conditions consistent between scenarios? How is infiltration handled in SFINCS relative to wflow?

The D-Flow FM model has an initialization spin-up adjusted to the models' inherent timescale, which is 3 days. For SFINCS, the model starts 5 days before TC Idai hits the case study area, i.e. 5 days before the effect of the TC becomes visible in the flood model forcing (including discharge, precipitation or coastal surge). During this period no flooding occurs, and can therefore be considered spin-up time. All this information can be found in the model building scripts, but is too detailed to be added in the manuscript.

The antecedent soil moisture conditions are kept constant between scenarios, which is in line with our storyline experiment. Within wflow, the available water for infiltration is taken as throughfall and stemflow (and snow runoff and glacier melt, if applicable). The actual infiltration depends on the vertical saturated conductivity and the soil moisture capacity. As SFINCS does not have a soil component, for the infiltration the simpler Curve Number method is used, where a fraction of the precipitation is assumed to be infiltrated. Curve Number values vary spatially based on land use, taken from the global dataset by Jaafar and Ahmad (2019).

- **Validation metrics**: The validation should report separate performance metrics for: coastal zones (surge-dominated), fluvial zones (discharge-dominated) and compound zones (driver interaction). This would strengthen confidence that the model captures the different flooding mechanisms appropriately.

We like the suggestion of the reviewer but argue it is beyond the scope of this paper. Additional runs would be necessary to define these separate zones. Moreover, with the considerable uncertainty in the satellite products, we argue that providing zone-specific hit rates will not provide a lot of new information to the notion that the lack of consistence between these satellite products do challenge any verification, which is already reported.

- **Meteorological forcing quality**: ERA5 underestimates TC intensity (appropriately addressed by Holland parametric winds), but the manuscript should clarify: Was the TC parametric wind model used throughout the entire modeling chain? If so, how do biases propagate? The Holland model performs well when fitted to observations or additional empirical relationships, but "out of the box" applications can have significant errors and miss asymmetric TC shapes. The 0.75 TC radius merging also needs explanation—how sensitive are results to this choice?

We used a parametric tropical cyclone model to generate wind and pressure fields for both D-Flow FM and SFINCS to ensure consistent forcing, particularly important for coastal areas. This was done according to the Holland model (Holland, 2008), fitted to TC Idai parameters from the IBTrACS database. The wind and pressure fields were thus defined over a large area around the TC track, extending well beyond the R34 radius of the TC (area of extreme winds), using the 'spiderweb' schematization, commonly applied for tropical cyclone modelling in D-Flow FM (Deltares, 2026, pp. 234–235). To ensure realistic meteorological conditions outside of the TC area of influence (e.g. during model spin up, before the TC enters the model domain), the parametric fields were merged with ERA5 reanalysis data at 0.75 of the 'spiderweb' forcing field radius (merge fraction parameter). This, however, does not affect the coastal surge generation in our area of interest, because the TC track passes directly through the case study region and surge is generated by winds well within the 0.75 of the TC forcing field radius. Because the 0.75 merge fraction does not influence the coastal water levels (and hence the attribution results), we removed it from the manuscript (L178-179); this technical detail remains documented in the published scripts.

3. Wave Setup and Coastal Process Assumption

- The **assumption that wave setup remains constant across counterfactual scenarios** is scientifically invalid and potentially introduces substantial error since wave setup scales with wave breaking intensity. A 10% wind reduction would generate lower wave heights, producing correspondingly lower setup—potentially 15-20% reduction if setup scales as Hs^2.

For similar reasons as given before, we consider this element beyond the scope of our study. Including a counterfactual dynamical wave scenario would require setting up and validating an additional model (deep-wave model forced by the counterfactual TC parametric wind model), as a simple assumption on the fractional effect of change in wind speed on wave height would not cover this uncertainty properly. However, we agree with the reviewer that including a counterfactual wave scenarios would be very interesting, and could cause additional impacts that can be potentially attributed to climate change. Therefore, we encourage future studies to include a counterfactual for this driver to our framework, as mentioned in L401 of the manuscript. We have also removed the word “all” from TC flood drivers in L87.

- Also, the **SnapWave approach over transects** is problematic since wave conditions aren't properly downscaled (ERA5 offshore waves are coarse), transects are poorly connected to actual water levels, and local nearshore processes (refraction, shoaling, breaking) may be inadequately represented in a transect approach

Apologies for the unclear description of our wave modelling approach. In our study, SnapWave is not used as a stand-alone transect model, nor are offshore ERA5 wave conditions directly imposed at the coastline. Instead, we employ a fully 2D flow–wave coupling through SFINCS–SnapWave to calculate wave-induced setup (Fig. 2 in manuscript), in which SnapWave is explicitly used to downscale offshore

ERA5 wave forcing and resolve local nearshore wave processes, including refraction, shoaling, and depth-limited breaking.

The coupled SFINCS–SnapWave simulations produce a wave-induced water level component, which is calculated as the difference between simulations with and without SnapWave, resulting in the targeted wave setup component. For practicality and to maintain computational consistency within our existing hydrodynamic modelling framework, the wave setup timeseries is subsequently extracted along coastline perpendicular transects and superimposed onto the nearest tide–surge water levels at Delft3D-FM output points (see S1.4). We have revised L145-150:

"*We combine the tide and surge with dynamically modelled wave setup, calculated from a coupled SFINCS-SnapWave simulation. The 2D SFINCS-SnapWave model has a spatially-varying grid with a resolution of 400 m offshore to 50 m at the coast, covering an area of 5400 km^2 (yellow domain in Fig. 2). The D-Flow FM output is generated around the 5-meter depth contour within the SFINCS domain at a 10-minute temporal resolution (Fig. S1). The wave setup output is also generated at a 10-minutes temporal resolution and saved at coastal transects*"

- I strongly recommend: (1) fully integrate SnapWave 2D within SFINCS for dynamic wave-surge coupling in both scenarios, OR (2) remove the wave coupling component entirely, acknowledge this as a limitation, and note it may introduce ~10 to 20% uncertainty in coastal flood depths. The current approach undermines the compound flooding framework's credibility.

While fully acknowledging that the current approach could be further improved, dynamically accounting for the wave contribution in a globally applicable approach is already a large advancement over current globally applicable approaches that tend to reply on simplistic parametric estimates or empirical estimates (Hinkel et al., 2021). SnapWave is very recently developed software (Roelvink et al., 2025), and at the time of our framework development, fully integrating SnapWave within SFINCS combined with all compound flood drivers was technically not yet possible (L78-81 in Supplement). We argue that having a better estimate of our factual scenario by including wave setup from SFINCS-SnapWave still adds value as it provides higher confidence in the simulated flooding and therefore in the attribution assessment. For this reason, we have chosen a hybrid approach by including a credible application to assess the contribution of waves on the event, without a full integration of the climate change impact on this contribution.

4. Flood Damage Modeling

- Depth-damage curve validation: The continental curves from Huizinga et al. (2017) assume European-style construction. Snel et al. (2019) showed Ethiopian traditional buildings experience 100% damage at 2m depth versus 5m for concrete structures. Mozambique's post-Idai assessments reported 111,163 completely destroyed houses, but no published studies validate these damage functions against actual losses. I recommend: 1) comparing aggregate model damage against reported sector-specific losses, 2) conducting sensitivity analyses with alternative damage curves for informal/traditional construction and 3) discussing this as a major uncertainty source.

We agree with the reviewer that these simplified depth-damage curves are uncertain but would like to stress that we work with the best available global data and state-of-the-art methods, allowing global applicability of our framework in data-scarce contexts. In response to this and the other comments, we have made our assumption explicit in L225-226, and made it more explicit that these damage curves are a major source of uncertainty in L411 of the discussion. Comparing our damage estimates with sector specific losses is too detailed for the scope of our study.

L225-226: "*The attributable change is conditional on the considered counterfactual flood drivers, and on the assumptions made in the model schematizations and input datasets.* "

5. Missing Elements: Uncertainty Quantification

This is the review's most critical concern. Every component carries substantial uncertainty:

- Counterfactual parameter choices (rainfall: ±2-3%, wind: ±5%, SLR: ±5cm)
- Meteorological forcing (ERA5 vs. parametric TC model inconsistencies)
- Hydrological model calibration
- Missing river bathymetry (bankfull approximation)
- Wave setup assumptions
- Exposure data completeness
- Damage function transferability

These uncertainties compound multiplicatively, not additively. The total framework uncertainty is substantial.

The manuscript MUST include:

1. Uncertainty quantification at each modeling step
2. Formal uncertainty propagation through the attribution framework
3. Comprehensive sensitivity analysis on key assumptions
4. Probabilistic framing of attribution statements with confidence intervals

Recent attribution papers explicitly report uncertainty ranges. Does climate change contribute 5-15% or 25-35% to damages? Without uncertainty bounds, readers cannot properly interpret the "31% damage attributable to climate change" conclusion.

As mentioned in the general response section and individual response to the reviewers comments, we have improved the manuscript as follows:

- Refined the scope of our study in L77-79, L87-90
- Clarified uncertainties and assumptions made within the scope of our study (L225-226).
- Throughout the manuscript improved the wording of our attribution assessment as being conditional, and using plausible climate trends for the constructions of counterfactual scenarios.
- Include climate trend uncertainty propagated in our counterfactual scenarios through the whole modelling chain for a low, middle and high scenario, and presenting our results as a

range of plausible values for the conditional attribution statement (Table 1 and 2 in the revised manuscript).

- Additional wflow hydrological model validation using GloFAS discharge data (Section S1.3)
- Additional SLR analysis and comparison with PSMSL data for the closest tide gauge (this rebuttal document).

As a result, these clarifications and additional experiments have helped to improve the interpretability of our results for the reader, leading to changes throughout the manuscript and in the abstract (L8-23).

Minor Comments

Exposure and Vulnerability Treatment (L285-290)

The manuscript states that exposure/vulnerability is held constant, but this critical assumption deserves more prominent discussion. The counterfactual answers: "What would 2019's exposed population experience under a pre-industrial climate?" not "What would the pre-industrial population experience?" This is correct for physical attribution, but should be explicitly stated in Section 2.3.2 rather than buried in the discussion.

We have explicitly included references to our assumptions on constant exposure and vulnerability between scenarios as part of Section 2.3.2 (L192-193) "*We assume no change of non-flood drivers, such as exposure and vulnerability, in the counterfactual scenarios*", per suggestion of the reviewer. We would like to take this opportunity to share that we are working on extending the framework to include a counterfactual exposure scenario in an upcoming paper.

Supplementary Figure S2 (Return Period Analysis)

The disconnection around 1-2 years is striking and unexplained. How was the fit performed? Was this a standard GEV/Gumbel distribution? The discontinuity suggests potential issues with the extreme value analysis or the underlying wflow discharge distribution. Please add a methods subsection describing the EVA approach and discuss this feature.

The extreme value analysis was done using the pyextremes Python package (Bocharov, 2023) that relies on standard, well-known fitting approaches to define extremes events (i.e. block maxima or peaks-over-threshold methods) and to estimate distribution parameters. Here, we selected yearly maxima from the time series and then fitted a GEV distribution, in accordance with the extreme value theorem that the GEV distribution is the limit distribution of independent and identically distributed block maxima samples (here, yearly maxima). In cases where the shape parameter is 0, this resulted in a Gumbel distribution. The selection between Gumbel or GEV was based on the Akaike Information Criteria (AIC) goodness-of-fit metric. The discontinuity observed is the result of a few years being less extreme than others and is mainly the result of the limited length (30 years) of the time series. As suggested by the reviewer, we have added more details on the EVA approach in section S1.2.

Line 175 (Holland Model Implementation)

"linearly fading the data at 0.75 fraction of the TC radius" - Why 0.75? This appears arbitrary and could significantly affect results. Show sensitivity or cite precedent. Also, how is the TC eye resolved in terms of rainfall distribution? The Holland wind model has asymmetric components—were these included?

The 0.75 merge fraction is explained in an earlier response. For asymmetry in the Holland wind model, the TC asymmetry between different quadrants was defined using Schwerdt et al. (1979), as common

in literature (e.g., Leijnse et al., 2021). While more advanced tropical cyclone wind models exist, data availability is often a limiting factor, and in our view, this makes application on a global and operational context infeasible. Considering the validation of the model, which is reported in section 3.2, S1.3 and S1.5, we consider our approach valid for the scope of our study.

Recommendations

Despite the substantial revisions required, this manuscript represents important and novel work. The technical execution is sophisticated, the application to Mozambique addresses a critical gap, and the compound flooding attribution framework is genuinely innovative. With careful attention to the major comments—particularly uncertainty quantification, counterfactual justification, and wave setup treatment—this can become a strong contribution to NHESS and the broader attribution literature.

Priority actions:

1. Add comprehensive uncertainty analysis (Monte Carlo or ensemble approaches)
2. Revise or remove the wave setup coupling
3. Strengthen counterfactual justifications with sensitivity analyses
4. Improve damage model validation against reported losses

The open-source, globally-applicable framework you've developed has significant potential for advancing attribution science in vulnerable, data-poor regions. I look forward to seeing the revised manuscript.

We would again like to sincerely thank the reviewer for their time to provide the detailed and elaborate comments on our manuscript. We believe these have strengthened our work significantly. Please refer to our earlier response to individual comments and the general response for the actions we have taken to include the reviewers suggestions.

Reply to reviewer 2

This study proposes and applies a storyline attribution framework, combining a multi-model chain to conduct climate attribution and impact attribution analysis for the compound flooding event induced by Tropical Cyclone Idai (2019). The research design is relatively complete, the methodology is advanced, and the attempt in a data-scarce region demonstrates certain innovation. However, the manuscript exhibits the following issues:

We thank the reviewer for the detailed comments and feedback they have provided. We have improved the manuscript in line with the scope of the paper to the best of our abilities.

Major Comments

1. Regarding the construction of the counterfactual scenarios, a uniform reduction of 8% in rainfall, 10% in wind speed, and the removal of 14 cm of sea-level rise were applied. While this method is operationally convenient and has some basis, it potentially overlooks the spatiotemporal heterogeneity of climate change. For tropical cyclones, climate change may affect not only their intensity but also their track, structure, translation speed, and spatial distribution of precipitation. The adjustment of only intensity parameters in this study may lead to an underestimation of the true impact of climate change.

Please see the general response regarding the additional counterfactual scenarios to capture climate trend uncertainty in TC flood drivers, as well as a explantion of the scope of our that is focused on conditional storyline attribution. In the revised manuscript, we acknowledge the current lack of our framework of not including heterogenous spatiotemporal effects of climate change on the TC flood drivers in the discussion (L392-397). We also mention in the discussion the inclusion of additional changes in TC size and translation speed due to climate change for future studies (L399-402). While we are aware that TC tracks also seem to shift poleward (e.g. Knutson et al, 2020), which could lead to changes in TC risk, this storyline approach requires constraining the event by fixing the TC track as explained in the general response (additional explanation added in L401 and L190-192).

L392-397: "*Our framework is built on simplified and uniform assumptions on the effect of climate change on TC rainfall and wind speed. The counterfactual rainfall is homogenously scaled according to plausible climate trends but neglects any TC specific estimates and changes in spatio-temporal patterns (Deng et al., 2025; Kim et al., 2022; Liu et al., 2019b). The same applies to the counterfactual scenarios of maximum wind speed, where simplified scaling the maximum wind speed with reductions of 1–10 % neglects the complex dynamics of TCs (Knutson et al., 2020).*"

L399-402: "*Moreover, we could evaluate the effect of climate change on additional flood drivers possibly increasing coastal flooding, such as change in TC size (Yamada et al., 2017), translation speed (Knutson et al., 2020; Seneviratne et al., 2021) and significant wave height (Thompson et al., 2021), while still conditioning on the TC track.*"

L190-192: "In line with storyline attribution, we constrain the TC track in all counterfactual scenarios, such that it is same to the one observed during the factual event (Feser and Shepherd, 2025; Mester et al., 2023; Strauss et al., 2021)."

2. The author employs GRDC discharge data from 1954–1984 for wflow model validation. Based on Figure S6, the simulated discharge performance is not satisfactory. And the simulated discharge exhibits a systematic overestimation, attributed by the authors to overestimation of ERA5 rainfall and the model being uncalibrated. This explanation is overly simplistic. Does

the lack of model calibration imply substantial parameter uncertainty, thereby casting doubt on the results. Furthermore, the factual event occurred in 2019, the hydrological response of the catchment may have undergone significant changes due to factors such as climate change and land-use alteration. Consequently, the representativeness and reliability of using data from over three decades ago to validate simulations of the current extreme event are questionable.

We agree with the reviewer that validating our wflow simulations using three decade old observations is questionable and have replaced our validation with available global modelled discharge data from GloFAS (L251-266 and Section S1.3), as it is another commonly used discharge dataset used in operational forecasts globally. These results show that discharge estimates for the major Buzi river are reasonable and that the high discharge we obtain can potentially be related to the finer spatial and temporal resolution (0.0083° and hourly resolution for wflow compared to 0.05° and daily resolution for GloFAS) used in our study. Interestingly, we find considerable uncertainty for the Pungwe river between GloFAS products (version 4.0 versus version 3.1). We recognize the uncertainty in our wflow results (L262-266) and highlight the need for recent and local observations in the Dicussion (L388-390).

L251-266: "*For discharge, we compare against modelled Global Flood Awareness System (GloFAS) discharge data (Grimaldi et al., 2023; Joint Research Center and Copernicus Emergency Management Service, 2020; Zsoter et al., 2021), as recent observations for the region are lacking. This comparison shows that the simulated discharge for the two major rivers in the region (the Pungwe and Buzi) is uncertain and differs significantly between GloFAS data versions (v4.0 and v3.1; Fig. S5 and S6). For the period of TC Idai, the summed daily discharges simulated by GloFAS v4.0 (v3.1) differ -19 % (-10 %) and -51 % (29 %) from the summed wflow discharges resampled to a daily time step for the Buzi and the Pungwe, respectively (Table S2). The overestimated discharge could be explained by the higher spatial and temporal resolution of our wflow model compared to GloFAS data. During the flood event, the simulated discharge is in the same order of magnitude as calculated by Eilander et al. (2023a). The agreement between our results and GloFAS for the Buzi river is reasonable (KGE for comparison with GloFAS v4.0 (v3.1) is 0.42 (0.61) for the Buzi river; Fig S6), although also here extremes are generally overestimated. For the Pungwe river, GloFAS discharge data vary significantly between versions, and this variability is also reflected in the comparison with our results (KGE for comparison with GloFAS v4.0 (v3.1) is 0.09 (0.75) for the Pungwe river; Fig S6). Recent local observations are required to better determine the performance of the wflow model.*"

L388-390: "*Echoing e.g. Eilander et al. (2023a) and Samadi et al. (2025), establishing high-quality observations should remain a priority for more accurate assessments in data-scarce regions and for providing more localized information on climate change impacts.*"

3. Due to the lack of river bathymetry data, the authors adopted a simplified approach: directly subtracting the estimated bankfull discharge (approximated by the 2-year return period discharge) from the discharge boundary conditions

    - However, has the applied semi-empirical relationship been validated locally in Mozambique? The relationship between discharge and return period can vary significantly across rivers under different climatic, geomorphological, and vegetation conditions.
    - As shown in Table S1, the estimated bankfull discharge for Gauge 1 (Buzi River) is 3887 m^3/s, but its 95% confidence interval spans [2935, 5140] m^3/s, representing a relative uncertainty exceeding ±30%. Using a parameter with such high uncertainty as a decisive "subtractor" directly transfers and amplifies its error into the input boundaries of SFINCS.

- This method neglected the mechanisms of channel storage and flood attenuation. This stands in fundamental contradiction to the complex two-dimensional flood dynamics that SFINCS aims to simulate. Although the authors mention in the supplementary material that this method may lead to inaccuracies in input discharge, its scientific rationale and practical implications have not been sufficiently justified.

We agree with the reviewer that our approach has inherent limitations and we have made those explicit in L19-23 in the supplement. We have not found further literature validating this approach for Mozambique. Our approach is thus the best we could do for a data-scarce context while ensuring global applicability. Concerning the mentioned ±30% uncertainty in bankfull discharge for gauge 1 (Buzi river; 1000–1300 m^3/s), this translates to only 4–5% of the peak discharge at the time of the event (27.000 m^3/s). While dynamics within the channel cannot be captured, using SFINCS still allows to better capture complex flood propagation and attenuation in the floodplains, of particular value for this study. We have clearly refined the scope of the study in L77-79 and L87-90, and made the assumptions of our conditional attribution assessment more explicit in L225-226.

L19-23 in supplement: "*Due to the lack of river bathymetry data, we remove the bankfull discharge from the discharge boundary conditions for SFINCS and assume that the incoming discharge represents out of banks discharge, thereby removing the need to burn in an (unknown) river conveyance in the digital elevation model. This approach may lead to an under- or overestimation in river discharge input for our SFINCS model simulations*."

L77-79: "*The goal of this paper is to demonstrate a storyline attribution framework that is applicable globally, including data-scarce regions, by attributing the effect of climate change on flood hazard and impact from TC Idai.*"

L87-90: "*We use a storyline attribution framework with a state-of-the-art modelling chain that dynamically simulates TC flood drivers and damages in factual and counterfactual scenarios, where plausible climate change trends are removed. The differences between the factual and counterfactual scenarios for flood hazard and impact are compared to construct conditional climate and impact attribution assessments.* "

L225-226: "*The attributable change is conditional on the considered counterfactual flood drivers, and on the assumptions made in the model schematizations and input datasets.*"

4. The simulated water levels are consistent with values from the literature but do not provide quantitative comparison metrics. This makes it difficult to objectively assess the simulation accuracy.

No in-situ measurements are available in or near the case study region. In this data-scarce context, we can therefore only compare the simulated storm surge by comparing maximum water levels with other studies and reported values (Eilander et al., 2023; Probst and Annunziato, 2019). These comparisons indicate that the simulated water levels for the factual scenario are consistent with previously reported ranges. In addition, the simulated factual flood extent shows good agreement with satellite-derived inundation observations. These qualitative validations provide confidence that the model performance is adequate for the scope and objectives of this study.

5. In the flood extent validation, although the Hit Rate is >76%, the False-Alarm Ratio is as high as 60% (based on the CEMS product), and the Critical Success Index is only 0.40, indicating limited overall predictive capability of the model. The significant discrepancy between the two

satellite products (UNOSAT and CEMS) also highlights the lack of a reliable ground truth flood extent benchmark, further increasing the uncertainty in model evaluation.

We agree with the reviewer that lack of in-situ observations in our case study region make it challenging to evaluate the model performance. At the same time, this data-scarce context was also a main motivation for applying our framework to this region.. The comparison of our simulated flood maps with the UNOSAT product has given us confidence in the factual flood map. We find it important to show both satellite products to highlight uncertainty in satellite observation for this region but we have more faith in the UNOSAT product as the CEMS product does not show any flooding in Beira. We have added this confidence in L100-101 of the Supplement: "*We have more trust in the UNOSAT product, as there is no flooding present in Beira for the CEMS product, even though flooding there is documented (e.g. ReliefWeb, 2019).*"

6. Changes in rainfall lead to the largest increase in flood volume and extent (9% and 2%, respectively), while the impacts of sea-level rise (SLR) and wind speed changes on volume and extent are less than 1%. However, SLR and wind jointly contribute to a 27% increase in damages, whereas rainfall contributes only 4%. Why do SLR and wind, which have minimal impact on inundation extent, result in such a significant rise in damages? It is recommended to enhance the process-based explanation of the attribution conclusions, rather than merely presenting statistical results.

We argue that we have sufficiently explained this process in L317-321 and L353-359.

L317-321: "*Even though changes in SLR and wind are negligible in terms of changes in flood volume and flood extent, these drivers have a larger impact on flood damage than changes in rainfall (Fig. 5). The relative change in impact is larger than the relative change in flooding, except for the rain-only scenario. Increased wind and SLR intensify coastal flooding, which is the main driver of damage in Beira, where total damages are concentrated due to the high density of buildings*"

L353-359: *"In the case of compound flooding from TC Idai, increased amounts of rainfall led to the largest increase in flood volume and flood extent, which can be explained by the flooding being largely driven by the high river discharges (Eilander et al., 2023). On the other hand, increased coastal flooding due to intensified wind speeds and SLR resulted in the largest increase in total damage, concentrated in the coastal areas. The coastal areas are most densely inhabited, especially the coastal city of Beira, which explains the large effect of intensified wind speeds and SLR on impacts despite the relatively small increase in flood depth, emphasizing the importance of accounting for exposure and vulnerability"*

Minor Comments

1. The sentence on line 30, "Compound flooding from tropical cyclones (TCs) is one of the most damaging climate extreme events and is exacerbated by climate change (Frame et al., 2020; Smith and Katz, 2013)," is somewhat broad. To aid reader comprehension, especially for those not specialized in this specific sub-field, it would be beneficial to briefly define the core concept of "compound flooding" immediately following its first mention.

We have incorporated the suggestion of the reviewer in L32: "*Compound flooding from tropical cyclones (TCs), driven by the co-occurrence and interaction of multiple flood drivers such as fluvial, pluvial, and coastal flooding (Zscheischler et al., 2018), is one of the most damaging climate extreme events and is exacerbated by climate change (Frame et al., 2020; Smith and Katz, 2013).*"

2. In lines 125, the description of removing permanent water bodies, based on the Global Surface Water dataset, is provided. However, the temporal relevance of this dataset during the flood event is not addressed. The static nature of the dataset may lead to the misclassification of dynamic water features, such as temporarily expanded rivers during the peak flood period, as permanent water bodies. Please provide more details.

As mentioned in the general response, we utilize the best globally available data and keep it static between scenarios, in line with storyline attribution. We use the version from 2019 (the year of TC Idai) of the permanent water layer from Pekel et al., (2016). We have decided to not describe all specific dataset versions in the manuscript, as readers can find these in the data catalog files of the published repository (scripts we use to manage all input data).

3. The authors highlight the applicability of their framework to global TC events and data-scarce regions as a strength. However, they do not explicitly acknowledge that the global data products used in this study may inherently carry greater uncertainty in these very regions. Furthermore, the discussion insufficiently addresses the model uncertainties that are particularly pronounced in data-scarce settings. These omissions may weaken the perceived reliability of the conclusions when the framework is applied in such contexts.

We agree that our attribution statements are contingent on the underlying assumptions and should be interpreted as plausible what-if scenarios. We have strengthened this throughout the entire manuscript, for example L87-90 and L225-226.

L87-90: "*We use a storyline attribution framework with a state-of-the-art modelling chain that dynamically simulates TC flood drivers and damages in factual and counterfactual scenarios, where plausible climate change trends are removed. The differences between the factual and counterfactual scenarios for flood hazard and impact are compared to construct conditional climate and impact attribution assessments.*"

L225-226: "*The attributable change is conditional on the considered counterfactual flood drivers, and on the assumptions made in the model schematizations and input datasets.*"

4. (Lines 320–325) The discussion emphasizes that "focusing on a single flood driver may not give a good representation of the total impact of climate change." However, the results of this study itself demonstrate that for flood volume and extent, rainfall is the overwhelmingly dominant driver (9%), while the individual contributions of SLR and wind are negligible (<1%). Conversely, for damages, the combined effect of SLR and wind (27%) far exceeds that of rainfall (4%). Therefore, whether an impact is "underestimated" depends entirely on the metric of concern. The discussion should more dialectically acknowledge that in compound flooding events, different impact metrics may be governed by distinct key drivers. Consequently, attribution statements should explicitly specify the targeted metric (hazard metric vs. impact metric) to avoid potential misinterpretation.

We agree with the reviewer and have incorporated the suggestion of more explicitly in L373-374: "*As a result, we highlight the importance of explicitly specifying the metrics used when making attribution statements.*"

We would again like to sincerely thank the reviewer for their time to provide the detailed and elaborate comments on our manuscript. We believe these have strengthened our work significantly.

Reply to reviewer 3

This article presents the results of an application of a global modeling framework that leverages multiple physics-based models to attribute increases in flood extent and damages from TC Idai to climate change (sea level rise, wind, rain). I particularly like that the authors show how climate change has a nonlinear impact on flood hazards and these nonlinearly impact damages. I commend the authors for all the modeling work they did and believe that it can be a valuable contribution after revisions.

We thank the reviewer for the detailed comments and feedback they have provided. We have improved the manuscript in line with the scope of the paper to the best of our abilities.

Major Comments

The goal of the paper is currently weakly stated (L75). The authors should rearticulate the gap or contribution of the paper to better frame the introduction and discussion. What is the new or useful information that the authors think this work contributes? I think the work has merit and has the potential to showcase how global models and frameworks can be leveraged in data scare regions. That said, there is almost no consideration for uncertainty, and it would be helpful if the authors could explain why they did not consider this in their analysis. The authors even suggest this in L336 where they state that "For areas with limited observational data, attribution statements should go hand in hand with a thorough uncertainty analysis."

We thank the reviewer for the suggestion to improve the description of the goal of our paper which is to emphasize the applicability of the framework globally, including data-scarce regions. This has now been reformulated in L77-79: "*The goal of this paper is to demonstrate a storyline attribution framework that is applicable globally, including data-scarce regions, by attributing the effect of climate change on flood hazard and impact from TC Idai*"

We agree that L336 (from the original manuscript) was ambiguous, and we have improved and elaborated on this sentence (L383-388 in revised manuscript). As mentioned in the general response, we have included additional counterfactual scenarios for plausible climate trends in the considered TC flood drivers.

L383-388: "*For areas without sufficient recent and local observations, providing robust attribution statements remains challenging due to limited opportunities for model validation, especially for high-impact low-likelihood events. In such contexts, storyline attribution assessments that consider plausible what-if scenarios can still provide highly informative insights (Sillmann et al., 2021). Multi-method attribution assessments could provide more confidence in the attribution assessment (Barriopedro et al., 2025; Thompson et al., 2025).*"

- What are the ranges of possible climate change factors for SLR, rain, wind? How would your results differ if you considered an ensemble of these? Is the modeling framework not suitable for conducting many simulations?

Please refer to the updated Table 1, Table 2, and Fig. 5, as well as justification for the additional counterfactual scenarios in Section 2.3.2.

- How much uncertainty in the results comes from model errors? Is this due to the coarse model inputs or model structure? There are mentions of this throughout the paper, but the discussion would benefit from a structured layout that addresses how these would alter the findings from the study (increase/decrease/no change)? You could conduct sensitivity tests to support these statements or evidence from other articles that use the same models.

Please also refer to the general response. We work with the best available global data and common practices, allowing global applicability of our framework. Sensitivity testing of model parameters is included to a reasonable and feasible extent, as considered within the scope of our study and our storyline experiment.

I like that this paper extends the analysis to exposure and shows how there is not a direct one-to-one relationship between changes in flood hazards and damages due to climate change. However, these exposure estimates are subject to the uncertainty in the flood hazards, and the authors have an opportunity to dive into the interplay more. Where are the buildings across the study area and how many are there? Is the fraction of the total buildings inundated in the coastal city higher or lower than the buildings impacted along the major rivers (you mentioned bias in L300)? Is fluvial flooding impacting 90% of the households in or near the floodplain even though the damages are small compared to the coastal area? You might consider breaking this down by political or watershed boundaries.

We thank the reviewer for this suggestion but would like to keep the scope of this paper on the non-linearity between climate and impact attribution, and on combining the climate change effect of multiple TC flood drivers. Therefore, a very detailed disaggregation of attribution statements is considered beyond the scope of this paper, but we are happy to announce that an upcoming paper is focused on this topic.

Minor Comments

Are the flood extent/volumes calculated at the grid or subgrid resolution?

Subgrid resolution of 25 m.

In L125 you mention you remove permanent water bodies… does this include the river network or just the major coastal water bodies? Could this lead to an overestimation of the contribution of rain/river to the flood extents?

In the flood maps of both factual and counterfactual scenarios we also removed the main rivers, such as the Buzi and Pungwe rivers.

Are buildings usually elevated off the ground (L155)? Would it be worthwhile to account for this uncertainty by using a range of depth thresholds (say 0.05-1m) before estimating exposure/damages?

It is possible that buildings are elevated off the ground, and an interesting sensitivity test (one of many possible) but beyond the scope of this study as mentioned in the general response.

L171 – what are the other global data sources? Maybe list in parenthesis with citations.

They can all be found in the data catalogs (scripts we use to manage all input data) of the published repository, with citations.

Line 181, you could strengthen this section by adding trends and citations for each flood driver mentioned – especially if they are trends for your study area/region.

As suggested by the reviewer, we have added additional scientific justification to this section for all counterfactual scenarios in L195-210: "*The plausible climate trend of TC rainfall, maximum wind speed and SLR is based on best available literature and global datasets. For the climate change effect on TC rainfall, some studies find that the trend is in line with the Clausius–Clapeyron relationship (7 %/°C of warming; Knutson et al., 2020), while other studies show trends higher than Clausius–Clapeyron (Guzman and Jiang, 2021; Liu et al., 2019; Patricola and Wehner, 2018), referred to as super Clausius–*

Clapeyron (14 %/°C of warming), and lower due to enhanced cooling from slower TC translation speeds in a warmer climate (Tu et al., 2022). As Idai took place in a ~1.1 °C warmer world, we adopt plausible reductions of rainfall of 4 %, 8 % and 16 % for low, medium and high counterfactual scenarios, respectively. For the climate change effect on TC maximum wind speeds, we use plausible reductions of 1%, 5% and 10 % for the low, medium and high counterfactual scenarios, respectively. The low and medium scenarios are based on the likely range of 1–5 % per °C of warming for the Southern Indian ocean from climate models (Knutson et al., 2020), and the high scenario of a 10 % wind speed reduction is based on regional trends from observed TCs (Mester et al., 2023) . For the climate change effect on SLR, we use plausible reductions of 5, 10 and 15 cm for the low, medium and high counterfactual scenario, respectively. The medium scenario is based on the dataset by Treu et al. (2024), used to estimate the SLR between the time of the event and pre-industrial levels, and the low and high scenarios are based on uncertainty bounds from Strauss et al. (2021)."

Table 1 – Including information on the storm rain rates and wind speeds (like the mean, max, 90 percentile) would be helpful

We thank the reviewer for the suggestion but prefer to keep the table simple, particularly given the additional layer of information introduced by the inclusion of multiple counterfactual scenarios. The magnitude of the forcing for both the factual and counterfactual cases is shown in Figs. S11 and S12.

L215 – The authors state that a lot of flooding is coming from the rivers which are being modeled using wflow which tends to perform poorly for extreme events (Fig S6). If I am understanding correctly, it seems that there are observational gauges near the SFINCS boundary. Why not use these as inflow to SFINCS to see how well the model performs compared to the satellite images and also to get an idea of the buildings/flood extent would be with a more precise discharge boundary condition? It might be a useful experiment especially given how impactful discharge (and the assumptions or error) are for this specific storm and study area.

This is a very good suggestion, but unfortunately there is no observed discharge for the period of the event (GRDC for our region is available from 1954-1984).

L234 – any idea why the KGE is so low (0.28) for the Pungwe compared to the Buzi?

In response to reviewer 2, we have redone the analysis using modelled discharge from GloFAS v3.1 and v4.0 (L251-266 and Sect. S1.3). This analysis shows considerable uncertainty between the GloFAS versions for the Pungwe river. Based on this, it is hard to identify the cause for this large difference but this can likely be attributed to the lack of recent observed discharge time series that reflect current catchment conditions and thus rely on little or no data or regionalization methods.

L251-266: "*For discharge, we compare against modelled Global Flood Awareness System (GloFAS) discharge data (Grimaldi et al., 2023; Joint Research Center and Copernicus Emergency Management Service, 2020; Zsoter et al., 2021), as recent observations for the region are lacking. This comparison shows that the simulated discharge for the two major rivers in the region (the Pungwe and Buzi) is uncertain and differs significantly between GloFAS data versions (v4.0 and v3.1; Fig. S5 and S6). For the period of TC Idai, the summed daily discharges simulated by GloFAS v4.0 (v3.1) differ -19 % (-10 %) and -51 % (29 %) from the summed wflow discharges resampled to a daily time step for the Buzi and the Pungwe, respectively (Table S2). The overestimated discharge could be explained by the higher spatial and temporal resolution of our wflow model compared to GloFAS data. During the flood event, the simulated discharge is in the same order of magnitude as calculated by Eilander et al. (2023a). The agreement between our results and GloFAS for the Buzi river is reasonable (KGE for comparison with*

GloFAS v4.0 (v3.1) is 0.42 (0.61) for the Buzi river; Fig S6), although also here extremes are generally overestimated. For the Pungwe river, GloFAS discharge data vary significantly between versions, and this variability is also reflected in the comparison with our results (KGE for comparison with GloFAS v4.0 (v3.1) is 0.09 (0.75) for the Pungwe river; Fig S6). Recent local observations are required to better determine the performance of the wflow model."

L236 – How much is ERA5 overestimating and how do you expect this would cascade to the runoff attribution? Is this mostly a problem for the discharge from wflow or is it also an issue for the rainfall directly on SFINCS?

Inaccuracies in ERA5 rainfall would affect both SFINCS (local pluvial flooding) and wflow (discharge boundary conditions) and constitutes an important uncertainty. However, due to the lack of recent local rain gauges data, uncertainty quantification is not readily implemented within the scope of this study. These limitations have been made more explicit in L383-385 and we highlight the need for local observations in L388-390.

L383-385: "*For areas without sufficient recent and local observations, providing robust attribution statements remains challenging due to limited opportunities for model validation, especially for high-impact low-likelihood events.*"

L388-390: "*Echoing e.g. Eilander et al. (2023a) and Samadi et al. (2025), establishing high-quality observations should remain a priority for more accurate assessments in data-scarce regions and for providing more localized information on climate change impacts.*"

Figure 4 – does this figure include the water bodies cells that are removed from the flood extent calculation? I would outline these so the reader knows what areas are excluded from the calculation.

They are indeed removed and we have added additional outlines of these so this is more clear in Fig. 4, shown here for ease:

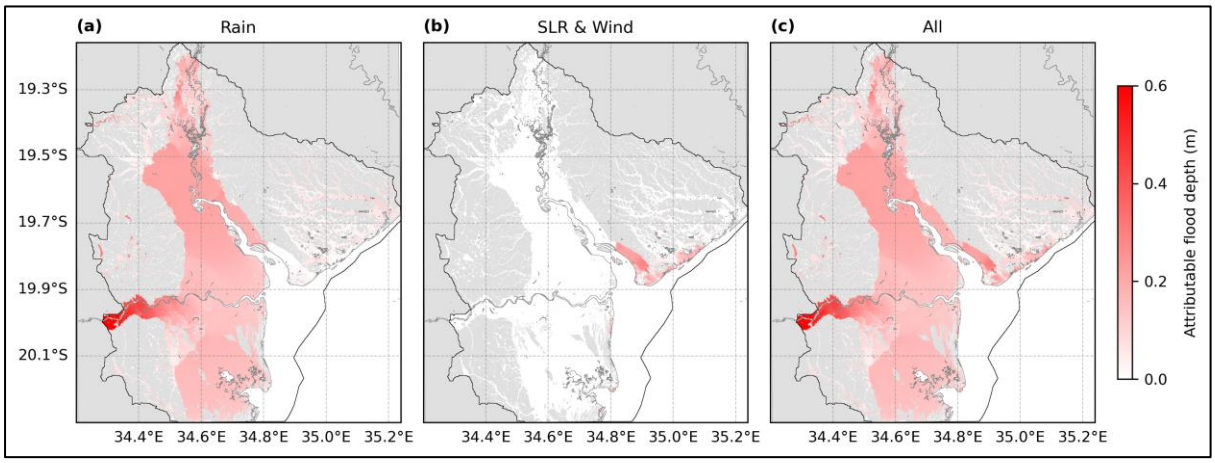

Figure 5 – add the number of buildings exposed to this would be helpful

We have included this suggestion in L313-315:

"*Comparing the factual and medium counterfactual scenario (low–high counterfactual scenario) shows that 21 % (8–35 %) of the flood damage, corresponding to 70 M USD (30–120 M USD), can be attributed to climate change, resulting in 7,000 (3,000–13,000) more buildings damaged.*"

L310 – I would avoid saying “accurately reproduces” here unless you have defined what this is and have statistics as proof. Consider rephrasing.

We agree with the suggestion of the reviewer and have revised the text in L351-353:

“*This framework provides an estimate of compound flooding from TC Idai using global data in line with observations and reported values in literature, and is applied for both climate and impact attribution assessments.*”

If you wanted to save some space, you could reduce the text that mentions the vulnerability aspect of flood risk (i.e., L290 and the last paragraph in the discussion). This is important to consider and should be mentioned as something that does matter when conducting risk assessments. However, this paper primarily focuses on the hazard and exposure (buildings) and focusing on the findings and key takeaways that we can gleam for your results regarding these components would help streamline the paper.

We thanks te reviewer for this suggestion, but have decided to keep the paragraph in the manuscript as it links well to the introduced difference between relative and absolute changes in damage for the attribution statement, and provides direction on exploring other forms of impact attribution.

We would again like to sincerely thank the reviewer for their time to provide the detailed and elaborate comments on our manuscript. We believe these have strengthened our work significantly.

References

Barriopedro, D., Jiménez-Esteve, B., Collazo, S., Garrido-Perez, J. M., Johnson, J. E., and García-Herrera, R.: A Multimethod Attribution Analysis of Spain's 2024 Extreme Precipitation Event, Bull. Am. Meteorol. Soc., 106, E2440–E2460, https://doi.org/10.1175/BAMS-D-25-0049.1, 2025.

Bocharov, G.: pyextremes (Version 2.3.3), https://github.com/georgebv/pyextremes, 2023.

Deltares: Delft3D fM Suite Simulation software for safe, sustainable and future deltas User Manual D-Flow Flexible Mesh, 2026.

Eilander, D., Couasnon, A., Leijnse, T., Ikeuchi, H., Yamazaki, D., Muis, S., Dullaart, J., Haag, A., Winsemius, H. C., and Ward, P. J.: A globally applicable framework for compound flood hazard modeling, Natural Hazards and Earth System Sciences, 23, 823–846, https://doi.org/10.5194/nhess-23-823-2023, 2023.

Feser, F. and Shepherd, T. G.: The concept of spectrally nudged storylines for extreme event attribution, Commun. Earth Environ., 6, 677, https://doi.org/10.1038/s43247-025-02659-6, 2025.

Frame, D. J., Wehner, M. F., Noy, I., and Rosier, S. M.: The economic costs of Hurricane Harvey attributable to climate change, Clim. Change, 160, 271–281, https://doi.org/10.1007/S10584-020-02692-8, 2020.

Grimaldi, S., Salamon, P., Disperati, J., Zsoter, E., Russo, C., Ramos, A., Carton De Wiart, C., Barnard, C., Hansford, E., Gomes, G., and Prudhomme, C.: River discharge and related forecasted data from the Global Flood Awareness System, https://doi.org/10.24381/cds.a4fdd6b9, 2023.

Guzman, O. and Jiang, H.: Global increase in tropical cyclone rain rate, Nature Communications 2021 12:1, 12, 5344-, https://doi.org/10.1038/s41467-021-25685-2, 2021.

Hinkel, J., Feyen, L., Hemer, M., Le Cozannet, G., Lincke, D., Marcos, M., Mentaschi, L., Merkens, J. L., de Moel, H., Muis, S., Nicholls, R. J., Vafeidis, A. T., van de Wal, R. S. W., Vousdoukas, M. I., Wahl, T., Ward, P. J., and Wolff, C.: Uncertainty and Bias in Global to Regional Scale Assessments of Current and Future Coastal Flood Risk, Earths Future, 9, e2020EF001882, https://doi.org/10.1029/2020EF001882, 2021.

Holgate, S. J., Matthews, A., Woodworth, P. L., Rickards, L. J., Tamisiea, M. E., Bradshaw, E., Foden, P. R., Gordon, K. M., Jevrejeva, S., and Pugh, J.: New Data Systems and Products at the Permanent Service for Mean Sea Level, J. Coast. Res., 29, 493–504, https://doi.org/10.2112/JCOASTRES-D-12-00175.1, 2013.

Holland, G.: A Revised Hurricane Pressure–Wind Model, Mon. Weather Rev., 136, 3432–3445, https://doi.org/10.1175/2008MWR2395.1, 2008.

Jaafar, H. and Ahmad, F.: GCN250, global curve number datasets for hydrologic modeling and design, https://doi.org/10.6084/m9.figshare.7756202.v1, 2019.

Joint Research Center and Copernicus Emergency Management Service: River discharge and related forecasted data from the Global Flood Awareness System, Early Warning Data Store (EWDS), https://doi.org/10.24381/cds.a4fdd6b9, 2020.

Knutson, T., Camargo, S. J., Chan, J. C. L., Emanuel, K., Ho, C. H., Kossin, J., Mohapatra, M., Satoh, M., Sugi, M., Walsh, K., and Wu, L.: Tropical Cyclones and Climate Change Assessment: Part II:

Projected Response to Anthropogenic Warming, Bull. Am. Meteorol. Soc., 101, E303–E322, https://doi.org/10.1175/BAMS-D-18-0194.1, 2020.

Leijnse, T., Van Ormondt, M., Nederhoff, K., and Van Dongeren, A.: Modeling compound flooding in coastal systems using a computationally efficient reduced-physics solver: Including fluvial, pluvial, tidal, wind-and wave-driven processes, Coastal Engineering, 163, 103796, https://doi.org/10.1016/j.coastaleng.2020.103796, 2021.

Liu, M., Vecchi, G. A., Smith, J. A., and Knutson, T. R.: Causes of large projected increases in hurricane precipitation rates with global warming, npj Climate and Atmospheric Science 2019 2:1, 2, 1–5, https://doi.org/10.1038/s41612-019-0095-3, 2019.

Lloyd, E. A. and Shepherd, T. G.: Environmental catastrophes, climate change, and attribution, Ann. N. Y. Acad. Sci., 1469, 105–124, https://doi.org/10.1111/NYAS.14308, 2020.

Lloyd, E. A. and Shepherd, T. G.: Climate change attribution and legal contexts: evidence and the role of storylines, Clim. Change, 167, 28, https://doi.org/10.1007/S10584-021-03177-Y, 2021.

Mester, B., Vogt, T., Bryant, S., Otto, C., Frieler, K., and Schewe, J.: Human displacements from Tropical Cyclone Idai attributable to climate change, Hazards Earth Syst. Sci, 23, 3467–3485, https://doi.org/10.5194/nhess-23-3467-2023, 2023.

Patricola, C. M. and Wehner, M. F.: Anthropogenic influences on major tropical cyclone events, Nature 2018 563:7731, 563, 339–346, https://doi.org/10.1038/s41586-018-0673-2, 2018.

Pekel, J. F., Cottam, A., Gorelick, N., and Belward, A. S.: High-resolution mapping of global surface water and its long-term changes, Nature, 540, 418–422, https://doi.org/10.1038/nature20584, 2016.

Permanent Service for Mean Sea Level (PSMSL): Tide Gauge Data, 2026.

Probst, P. and Annunziato, A.: Tropical Cyclone Idai: analysis of the wind, rainfall and storm surge impact, European Commission - Joint Research Centre, 2019.

ReliefWeb: Mozambique: Cyclone Idai & Floods Situation Report No. 2 (as of 3 April 2019) - Mozambique | ReliefWeb, 2019.

Roelvink, D., van Ormondt, M., Reyns, J., and van der Lugt, M.: SnapWave: fast, implicit wave transformation from offshore to nearshore, Geosci. Model Dev., https://doi.org/10.5194/gmd-18-9469-2025, 2025.

Samadi, V., Fowler, H. J., Lamond, J., Wagener, T., Brunner, M., Gourley, J., Moradkhani, H., Popescu, I., Wasko, C., Wright, D., Wu, H., Zhang, K., Arias, P. A., Duan, Q., Nazemi, A., van Oevelen, P. J., Prein, A. F., Roundy, J. K., Saberian, M., and Umutoni, L.: The Needs, Challenges, and Priorities for Advancing Global Flood Research, WIREs Water, 12, e70026, https://doi.org/https://doi.org/10.1002/wat2.70026, 2025.

Schwerdt, R. W., Ho, F. P., and Watkins, R. R.: Meteorological criteria for standard project hurricane and probable maximum hurricane windfields, gulf and east coasts of the United States, http://repository.library.noaa.gov/view/noaa/6948, 1979.

Shepherd, T. G.: A Common Framework for Approaches to Extreme Event Attribution, Curr. Clim. Change Rep., 2, 28–38, https://doi.org/10.1007/S40641-016-0033-Y, 2016.

Sillmann, J., Shepherd, T. G., van den Hurk, B., Hazeleger, W., Martius, O., Slingo, J., and Zscheischler, J.: Event-Based Storylines to Address Climate Risk, Earths Future, 9, e2020EF001783, https://doi.org/10.1029/2020EF001783, 2021.

Smith, A. B. and Katz, R. W.: US billion-dollar weather and climate disasters: Data sources, trends, accuracy and biases, Natural Hazards, 67, 387–410, https://doi.org/10.1007/S11069-013-0566-5, 2013.

Strauss, B. H., Orton, P. M., Bittermann, K., Buchanan, M. K., Gilford, D. M., Kopp, R. E., Kulp, S., Massey, C., Moel, H. de, and Vinogradov, S.: Economic damages from Hurricane Sandy attributable to sea level rise caused by anthropogenic climate change, Nat. Commun., 12, 2720, https://doi.org/10.1038/s41467-021-22838-1, 2021.

Thompson, V., Ermis, S., and Athanase, M.: The need for multi-method extreme event attribution, Weather, https://doi.org/10.1002/wea.7779, 2025.

Treu, S., Muis, S., Dangendorf, S., Wahl, T., Oelsmann, J., Heinicke, S., Frieler, K., and Mengel, M.: Reconstruction of hourly coastal water levels and counterfactuals without sea level rise for impact attribution, Earth Syst. Sci. Data, 16, 1121–1136, https://doi.org/10.5194/ESSD-16-1121-2024, 2024.

Tu, S., Chan, J. C. L., Xu, J., Zhong, Q., Zhou, W., and Zhang, Y.: Increase in tropical cyclone rain rate with translation speed, Nature Communications 2022 13:1, 13, 7325-, https://doi.org/10.1038/s41467-022-35113-8, 2022.

Zscheischler, J., Westra, S., Van Den Hurk, B. J. J. M., Seneviratne, S. I., Ward, P. J., Pitman, A., Aghakouchak, A., Bresch, D. N., Leonard, M., Wahl, T., and Zhang, X.: Future climate risk from compound events, Nature Climate Change 2018 8:6, 8, 469–477, https://doi.org/10.1038/s41558-018-0156-3, 2018.

Zsoter, E., Harrigan, S., Barnard, C., Wetterhall, F., Ferrario, I., Mazzetti, C., Alfieri, L., Salamon, P., and Prudhomme, C.: River discharge and related forecasted data from the Global Flood Awareness System, https://doi.org/10.24381/cds.a4fdd6b9, 2021.

Climate and impact attribution of compound flooding induced by tropical cyclone Idai in Mozambique

Doris M. Vertegaal[1,2], Bart J. J. M. van den Hurk[1,2], Anaïs Couasnon[1,2], Natalia Aleksandrova[1], Tycho Bovenschen[1], Fernaldi Gradiyanto[1], Tim W. B. Leijnse[1], Henrique M. D. Goulart[1,2], and Sanne Muis[1,2]

[1]Deltares, Delft, the Netherlands
[2]Institute for Environmental Studies (IVM), Vrije Universiteit Amsterdam, Amsterdam, the Netherlands

Correspondence to: Doris M. Vertegaal (doris.vertegaal@deltares.nl)

Abstract. In this study, we investigate the effect of climate change on tropical cyclone (TC) induced compound flooding and impacts for TC Idai, making landfall in Mozambique in 2019. TCs are one of the most damaging extreme events and are challenging to attribute using conventional, probabilistic methods. We develop a storyline attribution framework including a state-of-the-art modelling chain that combines hydrological, coastal, flood and impact models to simulate the changes in flooding and its impact under factual and counterfactual scenarios, with ~~the~~ a plausible range of the climate trend removed from TC rainfall, maximum wind speed and sea level rise (SLR). For the case of TC Idai, we find that climate trends in ~~sea level rise~~SLR and ~~change in~~ wind-driven storm surge lead to the largest increase in flood damage of 6–27 %, ~~(27 %~~ compared to the counterfactual~~s~~), while causing ~~a less than 1 %~~ the smallest increase in flood volume and flood extent of 0.2–0.8 % and 0.1–0.6 % , respectively. Climate trends in rainfall lead to the largest increase in flood volume and flood extent of ~~(9 %~~5–19 % and ~~2 %~~1–4 %, respectively, ~~compared to the counterfactual)~~ but account for the ~~a~~ smallest~~r~~ increase in flood damage of ~~(4 %~~2–8 %~~)~~. Changes in all drivers combined lead to about the same increase in flood volume and flood extent as the rain-only scenario ~~(9 %~~ (5–19 % and ~~2 %~~1-5 %, respectively) but the largest increase in flood damage of ~~(31 %~~8-35 %~~)~~. A non-linear relationship between flood hazard and flood damage results in a stronger climate footprint on TC impacts than hazards. Assessing the combination of all climate change-affected flood drivers is crucial for obtaining a comprehensive view on the effect of climate change. The attribution framework presented in this paper is applicable for TC-prone regions across the globe and can be applied in data-~~poor~~scarce, ~~yet~~ often highly impacted and vulnerable areas which are currently underrepresented in attribution studies.

Short summary (500 characters incl. spaces):

This study highlights the need to disentangle climate change effects on flood drivers using storyline attribution. Whether ~~the~~ information is presented as change in one or multiple drivers, or as change in hazard or impact, determines the attribution statement. For ~~the~~ compound flooding from tropical cyclone Idai~~, that hit~~ in Mozambique ~~in~~ (2019), we attribute ~~up to~~ 1–19 %~~9 %~~ of the flood hazard and 8-35 %~~31 %~~ of the damage to climate change. The attribution framework can be applied to other events worldwide.

1 Introduction

Compound flooding from tropical cyclones (TCs), driven by the co-occurrence and interaction of multiple flood drivers such as fluvial, pluvial, and coastal flooding (Zscheischler et al., 2018), is one of the most damaging climate extreme events and is exacerbated by climate change (Frame et al., 2020; Smith and Katz, 2013). This raises the question to what extent climate change is already worsening the occurrence and severity of TCs. This question is being addressed by climate attribution, which is a rapidly emerging academic field, aiming to assess the contribution of climate change to extreme events (Hegerl et al., 2010; Intergovernmental Panel on Climate Change (IPCC), 2014).

There are various attribution methods; ranging from probabilistic using climate model ensembles to (semi-)conditional analogues and storylines (Faranda et al., 2022; van Garderen et al., 2021; van Oldenborgh et al., 2021; Stott et al., 2004). Most climate attribution assessments focussing on flood events use a meteorological driver as a proxy to represent the flood hazard, such as 3-day annual maximum precipitation (Davenport et al., 2021; Otto et al., 2022; Wang et al., 2023). However, flooding involves many non-linear processes that depend not only on the amount and intensity of local rainfall. The rainfall–runoff response is controlled by catchment size, antecedent conditions, land cover, elevation, and other factors (Jahanshahi and Booij, 2023; Massari et al., 2023). Without the modelling of the flood event and associated drivers, it remains uncertain what aspect of the flood event is attributable to climate change (Scussolini et al., 2024). Moreover, attribution studies that do propagate the effect of climate change to flood hazard often model a single flood driver (Mester et al., 2023; Strauss et al., 2021), ignoring the interaction of multiple flood drivers, such as pluvial, fluvial or coastal flooding, that often co-occur during TC events (Ward et al., 2018).

TCs are particularly challenging to attribute using conventional, probabilistic attribution methods (Philp et al., 2022). The reason is that probabilistic attribution relies on accurate model representation and good quality observations, which both have been shown to be challenging for TCs due to their relatively small spatial scale compared to climate model resolution, limited understanding of the underlying physics, their short observational records, and large internal variability (Camargo et al., 2023; Knutson et al., 2019; Philip et al., 2020)

Instead of attributing all causal factors simultaneously, storyline attribution examines the causality chain through conditional explanations (e.g. conditioning on atmospheric dynamics) (Shepherd, 2016; Sillmann et al., 2021). Studying the plausibility rather than probability allows for assessing contributions of separate drivers affected by climate change, which is necessary for describing complex extremes such as TCs (Lloyd and Shepherd, 2021; Perkins-Kirkpatrick et al., 2024). A storyline approach is applicable for compound flooding from TCs and has been applied for event attribution (Mester et al., 2023).

By modelling a comprehensive causality chain between hazards and impacts, storyline attribution also enables impact attribution, which builds on climate attribution. Impact attribution propagates the effect of climate change from hazard to impact and includes elements of exposure and vulnerability contributing to societal impact (IPCC, 2023a; Mengel et al., 2021; Noy et al., 2024). By integrating the role of exposure and vulnerability, impact attribution helps improving climate impact assessments (IPCC, 2023a). It can be used to inform policies and actions, and can help improve the description of the links between climate phenomena and impacts (Hope et al., 2022).

Highly vulnerable and low-income regions, such as those in East Africa, remain underrepresented in attribution studies (Callaghan et al., 2021; Coumou et al., 2024; Perkins-Kirkpatrick et al., 2024). Most TC attribution studies focus on data-rich regions, like the United States (Bourdin et al., 2025; Grimley et al., 2024; Smiley et al., 2022; Strauss et al., 2021). This attribution gap is at least partly related to the lack of observational data. However, recent advances in global flood modelling (Ward et al., 2015; Wing et al., 2024) have created new information sources, including globally applicable methods for tropical-cyclone induced flooding (Benito et al., 2025; Eilander et al., 2023a). These developments pave the way for addressing the attribution gap and building a globally applicable method for storyline attribution of TC-induced flooding.

The goal of this paper is to demonstrate ~~the applicability of~~ a~~n~~ storyline attribution framework that is applicable globally, including data-scarce regions, ~~utilizing global data and methods~~ by attributing the effect~~s~~ of climate change on flood hazard and impact from TC Idai. TC Idai was one of the most devastating cyclones to ever hit the southern hemisphere Click or tap here to enter text.(Warren, 2019). On 14 March 2019, it made landfall close to Beira City in Mozambique. A seven-day accumulated rainfall of more than 600 mm, strong winds above 150 km/h and storm surge heights estimated at 2.5 to 4.4 m impacted Mozambique, Malawi and Zimbabwe (Probst and Annunziato, 2019; WMO, 2019). In Mozambique alone, it is estimated that Idai caused over 3 billion USD in economic costs, destroyed over 200,000 homes, and caused 600 fatalities (Nhundu et al., 2021; UN Office for the Coordination of Humanitarian Affairs (OCHA), 2019)Click or tap here to enter text.. The storm ultimately affected approximately 1.85 million people across Mozambique. Also in the future, Mozambique is expected to be the highest impacted country by TCs in East Africa (Benito et al., 2024).

We use a storyline attribution framework with a state-of-the-art modelling chain that dynamically simulates ~~all~~TC flood drivers and damages in factual and counterfactual scenarios, where plausible climate change trends are removed. The differences between the factual and counterfactual scenarios for flood hazard and impact are compared to construct conditional climate and impact attribution assessments. Finally, we discuss the results and recommend further improvements for our attribution framework and directions for climate and impact attribution assessment of compound flooding from TCs.

2 Methodology

The attribution framework (Fig. 1) for TC Idai (simulated for 9 to 25 March 2019) consists of multiple physics-based models for the different flood drivers (Sect. 2.1) and a flood impact model (Sect. 2.2). These models are used to simulate a factual scenario (Sect. 2.3.1) and multiple counterfactual scenarios with ~~the~~ plausible climate change trends removed from rainfall, wind and sea level (Sect. 2.3.2). The factual and counterfactual scenarios are compared in terms of change in flood hazard (volume and extent) and flood impact (direct damage) to determine ~~the~~ conditional climate- and impact attribution statements (Sect. 2.3.3). Our entire workflow is built on open-source models and is accessible on GitHub (Vertegaal et al., 2025).

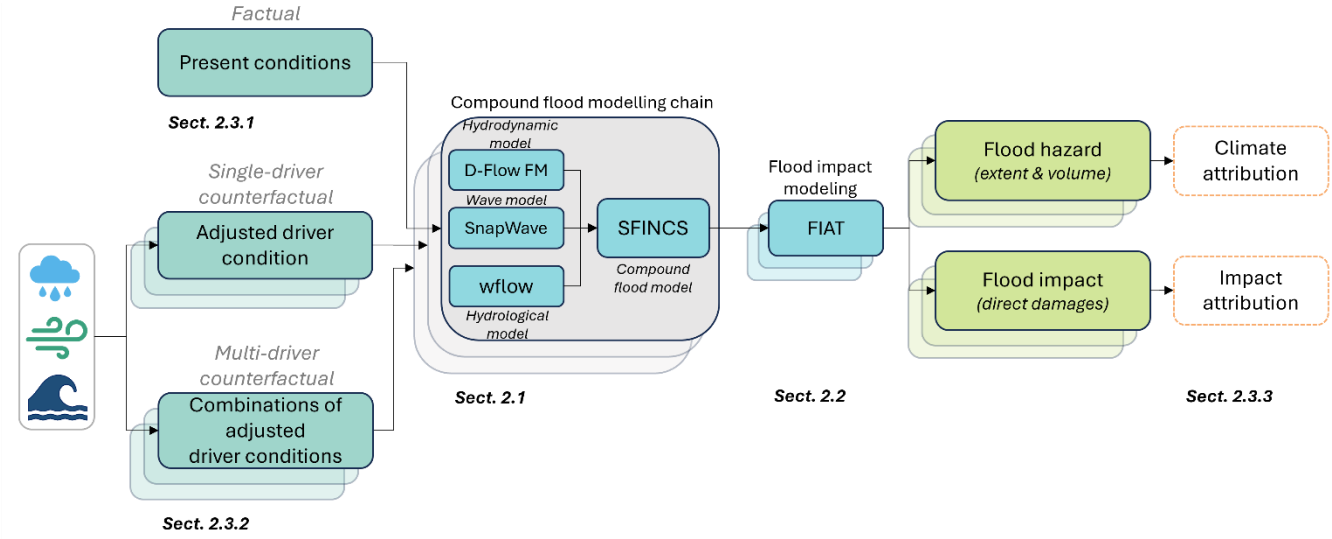

Figure 1: Attribution framework consisting of steps to assess climate- and impact attribution for compound flooding from TCs. The compound flood modelling (Sect. 2.1) and flood impact modelling (Sect. 2.2) is applied to a factual (Sect. 2.3.1) and multiple counterfactual scenarios (Sect. 2.3.2), and is used to simulate flood hazard (volume and extent) and flood impact (direct damages). The input data for the different counterfactuals is based on changes in wind, rainfall and sea level rise. Stacked boxes show multiple (combined) adjusted driver conditions, model simulations or analyses. Climate attribution refers to the changes due to climate change on the hazard, whereas impact attribution propagates the effect to impact (Sect. 2.3.3).

2.1 Compound flood modelling

The modelling chain we develop for simulating the TC-induced compound flooding (fluvial, pluvial and coastal) is based on the Super-Fast INundation of CoastS v2.2.0 (SFINCS) model (van Ormondt et al., 2025a), building on the globally-applicable method presented in Eilander et al. (2023a). Discharge boundary conditions are modelled with the hydrological model wflow v0.8.1 (van Verseveld et al., 2025). Coastal water level boundary conditions are modelled with hydrodynamic model D-Flow FM v2025.01 from the Delft3D Flexible Mesh Suite (Kernkamp et al., 2011) to compute tide and storm surge. Nearshore wave setup is modelled using the coupled wave model SnapWave (Roelvink et al., 2025), that is integrated into SFINCS (Leijnse et al., 2025). The forcing for the factual and counterfactual scenarios is described in Sect. 2.3. Details on model parameters can be found in the GitHub repository (Vertegaal et al., 2025). To setup the models and process the in- and output, we make use

of the python package Hydro Model Tools (HydroMT) with the model specific plugins (Deltares, 2025; Eilander et al., 2023b, 2024, 2025), except for the D-Flow FM model where we make use of dfm_tools v0.35 (Veenstra, 2025).

2.1.1 Compound flooding

Compound flooding is simulated using the SFINCS model, a reduced-complexity and computationally efficient model (Leijnse et al., 2021). SFINCS has been successfully used to simulate TC-induced flooding in various studies (Benito et al., 2024, 2025; Eilander et al., 2023a; Goulart et al., 2024; Grimley et al., 2024; Leijnse et al., 2025; Nederhoff et al., 2024). In this study, SFINCS is forced with river discharges (Sect. 2.1.2), coastal water levels (Sect. 2.1.3) and local rainfall (Sect. 2.3.1. & 2.3.2). The spatial resolution of the model is 100 m and the domain covers 8260 km^2 (pink domain in Fig. 2). To reduce computational costs, we make use of the subgrid functionality that applies corrections of the flow momentum and continuity equation for bed level and friction variability within a cell and downscale the results to the higher resolution digital elevation model of 25 m (van Ormondt et al., 2025b). For topobathy, we merge the global bathymetry dataset GEBCO (GEBCO Bathymetric Compilation Group 2024, 2024) with the FABDEM digital elevation model (Hawker et al., 2022). Land Manning roughness is based on the land use data from Buchhorn et al. (2020) and Curve Number infiltration data from Jaafar and Ahmad (2019). Flooded areas are identified by removing permanent water areas, using the Global Surface Water dataset (Pekel et al., 2016). A cell is considered as flooded if the water depth exceeds 0.05 meter.

2.1.2 River discharge

River discharge is simulated using the wflow model (van Verseveld et al., 2024), which is a distributed hydrological model. To account for the antecedent conditions, the wflow simulations consist of a warm-up run covering 365 days prior to the event, which provides the initial state for the event run. The wflow model has a spatial resolution of 0.0083° (~1 km). The model domain covers around 68,000 km^2, entailing the catchments ~~from~~ of the Pungwe and Buzi rivers (blue domain in Fig. 2). MERIT Hydro is used as hydrography data (Yamazaki et al., 2019), together with river geometries from Lin et al. (2019), and lakes and reservoirs from Lehner et al. (2022) and Linke et al. (2019). We use the same land cover dataset as for the SFINCS modelling (Buchhorn et al., 2020). Hourly output is generated at the river inflow points of the SFINCS model domain (Fig. S1) from which we remove the bankfull discharge (estimated as the 2-year return period; Wilkerson, 2008) to account for missing river bathymetry (Sect. S1.2).

2.1.3 Coastal water levels

Coastal water levels are composed of tides, storm surge, and wave setup (IPCC, 2023b). The tide and storm surge are simulated using a regional hydrodynamic D-Flow FM model. The spatially-varying grid has a resolution of ~2 km in the deep ocean and 450 m at the coast. The finest resolution aligns with that of the GEBCO bathymetry dataset (GEBCO Bathymetric Compilation Group 2024, 2024). The model stretches along the whole coast of Mozambique (white domain in Fig. 2), covering 1,117,000 km^2. We combine the tide and surge with dynamically modelled wave setup, calculated from ~~the~~ a coupled SFINCS-SnapWave

simulation. The 2D SFINCS-SnapWave model has a spatially-varying grid with a resolution of 400 m ~~off-shore~~offshore to 50 m at the coast, covering an area of 5400 km^2 (yellow domain in Fig. 2). The D-Flow FM output is generated around the 5-meter depth contour within the SFINCS domain at a 10-minute temporal resolution (Fig. S1). The ~~SnapWave~~ wave setup output is also generated at a 10-minutes temporal resolution ~~but for~~and saved at coastal transects. The wave setup is added to the D-Flow FM output at the same 5-meter depth contour (Sect. S1.4).

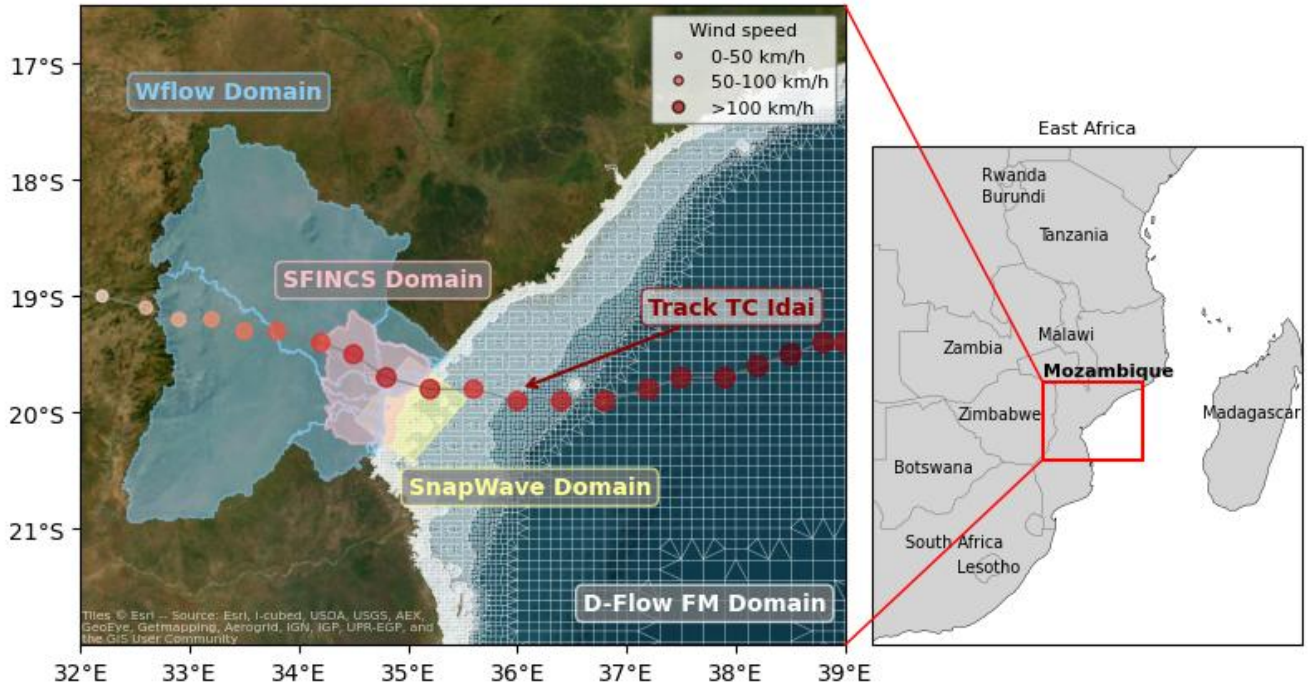

Figure 2: Overview of the different model domains to simulate the compound flooding (SFINCS domain in pink), river discharge (wflow domain in blue) and- coastal water levels (a part of the D-Flow FM domain in white; SnapWave domain in yellow). We also show the track of TC Idai from IBTrACS, where larger and more red coloured markers indicated higher wind speed.

2.2 Impact modelling

The fast impact assessment tool Delft-FIAT v0.3.2 (Wagenaar et al., 2017) is used to calculate direct flood damage by overlaying maximum flood depths with building footprints. The damage is calculated using the continental depth-damage curves for flooding and maximum potential damage per building type for Africa (Huizinga et al., 2017), similar to Eilander et al. (2023b) and Goulart et al. (2025). The currency of the maximum potential damage is in 2010 Euros, which is converted to 2019 US Dollars using a 2010 Euro-to-USD exchange rate of 1.327 and adjusted for inflation using a 2010-to-2019 USD rate of 1.172 (Archived Consumer Price Index Supplemental Files, 2025).

We use building footprints and type from OpenStreetMap (OSM; OpenStreetMap contributors, 2025) since it provides a recent and good coverage of the region, including rural areas and so-called informal settlements (Herfort et al., 2023; Wagenaar et

al., 2018a; Zhou et al., 2022). The output is generated as total and relative damage (damaged fraction of the total asset value) per building, which is aggregated to cells of 0.025° and to the total compound flood domain.

2.3 Scenarios for attribution

2.3.1 Factual scenario

For the factual scenario, we make use of various datasets as meteorological and hydrodynamic forcing. The main meteorological forcing used is the ERA5 reanalysis dataset (Hersbach et al., 2020), available at hourly and daily temporal resolution and 0.25° (~30 km) spatial resolution. ERA5 provides one of the best sources of globally complete and consistent historical climate data. The compound flood model SFINCS is forced with ERA5 hourly rainfall. The hydrological model wflow is forced with ERA5 daily (warm-up run) and hourly (event run) rainfall and temperature data. The wave model SnapWave is forced with ERA5 hourly wave conditions as the significant wave height, peak wave period and direction, at the offshore model boundary. Since ERA5 underestimates the intensity of TCs (Dullaart et al., 2020), we use best track data (IBTrACS; Gahtan et al., 2024; Knapp et al., 2010) in combination with the Holland parametric model (Holland, 2008; Holland et al., 2010) to define spatially-varying wind speed and pressure forcing fields ~~calculate TC wind and pressure forcing~~ for the D-Flow FM and SFINCS models. ~~The TC wind and pressure fields are merged with hourly background wind and pressure data from ERA5 by linearly fading the data at 0.75 fraction of the TC radius.~~ In addition to the meteorological forcing, the regional D-Flow FM model is forced with tidal boundary conditions derived from the Global Tides and Surge Model (GTSM) v4.1 (Wang et al., 2022).

2.3.2 Counterfactual scenarios

For the counterfactual scenario, we adjust the forcing of the factual scenario by removing ~~the~~ plausible long-term climate trends. Climate change is affecting TCs in multiple ways, with varying levels of scientific agreement. We focus on changes in rainfall, maximum wind speed and sea level rise (SLR), since there is a clear scientific consensus about the role of climate change on these drivers (Knutson et al., 2020), to create conditional attribution statements for these robust aspects of climate change. For the counterfactual scenarios, we adjust each of these drivers by removing ~~the~~low, medium, and high plausible climate change trends to capture a range of uncertainty in the attribution assessment. We assess the effect of changes for the three ~~individual~~ flood drivers individually, ~~as well as~~ the~~ir~~ combined effect of the coastal flood drivers, and the effect of all drivers combined (Table 1 ~~and S2~~). A complete description of the methodology that describes those changes is provided in Sect. S1.6. In line with storyline attribution, we constrain the TC track i~~I~~n all counterfactual scenarios, ~~we keep the same TC track as~~such that it is same to the one observed during the factual event (Feser and Shepherd, 2025; Mester et al., 2023; Strauss et al., 2021). We assume no change in non-flood drivers, such as exposure and vulnerability.

The plausible climate trend of TC rainfall, maximum wind speed and SLR is based on best available literature and global datasets. For the climate change effect on TC rainfall, some studies find that the trend is in line ~~to agree~~ with the ~~Similar to we adopt the~~ Clausius–Clapeyron relationship (7 %/°C of warming; Knutson et al., 2020), while other studies show ~~for the change in rainfall due to climate change.~~ trends higher than Clausius–Clapeyron (Guzman and Jiang, 2021; Liu et al., 2019a; Patricola and Wehner, 2018), referred to as super Clausius–Clapeyron (14 %/°C of warming), and lower due to enhanced cooling from slower TC translation speeds in a warmer climate (Tu et al., 2022). As Idai took place in a ~1.1 °C warmer world, we adopt ~~this results in~~ plausible reductions of rainfall of ~~a~~ 4 %, 8 % and 16 % ~~reduction of rainfall~~ for ~~the~~ low, medium and high counterfactual scenarios, respectively. For the climate change effect on TC maximum wind speeds~~llowing~~, we use plausible reductions of ~~a~~ 1%, 5% and 10 % ~~reduction in maximum wind speed~~ for the low, medium and high counterfactual scenarios, respectively. The~~is~~ low and medium scenarios are based on the likely range of 1–5 % per °C of warming for the Southern Indian ocean from climate models (Knutson et al., 2020), and the high scenario of a 10 % wind speed reduction ~~value~~ is based on regional trends from observed TCs (Mester et al., 2023)~~, and falls within the likely range of 2-11 % S~~. For the climate change effect on SLR, ~~W~~we use plausible reductions of 5, 10 and 15 cm for the low, medium and high counterfactual scenario, respectively. The medium scenario is based on the dataset by Treu et al. (2024), used to estimate the SLR between the time of the event and pre-industrial levels, and the low and high scenarios are based on uncertainty bounds from Strauss et al. (2021). ~~This results in a SLR of 14 cm for the counterfactual scenario, which is removed from the coastal boundary condition and initial water levels.~~

For all counterfactual scenarios, we assume that wave setup is the same as for the factual scenario. This simplification is made because our framework does not include a deep-water wave model, which would be required to generate a counterfactual scenario. For the case of TC Idai, we consider this a valid assumption given that waves are of limited importance for coastal flooding due to the shallow and gentle sloping coast that stimulates wave dissipation (van Dongeren et al., 2007).

Table 1: Overview of counterfactual ~~run~~scenarios where low, medium and high plausible ~~the~~ climate change trends are~~is~~ removed for rain, wind and sea level rise individually, for the coastal flood drivers (wind and SLR) combined, and for all drivers combined. ~~See Table S2 for all combinations of drivers.~~

Climate driver adjusted	Rainfall change	Wind change	SLR
Rain	-4 %, -8 %, -16 %	–	–
Wind	–	-1 %, -5 %, -10 %	–
SLR	–	–	-0.05 m, -0.10 m, -0.15 m
Wind & SLR	–	-1 %, -5 %, -10 %	-0.05 m, -0.10 m, -0.15 m

All	-4 %, -8 %, -16 %	-1 %, -5 %, -10 %	-0.05 m, -0.10 m, -0.15 m

2.3.3 Climate and impact attribution

The change in flood hazard and impact attributable to climate change is expressed following Eq. (1):

$$A(\%) = \frac{F-CF}{F} * 100\ \% \qquad (1)$$

Where A is the attributable change in %, F is the selected variable from the factual scenario and CF from the counterfactual scenario. The attributable change is conditional on the considered counterfactual flood drivers, and on the assumptions made in the model schematizations and input datasets.

For the climate attribution assessment, the flood volume and flood extent of the factual and counterfactual scenarios are compared, similar to Grimley et al. (2024) and Mester et al. (2023). The flood extent is calculated by summing the cell area of all cells considered as flooded. The flood volume is calculated by multiplying the cell area of every flooded cell with its flood depth, and then summing the volume of all flooded grid cells to obtain the total flood volume. For the impact attribution assessment, the total damage from Delft-FIAT is calculated by summing the flood damage of all flooded buildings.

3 Results

3.1 Description of the factual event

The compound flood modelling for the factual scenario indicates that TC Idai caused widespread flooding covering 3500 km^2, affecting mostly the floodplains of the Pungwe and Buzi rivers, and the city of Beira (Fig. 3, left panel). Most of the flooding is driven by the extensive fluvial flooding from the Buzi and the Pungwe rivers, with peak discharges of 27,000 m^3/s and 5,000 m^3/s, respectively, compared to 4,000 m^3/s and 2,000 m^3/s under normal conditions (Table S1). The extreme discharge in the Buzi river leads to flood depths of > 3.5 m along the river banks. Local rainfall, which amounted to a mean of 420 mm accumulated during the time of the event over the study area, partially flooded the more elevated area northeast of Beira. The flooding in the city of Beira, however, is largely driven by coastal flooding as a result of coastal water levels up to 4.3 m + m.s.l. (near Beira). Despite occurring close to neap tide, it exceeds water levels during normal high tide with about 0.6 meter, and coincides with the peak rainfall (Fig. S113). The wave setup accounted for 10 % of the maximum total water level.

In total, 842,000 buildings are estimated to be flooded with damages adding up to 3419 million USD. The flooding from TC Idai particularly impacts the city of Beira (Fig. 3, right panel). About 8179% of the total damage is situated in the Beira region. However, when considering relative damages (damaged fraction of the total asset value), the floodplains of the Pungwe and the Buzi, and the most southern estuary, are more severely damaged (Fig. 6).

3.2 Model validation

We compare the factual scenario against available observations and reported values in literature. Validating individual flood drivers is challenging due to lack of observations for rainfall and water levels during the event. For discharge, we ~~can only~~ compare against ~~observations~~ modelled Global Flood Awareness System (GloFAS) discharge data (Grimaldi et al., 2023; Joint Research Center and Copernicus Emergency Management Service, 2020; Zsoter et al., 2021), as recent observations for the region ~~for the period 1954-1984~~ are lacking. This comparison shows that the simulated discharge for the two major rivers in the region (the Pungwe and Buzi) is uncertain and differs significantly between GloFAS data versions (v4.0 and v3.1; Fig. S5 and S6). For the period of TC Idai, the summed daily discharges simulated by GloFAS v4.0 (v3.1) differ -19 % (-10 %) and -51 % (29 %) from the summed wflow discharges resampled to a daily time step for the Buzi and the Pungwe, respectively (Table S2). The overestimated discharge could be explained by the higher spatial and temporal resolution of our wflow model compared to GloFAS data. ~~For the event~~During the flood event, the simulated discharge is in the same order of magnitude as calculated by Eilander et al. (2023a). The agreement between our results and GloFAS for the Buzi river is ~~captures the seasonal and long-term dynamics~~ reasonable (KGE for comparison with GloFAS v4.0 (v3.1) is 0.42 (0.61) for the Buzi river; Fig S6), although also here extremes are generally overestimated. For the Pungwe river, GloFAS discharge data varies significantly between versions, and this variability is also reflected in the comparison with our results (KGE for comparison with GloFAS v4.0 (v3.1) is 0.09 (0.75) for the Pungwe river; Fig S6).~~to well (KGE 0.28 and 0.87 for the Pungwe and Buzi rivers, respectively; Fig S5), although extremes are generally overestimated (Fig. S6)~~ Recent local observations are required to better determine the performance of the wflow model. ~~The overestimation of extreme discharge may be related to the limited calibration of the wflow model and reported overestimation of ERA5 rainfall for tropical cyclone Idai~~ ~~For TC Idai, the simulated discharge is in the same order of magnitude as calculated by.~~ No tide gauge stations are available but our simulated coastal water levels are consistent with Probst & Annunziato (2019) and Eilander et al. (2023a). ~~However~~Regarding the effect of coastal waves, Eilander et al. (2023a) estimate a wave setup of up to 24 % of the total water level, calculated using a simplified empirical approach that is known to overestimate wave setup (Leijnse et al., 2025), compared to our estimate of 10 % wave setup resulting from dynamic wave modelling.

The maximum flood extent is validated against two satellite products, which show reasonable agreement (hit rate >76 %), but also considerable uncertainty in flood detection (Sect. S1.5). Our maximum flood extent is consistent with Mester et al. (2023) and Eilander et al. (2023a), although compared to the latter our results indicate more extensive coastal flooding in the Beira region. This can be explained by the ~~modelling setup with~~ higher-resolution regional coastal models of our modelling setup, which results in higher coastal boundary conditions (Benito et al., 2025).

With regards to the flood damage, the Government of Mozambique (2019) estimated the total housing damages at 410 million USD for the Sofala, Manica, Tete and Zambezia provinces in Mozambique. Our estimated damage of 3491 million USD only includes the most heavily impacted Sofala province and is thus in agreement with reported damages.

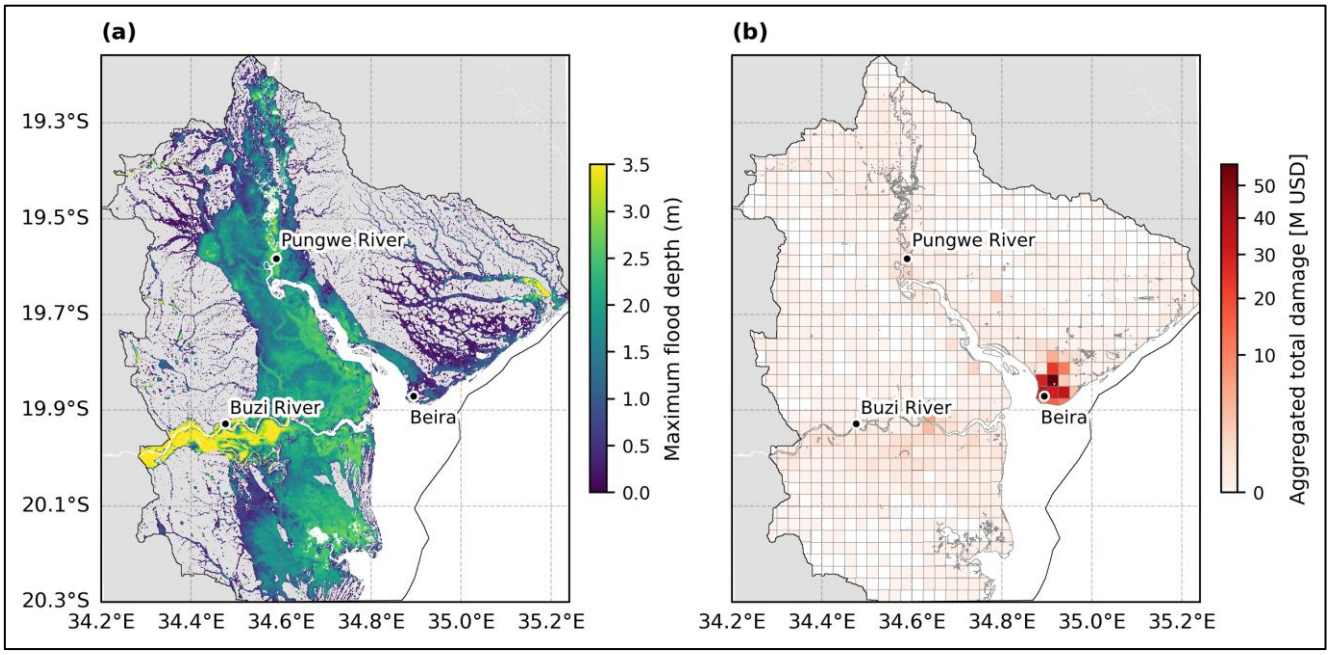

Figure 3: Simulated maximum flood depths in meters (a), and aggregated (0.025° grid cells) total damage in million (M) USD (b) due to flooding for the factual scenario of TC Idai. The compound flood model (SFINCS) domain is shown in black.

3.3 Climate and impact attribution

3.3.1 Climate attribution

The increase in flood volume ~~and flood extent~~ that can be attributed to climate change when comparing against the medium counterfactual scenario (low–high counterfactual scenario) for all flood drivers is ~~9~~10 % (5–19 %)~~and 2 %, respectively~~, corresponding to an increase of ~~>~~ 500 M m^3 (250–1000 M m^3; Table 2). The increase in flood extent that can be attributed to climate change is 2 % (1–5 %), corresponding to an increase of~~and >~~ 8~~5~~0 km^2 (40–170 km^2 ~~Table 2~~). The difference between change in flood volume and flood extent can be related to the region's topography, where higher elevated areas inhibit the extension of the flooded area. The climate change-increased~~duced~~ rainfall leads to the largest increase in flooding (Fig. 4), with an increase of 9 % (5–19 %) in flood volume and 2 % (1–4 %) in flood extent ~~when comparing against the counterfactual~~. The ~~C~~climate change-increased~~duced~~ wind speed ~~changes~~ and SLR lead to a less than 1 % increase in flood volume (0.2–0.8 %) and in flood extent (0.1–0.6 %). Still, changes in wind and SLR intensify the coastal flooding by elevating the coastal water levels, which primarily affects the Beira region, covering 23~~7~~0 km^2 for the medium counterfactual scenario. This is in contrast to the climate change-increased~~duced~~ rainfall, which intensifies river flooding ~~in a widespread area~~across most of the floodplain, covering 3300~~420~~ km^2. The intensified river flooding affects the floodplains of the Buzi river the most, with an

increase in flood depth of > 0.45 m. The increase in ~~intensified~~ coastal flooding ~~also reaches up to~~results in flood depths of > 0.25 m. Our results show that the counterfactual adjustment of individual flood drivers exhibits minimal ~~negligible~~ compounding effects in flood volume and flood extent due to the relatively small effect of climate change-in~~duced~~creased wind and SLR.

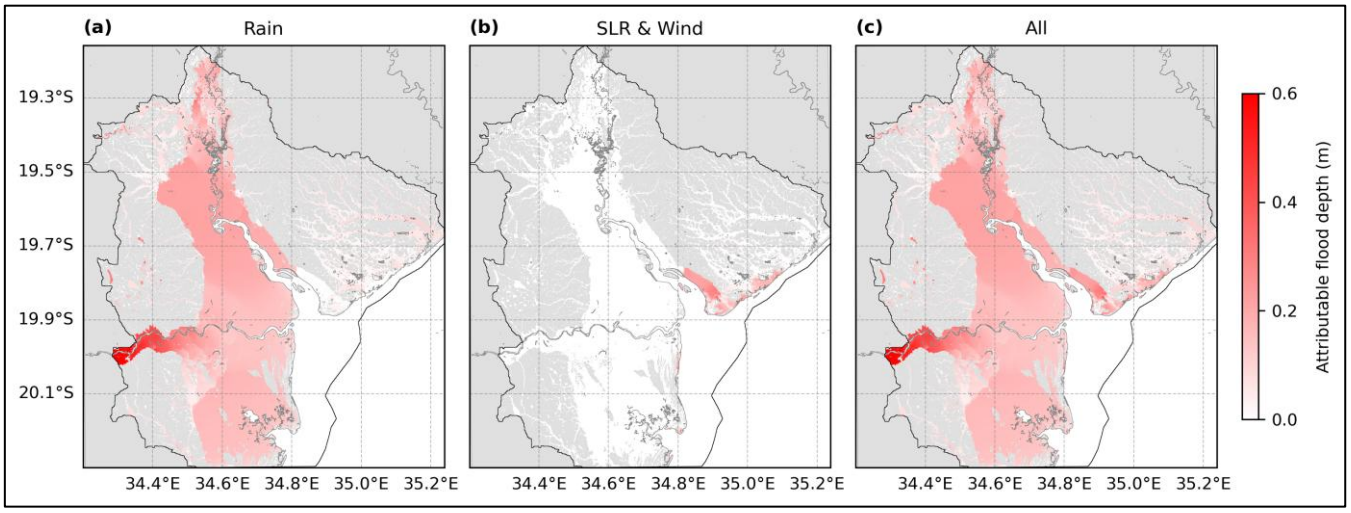

Figure 4: The flood depth attributable to climate change (~~factual~~ counterfactual medium scenario subtracted from factual scenario) ~~from~~ for different flood drivers; rain (a), wind and SLR (b), and all drivers combined (c). The compound flood model (SFINCS) domain is shown in black and the outline of removed permanent water bodies is shown as grey lines.

Table 2: The absolute and relative change in flood volume, flood extent and flood damage for factual (absolute values only) and medium counterfactual scenarios (low–high counterfactual scenarios in parentheses). The relative change in flooding and impact that is attributable to climate change is calculated by applying Eq. 1. Decimals are presented for values below 1.

	Flood volume		Flood extent		Flood damage	
Scenario	Absolute value [M m³]	Relative change	Absolute value [km²]	Relative change	Absolute value [M USD]	Relative change
Factual	5171	-	3525	-	341	-
Counterfactual						
Rain	4695 (4208–4934)	9 % (5–19 %)	3458 (3382–3492)	2 % (1–4 %)	328 (315–335)	4 % (2–8 %)
Wind	5156 (5142–5168)	0.3 % (0.1–0.6 %)	3515 (3506–3523)	0.3 % (0.1–0.5 %)	308 (275–335)	10 % (2–19 %)
SLR	5161 (5157–5166)	0.2 % (0.1–0.3 %)	3523 (3522–3524)	0.05 % (0.03–0.08 %)	317 (305–329)	7 % (4–11 %)
SLR & Wind	5147 (5131–5163)	0.5 % (0.2–0.8 %)	3513 (3503–3522)	0.3 % (0.1–0.6 %)	285 (251–322)	17 % (6–27 %)

All	4671 (4166–4925)	10 % (5–19 %)	3446 (3358–3489)	2 % (1–5 %)	270 (221–315)	21 % (8–35 %)

3.3.2 Impact attribution

Comparing the factual and medium counterfactual scenario (low–high counterfactual scenario) for all flood drivers ~~counterfactual scenarios~~ shows that ~~3~~21 % (8–35 %) ~~(109 M USD)~~ of the flood damage, corresponding to 70 M USD (30–120 M USD), can be attributed to climate change, resulting in 7,000 (3,000–13,000) more buildings damaged. Climate change-~~induced~~ increased ~~changes in~~ wind speed and SLR lead to the largest increase in damage of ~~2~~17 % (6–27 %), whereas climate change-~~induced~~ increased rainfall leads to an increase of 4 % (2–8 %; Table 2). Even though changes in SLR and wind are negligible in terms of changes in flood volume and flood extent, these drivers have a larger impact on flood damage than changes in rainfall (Fig. 5). The relative change in impact is larger than the relative change in flooding, except for the rain-only scenario. Increased wind and SLR intensify coastal flooding, which is the main driver of damage in Beira, where total damages are concentrated due to the high density of buildings (Fig. 3, Fig. S1~~2~~4). When adjusting wind and SLR individually, wind emerges as a more significant driver of flood damage than SLR (Table 2). Since wind and SLR both elevate coastal water levels, impacting the same coastal region, their individual impacts on damage are not additive; increases in flood depth translate non-linearly to damage due to the applied damage curves. In this case, there is a limited (< 1 %) compounding effect of attributing all flood drivers combined, as the minimal interaction of the intensified flood drivers translates non-linearly to higher flood damages ~~the increased rainfall driven flooding (pluvial and fluvial) impacts buildings in different areas than the increased coastal flooding~~. Changes in all drivers combined lead~~s~~ to the largest ~~changes~~ increase in flood damage. Our results show that propagating the effects of climate change from hazard to impact influences the attribution assessment. The location of climate change-increased~~duced~~ flooding is crucial in determining impacts, highlighting the role of exposure and vulnerability.

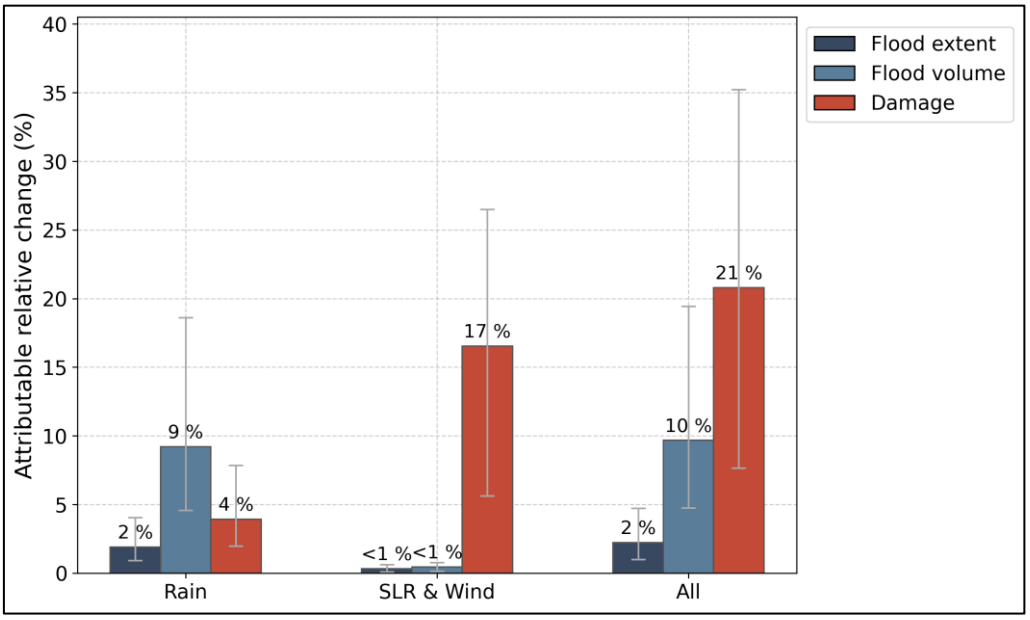

Figure 5: The relative change in flood extent (dark blue), flood volume (light blue), and flood damage (red) due to climate change ~~between the factual and counterfactual scenarios~~, driven by different flood drivers where "All" includes SLR, wind and rain. The bars present the medium counterfactual scenario, and the error bars present the low and high counterfactual scenarios. The relative change in flooding and impact is calculated by ~~subtracting the counterfactual from the factual value (~~Eq. 1~~:~~ (Sect. 2.5~~3.3~~).

Relative damage, i.e. damaged fraction of the total asset value, provides another perspective on the impacts of climate change. While Beira appears as a hotspot for total damage attributable to climate change (Fig. S1~~2~~4); when considering relative damages, areas across the floodplains become more prominent (Fig. 6). When focussing on relative damage, increased rainfall is the most important driver of additional damage compared to wind and SLR. Only looking at aggregated urban areas that are usually the hotspot of capital, and therefore more likely of total damage, provides a biased view on the impacts of climate change. Within urban areas, the compounding impacts of TC Idai have been found to increase inequality and highlight the need for local studies considering how the impact and response is distributed (Williamson et al., 2023).

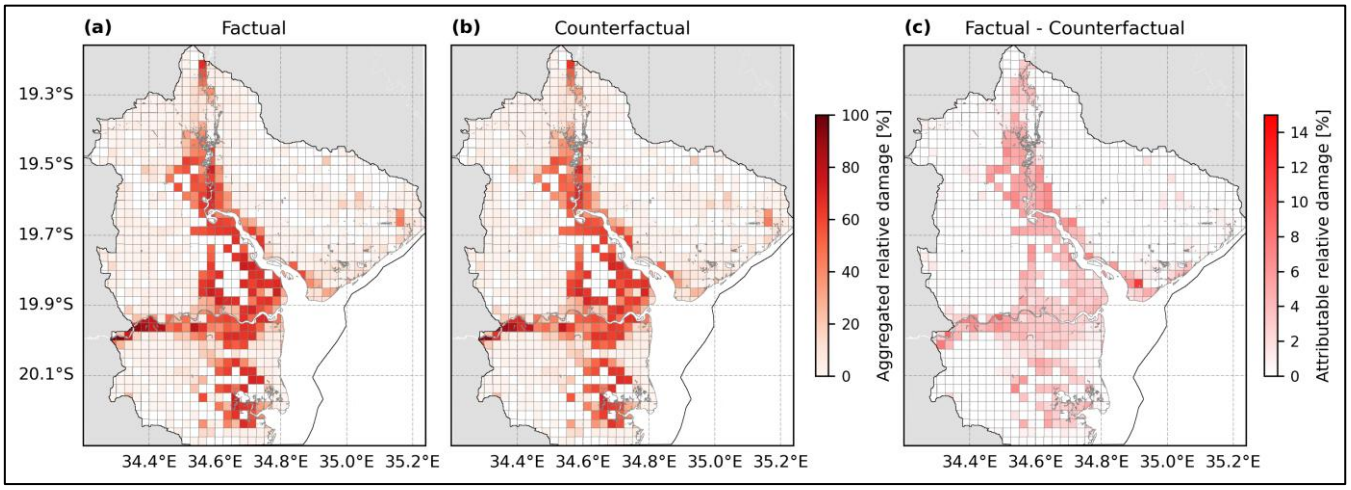

Figure 6: The aggregated (0.025° grid cells) relative damage (damaged fraction of total asset value) for the factual (a) and medium counterfactual (b) scenarios with all drivers combined, and the absolute difference (factual – medium counterfactual scenario) attributable to climate change (c). The compound flood model (SFINCS) domain is shown in black.

4 Discussion

In this paper, we present a storyline attribution framework with a state-of-the-art modelling chain for TC compound flooding. To our knowledge, this is the first framework resolving all TC flood drivers (local rainfall, discharge, tides, storm surge and wave setup) using physics-based models and attributing them to climate change. This framework ~~accurately reproduces~~provides an ~~credible~~ estimate of compound flooding from TC Idai using global data~~,~~ in line with observations and reported values in literature, ~~which~~ and is applied for both climate and impact attribution assessments. In the case of compound flooding from TC Idai, increased amounts of rainfall led to the largest increase in ~~the~~ flood ~~hazard~~volume and flood extent, which can be explained by the flooding being largely driven by the high river discharges (Eilander et al., 2023a). On the other hand, increased coastal flooding due to intensified wind speeds and SLR resulted in the largest increase in total damage, ~~specifically~~concentrated in the coastal areas. The coastal areas are most densely inhabited,~~—~~ especially the coastal city of Beira,~~—~~ which explains the large effect of intensified wind speeds and SLR on impacts~~,~~ despite the~~ir~~ relatively small increase in flood depth~~effect on the flooding itself~~, emphasizing the importance ~~role~~ of accounting for exposure and vulnerability. ~~In terms of~~When reporting changes in relative damage, however, all flood drivers contribute significantly~~;~~ because buildings outside of Beira are also substantially damaged but have a lower total asset value.

Our results show that propagating the effects of climate change from hazard to impact ~~for multiple flood drivers~~ influences the attribution assessment. Firstly, focussing on a single flood driver may misrepresent the total effect of climate change on the event~~not give a good representation of the total impact of climate change on~~for the severity of the flood event~~, depending on the considered impact metric~~. ~~speeds~~ In addition, ~~T~~treating compound drivers independently may provide incomplete and incorrect attribution statements, underestimating the impact of climate change (Perkins-Kirkpatrick et al., 2024). For

compound flooding, it is important to consider the dynamic interactions of the multiple flood drivers (Green et al., 2025). ~~Treating compound drivers independently may provide incomplete and incorrect attribution statements, underestimating the impact of climate change .~~ The relative contribution of compound processes in TC-induced flooding is found to become~~s~~ even more important in future climates (Grimley et al., 2024). Secondly, climate attribution results in different statements about the effect of climate change than impact attribution, which is explained by the non-linear relationship between flood hazard and damage~~s~~ (Huizinga et al., 2017; Pistrika et al., 2014). As a result, we highlight the importance of explicitly specifying the metrics used when making attribution statements. We also demonstrate the value ~~This highlights the relevance~~ of including both climate and impact attribution assessments for describing the impacts of climate change. Together, they provide comprehensive information to inform risk management and adaptation strategies (Carlson et al., 2024; Clarke et al., 2023; Coumou et al., 2024).

Our attribution framework is applicable to TC events anywhere on E~~e~~arth and could easily be extended to other type of flood events. Since the framework solely requires global datasets and open-source software, it has great potential to address the attribution gap and analyse climate impact on flood events in underrepresented, data-poor, yet severely impacted and highly vulnerable regions. This study highlights once again the value and need for observations to improve and validate model results, such as in situ rain and tide gauges (Mekonnen et al., 2023). For areas without sufficient recent and local observations, providing robust attribution statements remains challenging due to limited opportunities for model validation, especially for high-impact low-likelihood events. ~~For areas with limited observational data~~In such contexts, storyline attribution assessments that consider plausible what-if scenarios can still provide highly informative insights (Sillmann et al., 2021)~~lack of in situ sstatements should go hand in hand with~~ . Multi-method attribution assessments could provide more confidence in the attribution assessment (Barriopedro et al., 2025; Thompson et al., 2025). Echoing e.g. Eilander et al. (2023a) and Samadi et al. (2025), establishing high-quality observations should remain a priority for more accurate assessments in data-scarce regions and for providing more localized information on climate change impacts.

Our framework is built on simplified and uniform assumptions on the effect of climate change on TC rainfall and wind speed. The counterfactual rainfall is homogenously scaled according to plausible climate trends ~~the conservative Clausius–Clapeyron relationship and~~ but neglects any TC specific estimates and changes in spatio-temporal patterns (Deng et al., 2025; Kim et al., 2022; Liu et al., 2019b). The same applies to the counterfactual scenarios of maximum wind speed, where simplified scaling of the maximum wind speed with reductions of 1–10 % ~~also~~ neglects the complex dynamics of TCs ~~and may overestimate the climate change increased coastal flooding~~ (Knutson et al., 2020). The development of the counterfactual scenarios in this storyline attribution framework could be improved by further refining climate change trends in flood drivers, for example based on observed regional changes rather than global estimates. Moreover, we could evaluate the effect of climate change on additional flood drivers possibly increasing coastal flooding, such as change in TC size (Yamada et al., 2017), translation speed (Knutson et al., 2020; Seneviratne et al., 2021) and significant wave height (Thompson et al., 2021), while still conditioning

on the TC track~~which could also increase coastal flooding~~. As demonstrated by Dullaart et al. (2024) and Grimley et al. (2024), it is also possible to develop storyline approaches where the counterfactual is informed by TC statistics from pseudo global warming simulations. A promising but still developing method to construct comprehensive TC counterfactuals is the use of climate storyline simulations (Athanase et al., 2024b; Feser and Shepherd, 2025; Sánchez-Benítez et al., 2022). These simulations are nudged towards observed dynamics and can compare counterfactual realisations of near-real-time events. This method has been proven successful for mid- and high-latitude storms but is thus far limited for TCs due to the stronger role of convective processes (Athanase et al., 2024a; Goulart et al., 2024; Schubert-Frisius et al., 2017).

Our impact attribution is based on the calculation of damages to buildings using a simple but commonly used relationship between flood depth and damage, which is a major source of uncertainty. This method could be improved using multivariate depth damage curves that account for local characteristics of building types (Strauss et al., 2021) and other variables than flood depth influencing flood hazard such as duration, velocity, salinity or contamination (Adeke and Mugume, 2025; Delgado et al., 2016; Thieken et al., 2005). Impact attribution could be improved by including additional metrics of direct impacts, such as the displaced population (Mester et al., 2023); multi-hazard impacts, such as combined wind and flood damage (Wagenaar et al., 2018b); and indirect impacts, such as loss of livelihood options (Nhundu et al., 2021). Additionally, including dynamic changes in exposure and vulnerability, next to changes in the hazard, can improve our assessment of flood impact drivers. For example, the rising exposure and vulnerability in sub-Saharan Africa are found to increase damages from river flooding (Sauer et al., 2021). Such changes in exposure and vulnerability can be induced by climate change, but also by non-climatic drivers (Hope et al., 2022) such as land use change, urbanisation, or population growth (Paprotny et al., 2025; Rentschler et al., 2023; Rogers et al., 2025; Rogger et al., 2017). Lastly, total and relative damage provide different but incomplete perspectives on climate change impacts and we therefore recommend impact attribution to provide population differentiated assessments reflecting socio-spatial characteristics, such as age, gender and poverty (Puig et al., 2025). Differentiated assessments require a thorough understanding of the impacted population; studying population characteristics and their intersectionality as well as their response to different impact metrics. Such assessment can inform equitable and just adaptation measures to improve local resilience at the risks of climate change (Kind et al., 2017).

5 Conclusion

Our study advances climate and impact attribution of compound flooding from TCs by providing a framework that physically resolves multiple flood drivers (rainfall, river discharge, tide, surge and waves) using a state-of-the-art modelling chain. Our framework was applied to TC Idai, that devastated Mozambique in March 2019, and was shown to accurately reproduce compound flooding. We demonstrate that considering multiple flood drivers enables a comprehensive view on the impacts of climate change. For the case of TC Idai, we find that propagating the effects of climate change from hazard to impact affects the outcome of an attribution assessment, due to the non-linear relationship between flood hazard and damages. The conditional attribution ~~analysis~~ assessment shows that ~~9 %~~5–19 % of the flood volume, ~~2 %~~ 1–5 % of the flood extent, and ~~31 %~~8–35 %

of the flood damages can be attributed to climate change. The amplification from change in hazard to impact can be linked to the majority of the damages occurring near the city of Beira, where coastal flooding was increased by the intensification of wind speeds and by sea level rise. Our framework is applicable for TC-prone regions across the globe, including data-~~poor~~ scarce but highly impacted and vulnerable regions, potentially contributing to addressing the attribution gap.

Our S~~s~~toryline attribution framework improves the description of how plausible climate trends in TC ~~climate change exacerbated~~ flood drivers translate from hazard to impacts, which is relevant for anticipating further climate risks. Including the local context through the propagation to impact for specific extreme events has the potential to improve awareness by aligning closely with the lived experience of society. Our findings are sensitive to the applied impact metrics and simplified assumptions of the climate change effect on TC-induced flood drivers. Uncertainties in factual and counterfactual forcing persist in regions with a lack of long-term good quality observations, and stresses the ongoing priority for more observations and thorough uncertainty analyses. In the light of ongoing and intensifying climate change, we recommend research efforts to focus on extending climate to impact attribution for other highly impacted and vulnerable areas, and different type of compound events.

Code availability

The scripts and data used to set up the experiments in this study are available from Zenodo at https://doi.org/10.5281/zenodo.17107289 (Vertegaal et al., 2025).

Author contribution

DV, BvdH, AC, and SM conceived the idea for this study, jointly designed the experiments, and interpreted initial results. DV executed the experiments and set up the SFINCS, wflow and D-Flow FM models with help from NA, TB, and AC; NA helped with testing and setting up the D-Flow FM model; TB and AC helped with testing and setting up the wflow and SFINCS models; DV set up the Delft-FIAT model. FG and TL provided the necessary SnapWave simulations. DV conducted the computational processing and analysis of results with input from HMG and AC. DV wrote the manuscript with input from BvdH, AC, HMG, and SM.

Competing interests

The authors declare that they have no conflict of interest.

Acknowledgements

We would like to thank Albrecht Weerts for support with the wflow simulations, Jelmer Veenstra for support on the counterfactual SLR integration in the D-Flow FM model, and Brendan Dalmijn and Sarah Rautenbach for support with Delft-FIAT and HydroMT-FIAT. We also thank Dirk Eilander and Nadia Bloemendaal for their input during the initial discussions

of this work. We thank OpenAI's ChatGPT and GitHub Copilot for assistance with coding, and for suggestions on phrasing and text clarity during the preparation of this work.

Funding

This research was done as part of the "Compound extremes attribution of climate change: Towards an operational service" (COMPASS) project, which is funded by the European Union's HORIZON Research and Innovation Actions Programme under Grant Agreement No. 101135481.

References

Adeke, D. P. and Mugume, S. N.: A methodology for development of flood-depth-velocity damage functions for improved estimation of pluvial flood risk in cities, J. Hydrol. (Amst)., 653, 132736, https://doi.org/10.1016/J.JHYDROL.2025.132736, 2025.

Athanase, M., Sánchez-Benítez, A., Monfort, E., Jung, T., and Goessling, H. F.: How climate change intensified storm Boris' extreme rainfall, revealed by near-real-time storylines, Commun. Earth Environ., 5, 676, https://doi.org/10.1038/s43247-024-01847-0, 2024a.

Athanase, M., Sánchez-Benítez, A., Goessling, H. F., Pithan, F., and Jung, T.: Projected amplification of summer marine heatwaves in a warming Northeast Pacific Ocean, Commun. Earth Environ., 5, 53, https://doi.org/10.1038/s43247-024-01212-1, 2024b.

Barriopedro, D., Jiménez-Esteve, B., Collazo, S., Garrido-Perez, J. M., Johnson, J. E., and García-Herrera, R.: A Multimethod Attribution Analysis of Spain's 2024 Extreme Precipitation Event, Bull. Am. Meteorol. Soc., 106, E2440–E2460, https://doi.org/10.1175/BAMS-D-25-0049.1, 2025.

Benito, I., Aerts, J. C. J. H., Eilander, D., Ward, P. J., and Muis, S.: Stochastic coastal flood risk modelling for the east coast of Africa, npj Natural Hazards, 1, 10, https://doi.org/10.1038/s44304-024-00010-1, 2024.

Benito, I., Aerts, J. C. J. H., Ward, P. J., Eilander, D., and Muis, S.: A multiscale modelling framework of coastal flooding events for global to local flood hazard assessments, Natural Hazards and Earth System Sciences, 25, 2287–2315, https://doi.org/10.5194/NHESS-25-2287-2025, 2025.

Bourdin, S., Camargo, S. J., Lee, C. Y., Lin, J., Vrac, M., Vaittinada Ayar, P., and Faranda, D.: Improving analogues-based detection & attribution approaches for hurricanes, Environmental Research Letters, 20, 024042, https://doi.org/10.1088/1748-9326/ADAA8D, 2025.

Buchhorn, M., Smets, B., Bertels, L., De Roo, B., Lesiv, M., Tsendbazar, N. E., Linlin, L., and Tarko, A.: Copernicus Global Land Service: Land Cover 100m: Version 3 Globe 2015-2019: Product User Manual (Dataset v3.0, doc issue 3.3, https://doi.org/10.5281/zenodo.3938963, September 2020.

Callaghan, M., Schleussner, C. F., Nath, S., Lejeune, Q., Knutson, T. R., Reichstein, M., Hansen, G., Theokritoff, E., Andrijevic, M., Brecha, R. J., Hegarty, M., Jones, C., Lee, K., Lucas, A., van Maanen, N., Menke, I., Pfleiderer, P., Yesil, B.,

and Minx, J. C.: Machine-learning-based evidence and attribution mapping of 100,000 climate impact studies, Nat. Clim. Chang., 11, 966–972, https://doi.org/10.1038/s41558-021-01168-6, 2021.

Camargo, S. J., Murakami, H., Bloemendaal, N., Chand, S. S., Deshpande, M. S., Dominguez-Sarmiento, C., González-Alemán, J. J., Knutson, T. R., Lin, I. I., Moon, I. J., Patricola, C. M., Reed, K. A., Roberts, M. J., Scoccimarro, E., Tam, C. Y. (Francis), Wallace, E. J., Wu, L., Yamada, Y., Zhang, W., and Zhao, H.: An update on the influence of natural climate variability and anthropogenic climate change on tropical cyclones, Tropical Cyclone Research and Review, 12, 216–239, https://doi.org/10.1016/J.TCRR.2023.10.001, 2023.

Carlson, C. J., Mitchell, D., Carleton, T., Chersich, M., Gibb, R., Lavelle, T., Lukas-Sithole, M., North, M., Lippi, C., New, M., Ryan, S. J., Shumba, S., and Trisos, C.: Designing and describing climate change impact attribution studies: a guide to common approaches, https://doi.org/10.31223/X5CD7M, 2024.

Clarke, B., Otto, F., and Jones, R.: When don't we need a new extreme event attribution study?, Clim. Change, 176, 60, https://doi.org/10.1007/S10584-023-03521-4, 2023.

Coumou, D., Arias, P. A., Bastos, A., Gonzales, C. K. G., Hegerl, G. C., Hope, P., Jack, C., Otto, F., Saeed, F., Serdeczny, O., Shepherd, T. G., and Vautard, R.: How can event attribution science underpin financial decisions on Loss and Damage?, PNAS Nexus, 3, 277, https://doi.org/10.1093/PNASNEXUS/PGAE277, 2024.

Davenport, F. V, Burke, M., and Diffenbaugh, N. S.: Contribution of historical precipitation change to US flood damages, Proceedings of the National Academy of Sciences, 118, e2017524118, https://doi.org/10.1073/pnas.2017524118, 2021.

Delgado, J. M. P. Q., Guimarães, A. S., De Freitas, V. P., Antepara, I., Kočí, V., and Černý, R.: Salt Damage and Rising Damp Treatment in Building Structures, Advances in Materials Science and Engineering, 2016, 1280894, https://doi.org/10.1155/2016/1280894, 2016.

Deltares: HydroMT-FIAT: Automated and reproducible Delft-FIAT model building, https://github.com/Deltares/hydromt_fiat/releases/tag/v0.5.7, 3 September 2025.

Deng, E., Xiang, Q., Chan, J. C. L., Dong, Y., Tu, S., Chan, P. W., and Ni, Y. Q.: Increasing temporal stability of global tropical cyclone precipitation, NPJ Clim. Atmos. Sci., 8, 11, https://doi.org/10.1038/s41612-025-00896-2, 2025.

van Dongeren, A., Battjes, J., Janssen, T., van Noorloos, J., Steenhauer, K., Steenbergen, G., and Reniers, A.: Shoaling and shoreline dissipation of low-frequency waves, J. Geophys. Res. Oceans, 112, 2011, https://doi.org/10.1029/2006JC003701, 2007.

Dullaart, J. C. M., Muis, S., Bloemendaal, N., and Aerts, J. C. J. H.: Advancing global storm surge modelling using the new ERA5 climate reanalysis, Clim. Dyn., 54, 1007–1021, https://doi.org/10.1007/S00382-019-05044-0, 2020.

Dullaart, J. C. M., de Vries, H., Bloemendaal, N., Aerts, J. C. J. H., and Muis, S.: Improving our understanding of future tropical cyclone intensities in the Caribbean using a high-resolution regional climate model, Sci. Rep., 14, 6108, https://doi.org/10.1038/s41598-023-49685-y, 2024.

Eilander, D., Couasnon, A., Leijnse, T., Ikeuchi, H., Yamazaki, D., Muis, S., Dullaart, J., Haag, A., Winsemius, H. C., and Ward, P. J.: A globally applicable framework for compound flood hazard modeling, Natural Hazards and Earth System Sciences, 23, 823–846, https://doi.org/10.5194/nhess-23-823-2023, 2023a.

Eilander, D., Boisgontier, H., Bouaziz, L. J. e., Buitink, J., Couasnon, A., Dalmijn, B., Hegnauer, M., Jong, T. de, Loos, S., Marth, I., and Verseveld, W. van: HydroMT: Automated and reproducible model building and analysis, J. Open Source Softw., 8, 4897, https://doi.org/10.21105/JOSS.04897, 2023b.

Eilander, D., Couasnon, A., Sperna Weiland, F. C., Ligtvoet, W., Bouwman, A., Winsemius, H. C., and Ward, P. J.: Modeling compound flood risk and risk reduction using a globally applicable framework: a pilot in the Sofala province of Mozambique, Hazards Earth Syst. Sci, 23, 2251–2272, https://doi.org/10.5194/nhess-23-2251-2023, 2023c.

Eilander, D., de Goede, R., Leijnse, T., van Ormondt, M., Nederhoff, K., and Winsemius, H. C.: HydroMT-SFINCS, https://doi.org/10.5281/ZENODO.13693006, 2024.

Eilander, D., Boisgontier, H., van Verseveld, W., Bouaziz, L., Hegnauer, M., Buitink, J., and Dalmijn, B.: hydroMT-wflow, https://doi.org/10.5281/ZENODO.15182718, 2025.

Faranda, D., Bourdin, S., Ginesta, M., Krouma, M., Noyelle, R., Pons, F., Yiou, P., and Messori, G.: A climate-change attribution retrospective of some impactful weather extremes of 2021, Weather and Climate Dynamics, 3, 1311–1340, https://doi.org/10.5194/wcd-3-1311-2022, 2022.

Feser, F. and Shepherd, T. G.: The concept of spectrally nudged storylines for extreme event attribution, Commun. Earth Environ., 6, 677, https://doi.org/10.1038/s43247-025-02659-6, 2025.

Frame, D. J., Wehner, M. F., Noy, I., and Rosier, S. M.: The economic costs of Hurricane Harvey attributable to climate change, Clim. Change, 160, 271–281, https://doi.org/10.1007/S10584-020-02692-8, 2020.

Gahtan, J. , Knapp, K. R., Schreck, C. J., Diamond, H. J., Kossin, J. P., and Kruk, M. C.: International Best Track Archive for Climate Stewardship (IBTrACS) Project, Version 4r01, ALL, NOAA National Centers for Environmental Information, https://doi.org/10.25921/82ty-9e16, 2024.

van Garderen, L., Feser, F., and Shepherd, T. G.: A methodology for attributing the role of climate change in extreme events: A global spectrally nudged storyline, Natural Hazards and Earth System Sciences, 21, 171–186, https://doi.org/10.5194/NHESS-21-171-2021, 2021.

GEBCO Bathymetric Compilation Group 2024: GEBCO 2024 Grid - a continuous terrain model of the global oceans and land, NERC EDS British Oceanographic Data Centre, NOC, https://doi.org/10.5285/1c44ce99-0a0d-5f4f-e063-7086abc0ea0f, 2024.

Goulart, H. M. D., Benito Lazaro, I., Van Garderen, L., Van Der Wiel, K., Le Bars, D., Koks, E., and Van Den Hurk, B.: Compound flood impacts from Hurricane Sandy on New York City in climate-driven storylines, Natural Hazards and Earth System Sciences, 24, 29–45, https://doi.org/10.5194/nhess-24-29-2024, 2024.

Goulart, H. M. D., Athanasiou, P., van Ginkel, K., van der Wiel, K., Winter, G., Pinto, I., and van den Hurk, B.: Exploring coastal climate adaptation through storylines: Insights from cyclone Idai in Beira, Mozambique, Cell Reports Sustainability, 2, 100270, https://doi.org/10.1016/J.CRSUS.2024.100270, 2025.

Government of Mozambique: Mozambique Cyclone Idai Post Disaster Needs Assessment Conference Version, 2019.

Green, J., Haigh, I. D., Quinn, N., Neal, J., Wahl, T., Wood, M., Eilander, D., De Ruiter, M., Ward, P., and Camus, P.: A comprehensive review of compound flooding literature with a focus on coastal and estuarine regions, Hazards Earth Syst. Sci, 25, 747–816, https://doi.org/10.5194/nhess-25-747-2025, 2025.

Grimaldi, S., Salamon, P., Disperati, J., Zsoter, E., Russo, C., Ramos, A., Carton De Wiart, C., Barnard, C., Hansford, E., Gomes, G., and Prudhomme, C.: River discharge and related forecasted data from the Global Flood Awareness System, https://doi.org/10.24381/cds.a4fdd6b9, 2023.

Grimley, L. E., Hollinger Beatty, K. E., Sebastian, A., Bunya, S., and Lackmann, G. M.: Climate change exacerbates compound flooding from recent tropical cyclones, npj Natural Hazards, 1, 45, https://doi.org/10.1038/s44304-024-00046-3, 2024.

Guzman, O. and Jiang, H.: Global increase in tropical cyclone rain rate, Nature Communications 2021 12:1, 12, 5344-, https://doi.org/10.1038/s41467-021-25685-2, 2021.

Hawker, L., Uhe, P., Paulo, L., Sosa, J., Savage, J., Sampson, C., and Neal, J.: A 30 m global map of elevation with forests and buildings removed, Environmental Research Letters, 17, 024016, https://doi.org/10.1088/1748-9326/AC4D4F, 2022.

Hegerl, G. C., Hoegh-Guldberg, O., Casassa, G., Hoerling, M., Kovats, S., Parmesan, C., Pierce, D., and Stott, P.: Good Practice Guidance Paper on Detection and Attribution Related to Anthropogenic Climate Change, in: Meeting Report of the Intergovernmental Panel on Climate Change Expert Meeting on Detection and Attribution of Anthropogenic Climate Change, edited by: Stocker, T., Field, C., Dahe, Q., Plattner, G.-K., Tignor, M., Midgley, P., and Ebi, K., IPCC Working Group I Technical Support Unit, University of Bern, Bern, Switzerland, 2010.

Herfort, B., Lautenbach, S., Porto De Albuquerque, J., Anderson, J., and Zipf, A.: A spatio-temporal analysis investigating completeness and inequalities of global urban building data in OpenStreetMap, Nat. Commun., 14, 3985, https://doi.org/10.1038/s41467-023-39698-6, 2023.

Hersbach, H., Bell, B., Berrisford, P., Hirahara, S., Horányi, A., Muñoz-Sabater, J., Nicolas, J., Peubey, C., Radu, R., Schepers, D., Simmons, A., Soci, C., Abdalla, S., Abellan, X., Balsamo, G., Bechtold, P., Biavati, G., Bidlot, J., Bonavita, M., De Chiara, G., Dahlgren, P., Dee, D., Diamantakis, M., Dragani, R., Flemming, J., Forbes, R., Fuentes, M., Geer, A., Haimberger, L., Healy, S., Hogan, R. J., Hólm, E., Janisková, M., Keeley, S., Laloyaux, P., Lopez, P., Lupu, C., Radnoti, G., de Rosnay, P., Rozum, I., Vamborg, F., Villaume, S., and Thépaut, J. N.: The ERA5 global reanalysis, Quarterly Journal of the Royal Meteorological Society, 146, 1999–2049, https://doi.org/10.1002/QJ.3803, 2020.

Holland, G.: A Revised Hurricane Pressure–Wind Model, Mon. Weather Rev., 136, 3432–3445, https://doi.org/10.1175/2008MWR2395.1, 2008.

Holland, G. J., Belanger, J. I., and Fritz, A.: A revised model for radial profiles of hurricane winds, Mon. Weather Rev., 138, 4393–4401, https://doi.org/10.1175/2010MWR3317.1, 2010.

Hope, P., W. Cramer, M. van Aalst, G. Flato, K. Frieler, N. Gillett, C. Huggel, J. Minx, F. Otto, C. Parmesan, J. Rogelj, M. Rojas, S.I. Seneviratne, A. Slangen, D. Stone, L. Terray, R. Vautard, and X. Zhang: Cross-Working Group Box ATTRIBUTION | Attribution in the IPCC Sixth Assessment Report, in: Climate Change 2022: Impacts, Adaptation and Vulnerability. Contribution of Working Group II to the Sixth Assessment Report of the Intergovernmental Panel on Climate Change, edited by: Pörtner, H.-O., Roberts, D. C., Tignor, M., Poloczanska, E. S., Mintenbeck, K., Alegría, A., Craig, M., Langsdorf, S., Löschke, S., Möller, V., Okem, A., and Rama, B., Cambridge University Press, Cambridge, UK and New York, NY, USA, 149–152, 2022.

Huizinga, J., Moel, H. d., and Szewczyk, W.: Global flood depth-damage functions: Methodology and the database with guidelines, Publications Office of the European Union, Luxembourg (Luxembourg), https://doi.org/10.2760/16510, 2017.

Intergovernmental Panel on Climate Change (IPCC): Climate Change 2014: Synthesis Report. Contribution of Working Groups I, II and III to the Fifth Assessment Report of the Intergovernmental Panel on Climate Change [Core Writing Team, R.K. Pachauri and L.A. Meyer (eds.)], IPCC, Geneva, Switserland, 151, 2014.

Intergovernmental Panel on Climate Change (IPCC): Key Risks across Sectors and Regions, Climate Change 2022 – Impacts, Adaptation and Vulnerability, 2411–2538, https://doi.org/10.1017/9781009325844.025, 2023a.

Intergovernmental Panel on Climate Change (IPCC): Ocean, Cryosphere and Sea Level Change, in: Climate Change 2021 – The Physical Science Basis: Working Group I Contribution to the Sixth Assessment Report of the Intergovernmental Panel on Climate Change, Cambridge University Press, Cambridge, 1211–1362, https://doi.org/10.1017/9781009157896.011, 2023b.

Jaafar, H. and Ahmad, F.: GCN250, global curve number datasets for hydrologic modeling and design, https://doi.org/10.6084/m9.figshare.7756202.v1, 2019.

Jahanshahi, A. and Booij, M. J.: Exploring controls on rainfall-runoff events: spatial dynamics of event runoff coefficients in Iran, Hydrological Sciences Journal, 68, 954–966, https://doi.org/10.1080/02626667.2023.2193297, 2023.

Joint Research Center and Copernicus Emergency Management Service: River discharge and related forecasted data from the Global Flood Awareness System, Early Warning Data Store (EWDS), https://doi.org/10.24381/cds.a4fdd6b9, 2020.

Kernkamp, H. W. J., Van Dam, A., Stelling, G. S., and De Goede, E. D.: Efficient scheme for the shallow water equations on unstructured grids with application to the Continental Shelf, Ocean Dyn., 61, 1175–1188, https://doi.org/10.1007/S10236-011-0423-6, 2011.

Kim, D., Park, D. S. R., Nam, C. C., and Bell, M. M.: The parametric hurricane rainfall model with moisture and its application to climate change projections, NPJ Clim. Atmos. Sci., 5, 86, https://doi.org/10.1038/S41612-022-00308-9, 2022.

Kind, J., Wouter Botzen, W. J., and Aerts, J. C. J. H.: Accounting for risk aversion, income distribution and social welfare in cost-benefit analysis for flood risk management, Wiley Interdiscip. Rev. Clim. Change, 8, e446, https://doi.org/10.1002/WCC.446, 2017.

Knapp, K. R., Kruk, M. C., Levinson, D. H., Diamond, H. J., and Neumann, C. J.: The International Best Track Archive for Climate Stewardship (IBTrACS): Unifying Tropical Cyclone Data, Bull. Am. Meteorol. Soc., 91, 363–376, https://doi.org/10.1175/2009BAMS2755.1, 2010.

Knutson, T., Camargo, S. J., Chan, J. C. L., Emanuel, K., Ho, C. H., Kossin, J., Mohapatra, M., Satoh, M., Sugi, M., Walsh, K., and Wu, L.: Tropical Cyclones and Climate Change Assessment: Part I: Detection and Attribution, Bull. Am. Meteorol. Soc., 100, 1987–2007, https://doi.org/10.1175/BAMS-D-18-0189.1, 2019.

Knutson, T., Camargo, S. J., Chan, J. C. L., Emanuel, K., Ho, C. H., Kossin, J., Mohapatra, M., Satoh, M., Sugi, M., Walsh, K., and Wu, L.: Tropical Cyclones and Climate Change Assessment: Part II: Projected Response to Anthropogenic Warming, Bull. Am. Meteorol. Soc., 101, E303–E322, https://doi.org/10.1175/BAMS-D-18-0194.1, 2020.

Lehner, B., Messager, M. L., Korver, M. C., and Linke, S.: Global hydro-environmental lake characteristics at high spatial resolution, Sci. Data, 9, 351, https://doi.org/10.1038/s41597-022-01425-z, 2022.

Leijnse, T., Van Ormondt, M., Nederhoff, K., and Van Dongeren, A.: Modeling compound flooding in coastal systems using a computationally efficient reduced-physics solver: Including fluvial, pluvial, tidal, wind-and wave-driven processes, Coastal Engineering, 163, 103796, https://doi.org/10.1016/j.coastaleng.2020.103796, 2021.

Leijnse, T. W. B., van Dongeren, A., van Ormondt, M., de Goede, R., and Aerts, J. C. J. H.: The importance of waves in large-scale coastal compound flooding: A case study of Hurricane Florence (2018), Coastal Engineering, 199, 104726, https://doi.org/10.1016/j.coastaleng.2025.104726, 2025.

Lin, P., Pan, M., Allen, G., Frasson, R., Zeng, Z., Yamazaki, D., and Wood, E.: Global estimates of reach-level bankfull river width leveraging big-data geospatial analysis, https://doi.org/10.5281/ZENODO.3552776, 2019.

Linke, S., Lehner, B., Ouellet Dallaire, C., Ariwi, J., Grill, G., Anand, M., Beames, P., Burchard-Levine, V., Maxwell, S., Moidu, H., Tan, F., and Thieme, M.: Global hydro-environmental sub-basin and river reach characteristics at high spatial resolution, Sci. Data, 6, 283, https://doi.org/10.1038/s41597-019-0300-6, 2019.

Liu, M., Vecchi, G. A., Smith, J. A., and Knutson, T. R.: Causes of large projected increases in hurricane precipitation rates with global warming, npj Climate and Atmospheric Science 2019 2:1, 2, 1–5, https://doi.org/10.1038/s41612-019-0095-3, 2019a.

Liu, M., Vecchi, G. A., Smith, J. A., and Knutson, T. R.: Causes of large projected increases in hurricane precipitation rates with global warming, NPJ Clim. Atmos. Sci., 2, 38, https://doi.org/10.1038/s41612-019-0095-3, 2019b.

Lloyd, E. A. and Shepherd, T. G.: Climate change attribution and legal contexts: evidence and the role of storylines, Clim. Change, 167, 28, https://doi.org/10.1007/S10584-021-03177-Y, 2021.

Massari, C., Pellet, V., Tramblay, Y., Crow, W. T., Gründemann, G. J., Hascoetf, T., Penna, D., Modanesi, S., and Brocca, L.: On the relation between antecedent basin conditions and runoff coefficient for European floods, J. Hydrol. (Amst)., 625, 130012, https://doi.org/10.1016/j.jhydrol.2023.130012, 2023.

Mekonnen, K., Velpuri, N. M., Leh, M., Akpoti, K., Owusu, A., Tinonetsana, P., Hamouda, T., Ghansah, B., Paranamana, T. P., and Munzimi, Y.: Accuracy of satellite and reanalysis rainfall estimates over Africa: A multi-scale assessment of eight products for continental applications, J. Hydrol. Reg. Stud., 49, 101514, https://doi.org/10.1016/J.EJRH.2023.101514, 2023.

Mengel, M., Treu, S., Lange, S., and Frieler, K.: ATTRICI v1.1 - Counterfactual climate for impact attribution, Geosci. Model Dev., 14, 5269–5284, https://doi.org/10.5194/GMD-14-5269-2021, 2021.

Mester, B., Vogt, T., Bryant, S., Otto, C., Frieler, K., and Schewe, J.: Human displacements from Tropical Cyclone Idai attributable to climate change, Hazards Earth Syst. Sci, 23, 3467–3485, https://doi.org/10.5194/nhess-23-3467-2023, 2023.

Nederhoff, K., van Ormondt, M., Veeramony, J., van Dongeren, A., Antolínez, J. A. Á., Leijnse, T., and Roelvink, D.: Accounting for uncertainties in forecasting tropical-cyclone-induced compound flooding, Geosci. Model Dev., 17, 1789–1811, https://doi.org/10.5194/gmd-17-1789-2024, 2024.

Nhundu, K., Sibanda, M., and Chaminuka, P.: Economic Losses from Cyclones Idai and Kenneth and Floods in Southern Africa: Implications on Sustainable Development Goals, in: Cyclones in Southern Africa: Volume 3: Implications for the Sustainable Development Goals, Springer International Publishing, Cham, 289–303, https://doi.org/10.1007/978-3-030-74303-1_19, 2021.

Noy, I., Stone, D., and Uher, T.: Extreme events impact attribution: A state of the art, Cell Reports Sustainability, 1, 100101, https://doi.org/10.1016/J.CRSUS.2024.100101, 2024.

van Oldenborgh, G. J., van der Wiel, K., Kew, S., Philip, S., Otto, F., Vautard, R., King, A., Lott, F., Arrighi, J., Singh, R., and van Aalst, M.: Pathways and pitfalls in extreme event attribution, Clim. Change, 166, 13, https://doi.org/10.1007/s10584-021-03071-7, 2021.

OpenStreetMap contributors: OpenStreetMap, https://www.openstreetmap.org, 2025.

van Ormondt, M., Leijnse, T., Nederhoff, K., de Goede, R., van Dongeren, A., Bovenschen, T., and van Asselt, K.: SFINCS: Super-Fast INundation of CoastS model Version 2.2.0 col d'Eze Release 2025.01, https://doi.org/10.5281/ZENODO.13691724, 2025a.

van Ormondt, M., Leijnse, T., de Goede, R., Nederhoff, K., and van Dongeren, A.: Subgrid corrections for the linear inertial equations of a compound flood model - a case study using SFINCS 2.1.1 Dollerup release, Geosci. Model Dev., 18, 843–861, https://doi.org/10.5194/GMD-18-843-2025, 2025b.

Otto, F. E. L., Zachariah, M., Wolski, P., Pinto, I., Barimalala, R., Nhamtumbo, B., Bonnet, R., Vautard, R., Philip, S., Kew, S., Luu, L. N., Heinrich, D., Vahlberg, M., Singh, R., Arrighi, J., Thalheimer, L., Van Aalst, M., Li, S., Sun, J., Vecchi, G., and Harrington, L. J.: Climate change increased rainfall associated with tropical cyclones hitting highly vulnerable communities in Madagascar, Mozambique & Malawi, 2022.

Paprotny, D., 't Hart, C. M. P., and Morales-Nápoles, O.: Evolution of flood protection levels and flood vulnerability in Europe since 1950 estimated with vine-copula models, Natural Hazards, 121, 6155–6184, https://doi.org/10.1007/S11069-024-07039-5, 2025.

Patricola, C. M. and Wehner, M. F.: Anthropogenic influences on major tropical cyclone events, Nature 2018 563:7731, 563, 339–346, https://doi.org/10.1038/s41586-018-0673-2, 2018.

Pekel, J. F., Cottam, A., Gorelick, N., and Belward, A. S.: High-resolution mapping of global surface water and its long-term changes, Nature, 540, 418–422, https://doi.org/10.1038/nature20584, 2016.

Perkins-Kirkpatrick, S. E., Alexander, L. V., King, A. D., Kew, S. F., Philip, S. Y., Barnes, C., Maraun, D., Stuart-Smith, R. F., Jézéquel, A., Bevacqua, E., Burgess, S., Fischer, E., Hegerl, G. C., Kimutai, J., Koren, G., Lawal, K. A., Min, S.-K., New,

M., Odoulami, R. C., Patricola, C. M., Pinto, I., Ribes, A., Shaw, T. A., Thiery, W., Trewin, B., Vautard, R., Wehner, M., and Zscheischler, J.: Frontiers in attributing climate extremes and associated impacts, Frontiers in Climate, 6, https://doi.org/10.3389/fclim.2024.1455023, 2024.

Philip, S., Kew, S., van Oldenborgh, G. J., Otto, F., Vautard, R., van der Wiel, K., King, A., Lott, F., Arrighi, J., Singh, R., and van Aalst, M.: A protocol for probabilistic extreme event attribution analyses, Adv. Stat. Climatol. Meteorol. Oceanogr., 6, 177–203, https://doi.org/10.5194/ASCMO-6-177-2020, 2020.

Philp, T. J., Champion, A. J., Hodges, K. I., Pigott, C., MacFarlane, A., Wragg, G., and Zhao, S.: Identifying Limitations when Deriving Probabilistic Views of North Atlantic Hurricane Hazard from Counterfactual Ensemble NWP Re-forecasts, in: Hurricane Risk in a Changing Climate, edited by: Collins, J. M. and Done, J. M., Springer International Publishing, Cham, 233–254, https://doi.org/10.1007/978-3-031-08568-0_10, 2022.

Pistrika, A., Tsakiris, G., and Nalbantis, I.: Flood Depth-Damage Functions for Built Environment, Environmental Processes, 1, 553–572, https://doi.org/10.1007/S40710-014-0038-2, 2014.

Probst, P. and Annunziato, A.: Tropical Cyclone Idai: analysis of the wind, rainfall and storm surge impact, European Commission - Joint Research Centre, 2019.

Puig, D., Adger, N. W., Barnett, J., Vanhala, L., and Boyd, E.: Improving the effectiveness of climate change adaptation measures, Clim. Change, 178, 7, https://doi.org/10.1007/S10584-024-03838-8, 2025.

Rentschler, J., Avner, P., Marconcini, M., Su, R., Strano, E., Vousdoukas, M., and Hallegatte, S.: Global evidence of rapid urban growth in flood zones since 1985, Nature, 622, 87–92, https://doi.org/10.1038/S41586-023-06468-9, 2023.

Roelvink, D., van Ormondt, M., Reyns, J., and van der Lugt, M.: SnapWave: fast, implicit wave transformation from offshore to nearshore, Geosci. Model Dev., https://doi.org/10.5194/gmd-18-9469-2025, 2025.

Rogers, J. S., Maneta, M. M., Sain, S. R., Madaus, L. E., and Hacker, J. P.: The role of climate and population change in global flood exposure and vulnerability, Nat. Commun., 16, 1287, https://doi.org/10.1038/S41467-025-56654-8, 2025.

Rogger, M., Agnoletti, M., Alaoui, A., Bathurst, J. C., Bodner, G., Borga, M., Chaplot, V., Gallart, F., Glatzel, G., Hall, J., Holden, J., Holko, L., Horn, R., Kiss, A., Kohnová, S., Leitinger, G., Lennartz, B., Parajka, J., Perdigão, R., Peth, S., Plavcová, L., Quinton, J. N., Robinson, M., Salinas, J. L., Santoro, A., Szolgay, J., Tron, S., van den Akker, J. J. H., Viglione, A., and Blöschl, G.: Land use change impacts on floods at the catchment scale: Challenges and opportunities for future research, Water Resour. Res., 53, 5209–5219, https://doi.org/10.1002/2017WR020723, 2017.

Samadi, V., Fowler, H. J., Lamond, J., Wagener, T., Brunner, M., Gourley, J., Moradkhani, H., Popescu, I., Wasko, C., Wright, D., Wu, H., Zhang, K., Arias, P. A., Duan, Q., Nazemi, A., van Oevelen, P. J., Prein, A. F., Roundy, J. K., Saberian, M., and Umutoni, L.: The Needs, Challenges, and Priorities for Advancing Global Flood Research, WIREs Water, 12, e70026, https://doi.org/https://doi.org/10.1002/wat2.70026, 2025.

Sánchez-Benítez, A., Goessling, H., Pithan, F., Semmler, T., and Jung, T.: The July 2019 European Heat Wave in a Warmer Climate: Storyline Scenarios with a Coupled Model Using Spectral Nudging, J. Clim., 35, 2373–2390, https://doi.org/10.1175/JCLI-D-21-0573.1, 2022.

Sauer, I. J., Reese, R., Otto, C., Geiger, T., Willner, S. N., Guillod, B. P., Bresch, D. N., and Frieler, K.: Climate signals in river flood damages emerge under sound regional disaggregation, Nat. Commun., 12, 2128, https://doi.org/10.1038/s41467-021-22153-9, 2021.

Schubert-Frisius, M., Feser, F., von Storch, H., and Rast, S.: Optimal Spectral Nudging for Global Dynamic Downscaling, Mon. Weather Rev., 145, 909–927, https://doi.org/10.1175/MWR-D-16-0036.1, 2017.

Scussolini, P., Luu, L. N., Philip, S., Berghuijs, W. R., Eilander, D., Aerts, J. C. J. H., Kew, S. F., van Oldenborgh, G. J., Toonen, W. H. J., Volkholz, J., and Coumou, D.: Challenges in the attribution of river flood events, WIREs Climate Change, 15, e874, https://doi.org/10.1002/WCC.874, 2024.

Seneviratne, S. I., Zhang, X., Adnan, M., Badi, W., Dereczynski, C., Di Luca, A., Ghosh, S., Iskander, I., Kossin, J., and Lewis, S.: Weather and climate extreme events in a changing climate, in: Climate Change 2021: The Physical Science Basis. Contribution of Working Group I to the Sixth Assessment Report of the Intergovernmental Panel on Climate Change, edited by: Masson-Delmotte, V., Zhai, P., Pirani, A., Connors, S. L., Péan, C., Berger, S., Caud, N., Chen, Y., Goldfarb, L., Gomis, M. I., Huang, M., Leitzell, K., Lonnoy, E., Matthews, J. B. R., Maycock, T. K., Waterfield, T., Yelekçi, O., Yu, R., and Zhou, B., Cambridge University Press, Cambridge, United Kingdom and New York, NY, USA, 1513–1766, https://doi.org/10.1017/9781009157896.013, 2021.

Shepherd, T. G.: A Common Framework for Approaches to Extreme Event Attribution, Curr. Clim. Change Rep., 2, 28–38, https://doi.org/10.1007/S40641-016-0033-Y, 2016.

Sillmann, J., Shepherd, T. G., van den Hurk, B., Hazeleger, W., Martius, O., Slingo, J., and Zscheischler, J.: Event-Based Storylines to Address Climate Risk, Earths Future, 9, e2020EF001783, https://doi.org/10.1029/2020EF001783, 2021.

Smiley, K. T., Noy, I., Wehner, M. F., Frame, D., Sampson, C. C., and Wing, O. E. J.: Social inequalities in climate change-attributed impacts of Hurricane Harvey, Nat. Commun., 13, 3418, https://doi.org/10.1038/s41467-022-31056-2, 2022.

Smith, A. B. and Katz, R. W.: US billion-dollar weather and climate disasters: Data sources, trends, accuracy and biases, Natural Hazards, 67, 387–410, https://doi.org/10.1007/S11069-013-0566-5, 2013.

Stott, P. A., Stone, D. A., and Allen, M. R.: Human contribution to the European heatwave of 2003, Nature, 432, 610–614, https://doi.org/10.1038/NATURE03089, 2004.

Strauss, B. H., Orton, P. M., Bittermann, K., Buchanan, M. K., Gilford, D. M., Kopp, R. E., Kulp, S., Massey, C., Moel, H. de, and Vinogradov, S.: Economic damages from Hurricane Sandy attributable to sea level rise caused by anthropogenic climate change, Nat. Commun., 12, 2720, https://doi.org/10.1038/s41467-021-22838-1, 2021.

Thieken, A. H., Müller, M., Kreibich, H., and Merz, B.: Flood damage and influencing factors: New insights from the August 2002 flood in Germany, Water Resour. Res., 41, W12430, https://doi.org/10.1029/2005WR004177, 2005.

Thompson, C., Barthe, C., Bielli, S., Tulet, P., and Pianezze, J.: Projected Characteristic Changes of a Typical Tropical Cyclone under Climate Change in the South West Indian Ocean, Atmosphere (Basel)., 12, 232, https://doi.org/10.3390/atmos12020232, 2021.

Thompson, V., Ermis, S., and Athanase, M.: The need for multi-method extreme event attribution, Weather, https://doi.org/10.1002/wea.7779, 2025.

Treu, S., Muis, S., Dangendorf, S., Wahl, T., Oelsmann, J., Heinicke, S., Frieler, K., and Mengel, M.: Reconstruction of hourly coastal water levels and counterfactuals without sea level rise for impact attribution, Earth Syst. Sci. Data, 16, 1121–1136, https://doi.org/10.5194/ESSD-16-1121-2024, 2024.

Tu, S., Chan, J. C. L., Xu, J., Zhong, Q., Zhou, W., and Zhang, Y.: Increase in tropical cyclone rain rate with translation speed, Nature Communications 2022 13:1, 13, 7325-, https://doi.org/10.1038/s41467-022-35113-8, 2022.

UN Office for the Coordination of Humanitarian Affairs (OCHA): Mozambique: Cyclone Idai & Floods Situation Report No. 2, ReliefWeb, 2019.

Archived Consumer Price Index Supplemental Files: https://www.bls.gov/cpi/tables/supplemental-files/, last access: 27 August 2025.

Veenstra, J.: dfm_tools: A Python package for pre- and postprocessing D-FlowFM model input and output files (v0.35.0), Zenodo, https://doi.org/10.5281/zenodo.14901200, 2025.

van Verseveld, W. J., Weerts, A. H., Visser, M., Buitink, J., Imhoff, R. O., Boisgontier, H., Bouaziz, L., Eilander, D., Hegnauer, M., Ten Velden, C., and Russell, B.: Wflow-sbm v0.7.3, a spatially distributed hydrological model: From global data to local applications, Geosci. Model Dev., 17, 3199–3234, https://doi.org/10.5194/GMD-17-3199-2024, 2024.

van Verseveld, W., Visser, M., Buitink, J., Bouaziz, L., Boisgontier, H., Bootsma, H., Weerts, A., Baptista, C. F., Pronk, M., Eilander, D., Hartgring, S., Dalmijn, B., Hofer, J., Hegnauer, M., and Mendoza, R.: Deltares/Wflow.jl, https://github.com/Deltares/Wflow.jl/releases/tag/v0.8.1, 2025.

Vertegaal, D. M., Aleksandrova, N., Bovenschen, T., Couasnon, A., and Goulart, H. M. D.: Climate and impact attribution of TC Idai, https://doi.org/10.5281/zenodo.17107289, 12 September 2025.

Wagenaar, B. H., Augusto, O., Ásbjörnsdóttir, K., Akullian, A., Manaca, N., Chale, F., Muanido, A., Covele, A., Michel, C., Gimbel, S., Radford, T., Girardot, B., and Sherr, K.: Developing a representative community health survey sampling frame using open-source remote satellite imagery in Mozambique, Int. J. Health Geogr., 17, 37, https://doi.org/10.1186/s12942-018-0158-4, 2018a.

Wagenaar, D., Slager, K., and Calero, J. S.: Delft-FIAT: An open-source flood impact analysis tool, Zenodo, https://doi.org/https://doi.org/10.5281/zenodo.1400183, 2017.

Wagenaar, D., Lüdtke, S., Schröter, K., Bouwer, L. M., and Kreibich, H.: Regional and Temporal Transferability of Multivariable Flood Damage Models, Water Resour. Res., 54, 3688–3703, https://doi.org/10.1029/2017WR022233, 2018b.

Wang, J., Chen, Y., Tett, S. F. B., Stone, D., Nie, J., Feng, J., Yan, Z., Zhai, P., and Ge, Q.: Storyline attribution of human influence on a record-breaking spatially compounding flood-heat event, Sci. Adv., 9, eadi2714, https://doi.org/10.1126/sciadv.adi2714, 2023.

Wang, X., Verlaan, M., Veenstra, J., and Lin, H. X.: Data-assimilation-based parameter estimation of bathymetry and bottom friction coefficient to improve coastal accuracy in a global tide model, Ocean Science, 18, 881–904, https://doi.org/10.5194/OS-18-881-2022, 2022.

Ward, P. J., Jongman, B., Salamon, P., Simpson, A., Bates, P., De Groeve, T., Muis, S., De Perez, E. C., Rudari, R., Trigg, M. A., and Winsemius, H. C.: Usefulness and limitations of global flood risk models, Nat. Clim. Chang., 5, 712–715, https://doi.org/10.1038/nclimate2742, 2015.

Ward, P. J., Couasnon, A., Eilander, D., Haigh, I. D., Hendry, A., Muis, S., Veldkamp, T. I. E., Winsemius, H. C., and Wahl, T.: Dependence between high sea-level and high river discharge increases flood hazard in global deltas and estuaries, Environmental Research Letters, 13, 084012, https://doi.org/10.1088/1748-9326/AAD400, 2018.

Warren, M.: Why Cyclone Idai is one of the Southern Hemisphere's most devastating storms, Nature, https://doi.org/10.1038/D41586-019-00981-6, 2019.

Wilkerson, G. V.: Improved bankfull discharge prediction using 2-year recurrence-period discharge, J. Am. Water Resour. Assoc., 44, 243–257, https://doi.org/10.1111/J.1752-1688.2007.00151.X, 2008.

Williamson, C., McCordic, C., and Doberstein, B.: The compounding impacts of Cyclone Idai and their implications for urban inequality, International Journal of Disaster Risk Reduction, 86, 103526, https://doi.org/10.1016/J.IJDRR.2023.103526, 2023.

Wing, O. E. J., Bates, P. D., Quinn, N. D., Savage, J. T. S., Uhe, P. F., Cooper, A., Collings, T. P., Addor, N., Lord, N. S., Hatchard, S., Hoch, J. M., Bates, J., Probyn, I., Himsworth, S., Rodríguez González, J., Brine, M. P., Wilkinson, H., Sampson, C. C., Smith, A. M., Neal, J. C., and Haigh, I. D.: A 30 m Global Flood Inundation Model for Any Climate Scenario, Water Resour. Res., 60, e2023WR036460, https://doi.org/10.1029/2023WR036460, 2024.

World Meteorological Organisation (WMO): Tropical Cyclone Idai hits Mozambique, 2019.

Yamada, Y., Satoh, M., Sugi, M., Kodama, C., Noda, A. T., Nakano, M., and Nasuno, T.: Response of Tropical Cyclone Activity and Structure to Global Warming in a High-Resolution Global Nonhydrostatic Model, J. Clim., 30, 9703–9724, https://doi.org/10.1175/JCLI-D-17-0068.1, 2017.

Yamazaki, D., Ikeshima, D., Sosa, J., Bates, P. D., Allen, G. H., and Pavelsky, T. M.: MERIT Hydro: A High-Resolution Global Hydrography Map Based on Latest Topography Dataset, Water Resour. Res., 55, 5053–5073, https://doi.org/10.1029/2019WR024873, 2019.

Zhou, Q., Zhang, Y., Chang, K., and Brovelli, M. A.: Assessing OSM building completeness for almost 13,000 cities globally, Int. J. Digit. Earth, 15, 2400–2421, https://doi.org/10.1080/17538947.2022.2159550, 2022.

Zscheischler, J., Westra, S., Van Den Hurk, B. J. J. M., Seneviratne, S. I., Ward, P. J., Pitman, A., Aghakouchak, A., Bresch, D. N., Leonard, M., Wahl, T., and Zhang, X.: Future climate risk from compound events, Nature Climate Change 2018 8:6, 8, 469–477, https://doi.org/10.1038/s41558-018-0156-3, 2018.

Zsoter, E., Harrigan, S., Barnard, C., Wetterhall, F., Ferrario, I., Mazzetti, C., Alfieri, L., Salamon, P., and Prudhomme, C.: River discharge and related forecasted data from the Global Flood Awareness System, https://doi.org/10.24381/cds.a4fdd6b9, 2021.

Supplementary material

S1 Method material

S1.1 SFINCS Basemap

Figure S1 shows the SFINCS model domain with its elevation, in- and -outflow boundaries and output points for timeseries analyses. SFINCS uses the simulated wflow discharge as input for the fluvial flooding, and the D-Flow FM – SnapWave simulated coastal water levels as input for the coastal flooding.

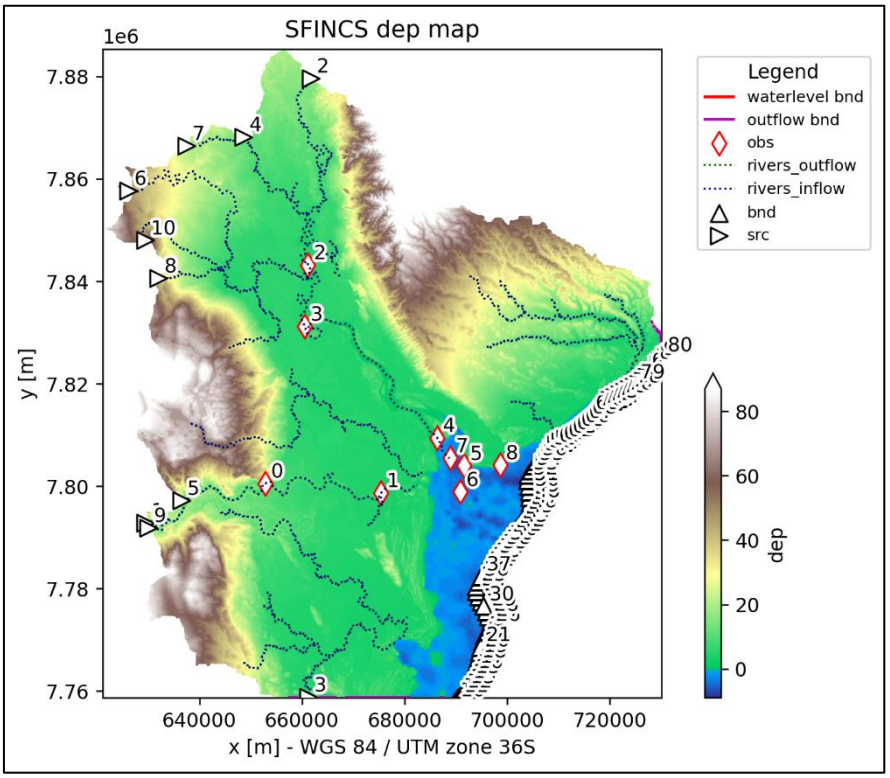

Figure S1: Basemap of the local SFINCS model with the boundary conditions coupling the wflow discharge output (src), water level boundary coupling the D-Flow FM – SnapWave output (bnd), outflow boundary (outflow bnd), rivers, elevation (dep), and the SFINCS output points for timeseries data (obs).

S1.2 Wflow bankfull discharge

Figure S2 shows the estimated return values for extreme discharge in the two largest rivers, the Buzi (Gauge 1) and the Pungwe (Gauge 2), see Figure S~~1~~4 for gauge locations. ~~The~~We derive the 2-year return period ~~is estimated~~ for all gauges (Table S1) by extracting annual maxima from the discharge time series from the 30-year wflow simulation (1989-2019) and fitting a

Generalized Extreme Value (GEV) or Gumbel distribution (a specific case of the GEV distribution with the shape parameter being 0) to the extremes, based on the Akaike Information Criterion goodness-of-fit metric~~ir distribution~~, as implemented in the pyextremes Python package (Bocharov, 2023)~~ and~~. The estimated 2-year return period is ~~-~~removed from the wflow simulated discharge of the event (example for the Buzi river in Fig. S3). The 2-year return period represents an approximation of the bankfull river discharge and this relationship is based on semi-empirical relationships (Liu et al., 2024). Due to the lack of river bathymetry data, we remove the bankfull discharge from the discharge boundary conditions for SFINCS and assume that the incoming discharge represents out of banks discharge, thereby removing the need to burn in an (unknown) river conveyance in the digital elevation model. This approach may lead to an under- or overestimation in river discharge input for our SFINCS model simulations.

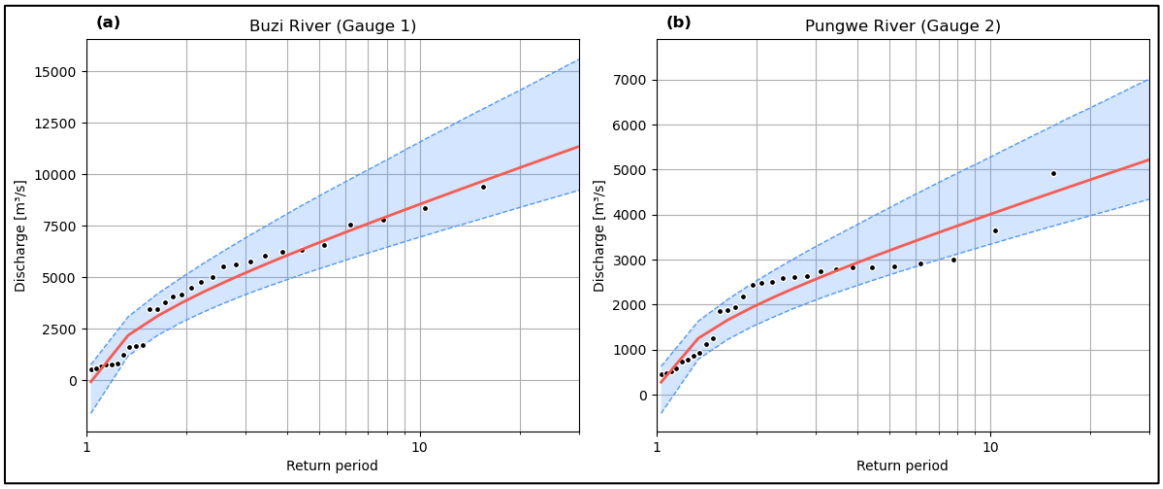

Figure S2: ~~The estimated return values for maximum~~Discharge return levels ~~discharge~~ (m³/s) obtained for ~~in~~ the Buzi (a) and the Pungwe (b) rivers, based on a Gumbel distribution ~~an extreme value analysis~~ (Bocharov, 2023) ~~using block maxima for a 30 year wflow simulation (1989-2019).~~ . The fit ~~(red)~~ obtained is shown in red and confidence interval (5-95%~~; blue~~) in blue. The ranked yearly maxima from the 30-year time series (1989-2019) are ~~plotted next to the annual maxima~~shown in black.

Table S1: The estimated 2-year return period (bankfull discharge) in m³/s from ~~a 30 year wflow simulation (1989-2019)~~the GEV or Gumbel fit (based on the Akaike Information Criterion goodness-of-fit metric) for all discharge boundary points of the SFINCS model domain (see Fig. S~~1~~4 for locations), together with the upper and lower 95% confidence intervals (CI) in m³/s.

Gauge ID	Bankfull Discharge (m³/s)	Lower 95% CI (m³/s)	Upper 95% CI (m³/s)
1	3888	2921	5212
2	1992	1566	2515
3	102	72	174
4	179	136	237

5	197	143	272
6	99	70	155
7	30	23	40
8	15	10	27
9	89	62	123
10	11	7	18

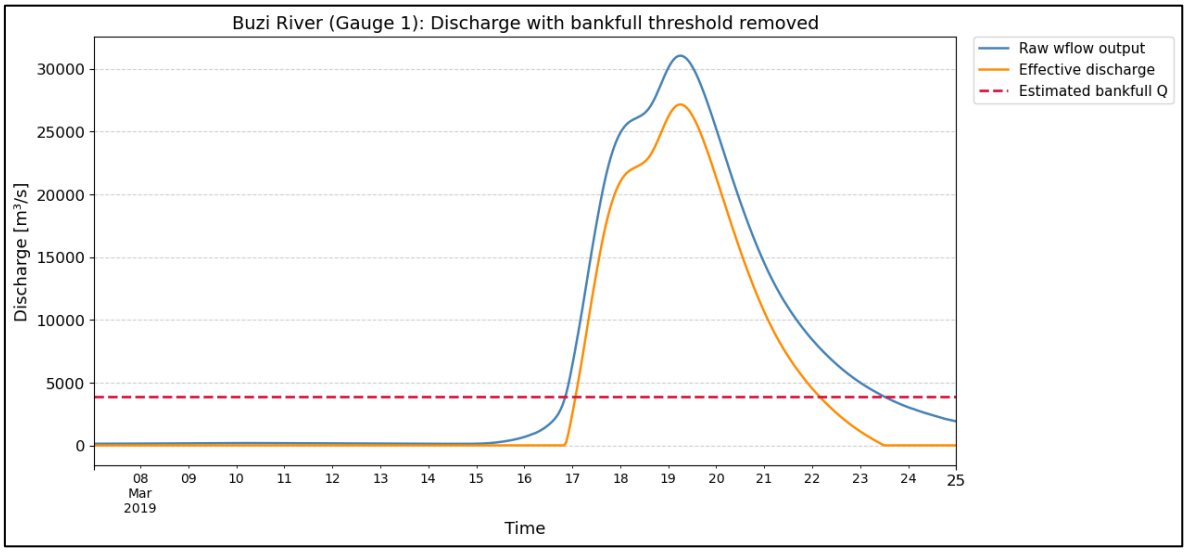

Figure S3: Example of bankfull discharge removal for the Buzi river (Gauge 1) for the period of TC Idai. The estimated 2-year return period (red) is removed from the wflow output (blue) to correct for missing river bathymetry before provided as effective discharge (orange)~~boundary~~ to SFINCS.

S1.3 Simulated discharge comparison with modelled GloFAS data~~GRDC stations~~

The 30-year warm-up simulation of ~~same~~ the wflow model ~~as for Sect. 1.2 is run for 30 years that align with the available Global Runoff Data Centre (GRDC)~~ is compared with two versions (v4.0 and v3.1) of the Global Flood Awareness System (GloFAS) modelled discharge data (Grimaldi et al., 2023; Joint Research Center and Copernicus Emergency Management Service, 2020; Zsoter et al., 2021), also using the ERA5 reanalysis dataset as meteorological forcing but the hydrological and channel routing model LISFLOOD ~~within the region (1954-1984, Fig. S4), using ERA5 daily rainfall and temperature forcing~~. The ~~climatology~~ event discharge and 30-year daily timeseries for ~~GRDC~~ GloFAS grid cells ~~stations~~ closest to the ~~SFINCS model domain~~ wflow gauges for the major Buzi and Pungwe rivers (gauges 1 and 2 in Fig. S4) are compared to the simulated wflow discharge data for these gauges (Figs. S5 and S6). For the period of TC Idai, the summed daily discharges simulated by GloFAS v4.0 (v3.1) differ -19 % (-10 %) and -51 % (29 %) from the summed wflow discharges resampled to a daily time step for the Buzi and the Pungwe, respectively (Table S2). The overestimated discharge could be explained by the higher spatial

resolution of our wflow model compared to GloFAS data. For the event, the simulated discharge is in the same order of magnitude as calculated by Eilander et al. (2023a). The agreement between our results and GloFAS for the Buzi river is ~~captures the seasonal and long-term dynamics~~ reasonable ~~to well~~ (KGE for comparison with GloFAS v4.0 (v3.1) is 0.42 (0.61) for the Buzi river; Fig S6), although also here extremes are generally overestimated, but uncertain for the Pungwe river as GloFAS result varies significantly between data versions (KGE for comparison with GloFAS v4.0 (v3.1) is 0.09 (0.75) for the Pungwe river; Fig S6) and would require recent local observations to determine the ground truth. ~~The seasonality and long term dynamics are simulated reasonable to well (KGE 0.28 and 0.87 for the Pungwe and Buzi rivers, respectively) but the extremes are generally overpredicted.~~

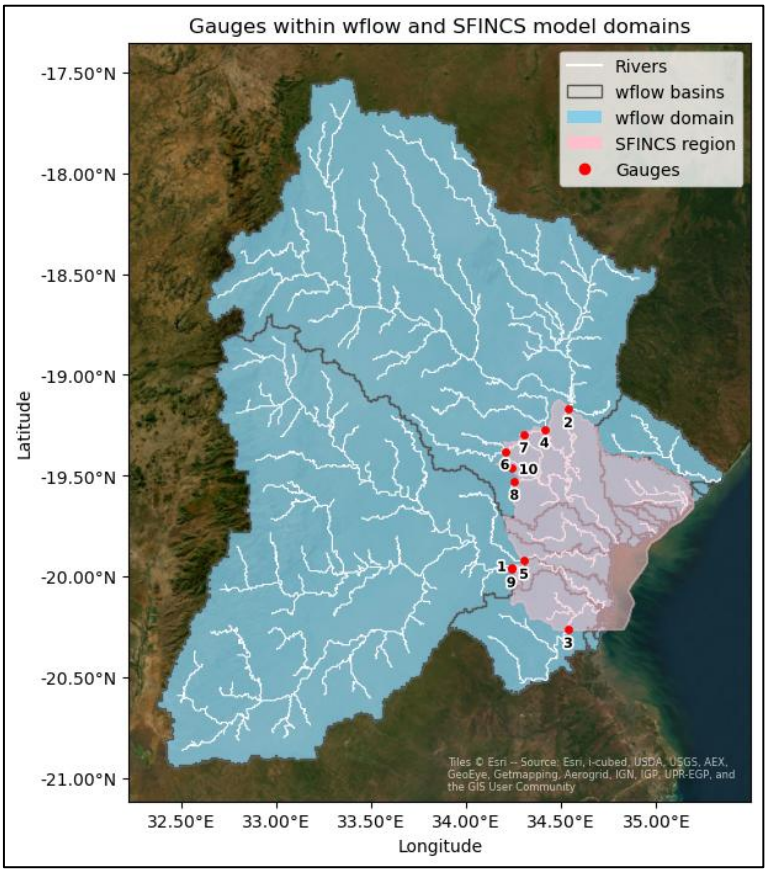

Figure S4: The ~~selected GRDC gauges (blue) and closest~~ wflow ~~gauges grid points~~ (red~~orange~~) as output of the hydrological wflow model and input to the SFINCS compound flood model. ~~compare historical discharge in the Sofala province, Mozambique, for t~~The major Buzi ~~(G1 and Q1),~~ and Pungwe ~~(G2 and Q2)~~ rivers are modelled as gauge 1 and 2 and have the largest upstream area in the domain. The wflow and SFINCS domains are shown in blue and pink, respectively, as well as the river geometries in white.

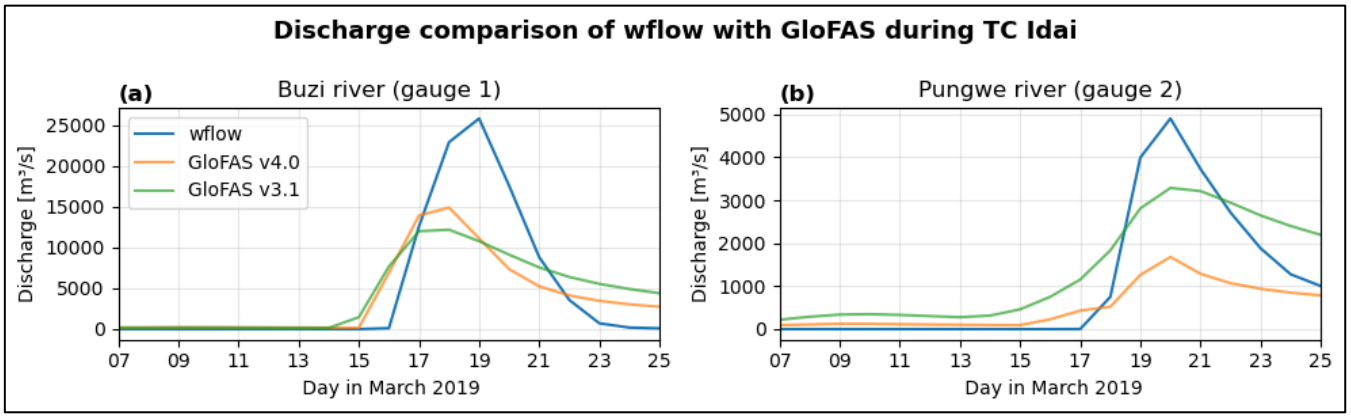

Figure S5: The ~~monthly mean~~ daily simulated discharge during TC Idai ~~(climatology)~~ in m^3/s for the Buzi (a) and the Pungwe (b) rivers for the wflow model used in this study (blue), and versions 4.0 (orange) and 3.1 (green) of the globally available GloFAS discharge dataset (wflow is modelled hourly but shown as daily for comparison with GloFAS), ~~using the GRDC discharge data and a 30-year wflow simulation for the GRDC available stations within the Sofala region and available time period (1954-1984)~~.

Tabel S2: The total discharge during event of TC Idai (7 to 25 March 2019) for the major Buzi (gauge 1) and Pungwe (gauge 2) rivers as simulated by the wflow model used in this study, and version 4.0 and 3.1 of the globally available GloFAS discharge dataset.

Gauge number	wflow [10^{15} m³]	GloFAS [10^{15} m³]		$\frac{GloFAS - wflow}{wflow}$ [%]	
		v4.0	v3.1	v4.0	v3.1
1	7,99	6,45	7,20	-19	-10
2	1,75	8.65	2,26	-51	29

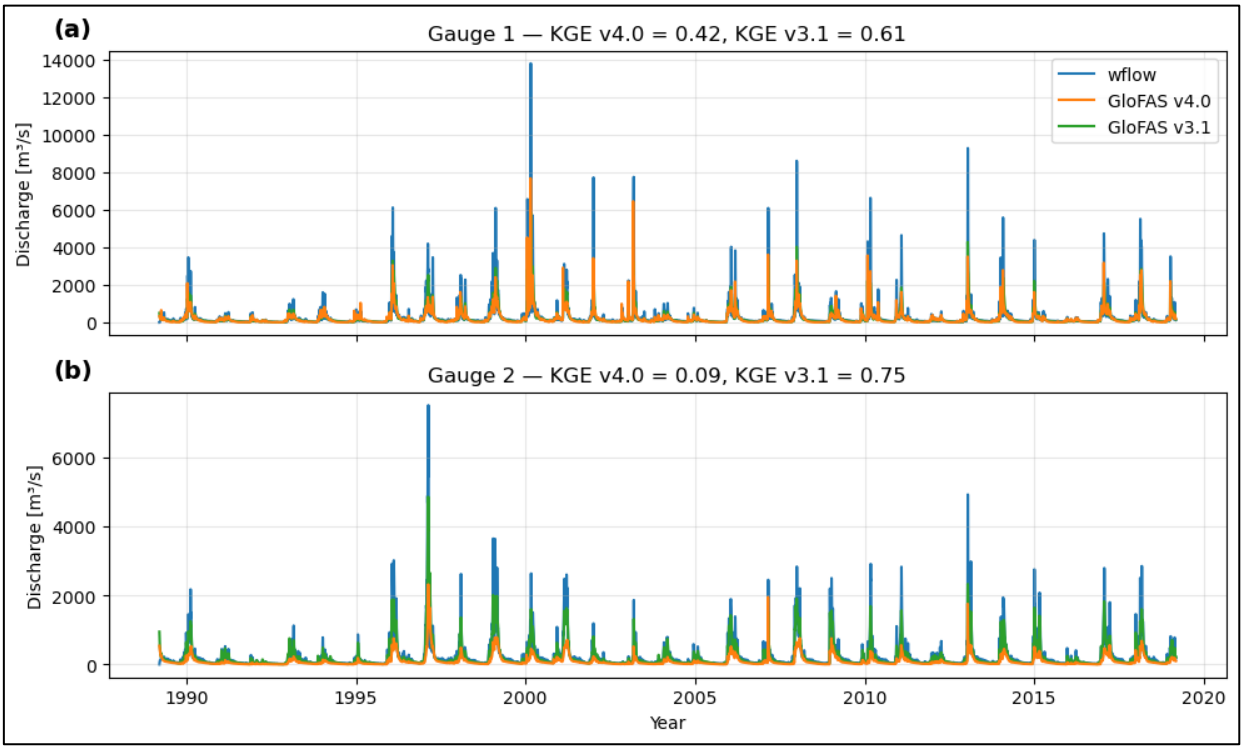

Figure S6: The daily discharge in m^3/s for the Buzi (a) and the Pungwe (b) rivers for the 30-year period prior to the event (1989–2019), ~~using~~ for the wflow model used in this study (blue), and ~~the GRDC~~ version 4.0 (orange) and 3.1 (green) of the globally available GloFAS discharge dataset. ~~(1954-1984) and corresponding wflow simulation performed at the daily timestep, available stations within the Sofala region and available time period (1954-1984).~~

S1.4 SnapWave

Figure S7 shows which SnapWave ~~coastal transects~~output points are matched to D-Flow FM output points, with an example of the timeseries for station 62 (panel b). Ideally, the SnapWave coupling would be fully integrated into the SFINCS model of the ~~SFINCS~~ modelling chain, ~~model of SFINCS~~ together with all compound flood drivers simultaneously~~to prevent potential wave dissipation due to the shallow and sloping coast~~; however, this was not yet possible at the time of preparation of this paper. Therefore, a nested approach was utilized with 2 different SFINCS simulations. ~~For station 62 (panel b), as for many other stations, the maximum wave setup does not totally align in time with the maximum water level from tide and surge due a time mismatch (up to 30 min) resulting from the spatial difference between the D-Flow FM and SnapWave output.~~

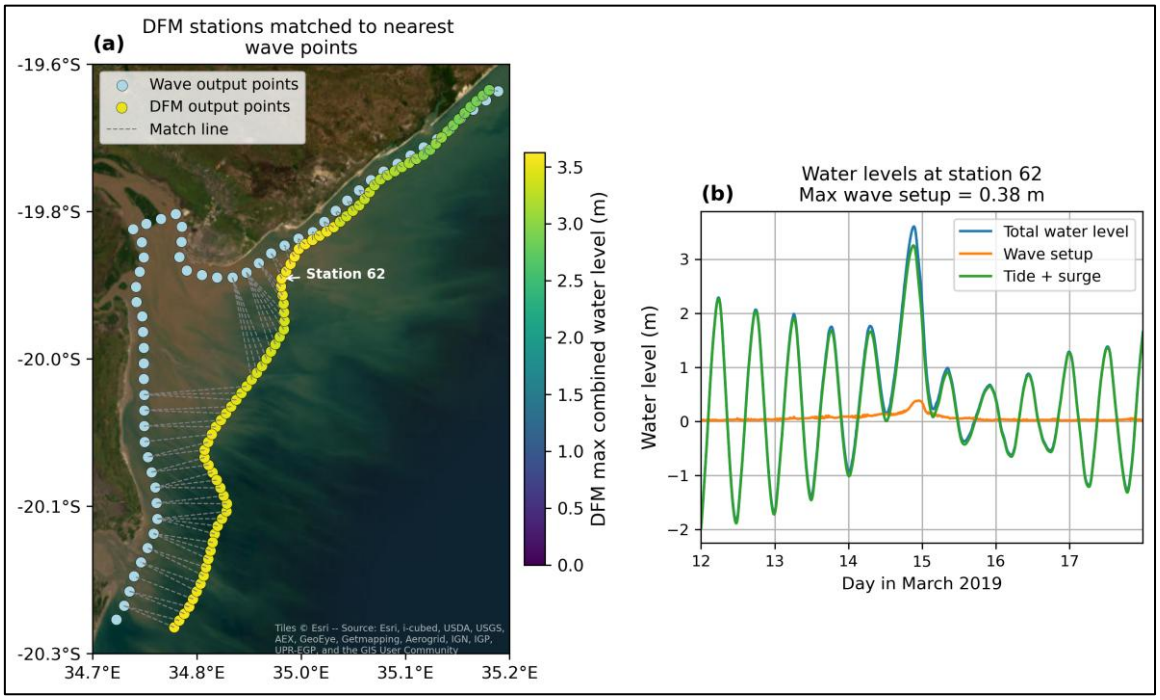

Figure S7: Panel a shows the output points of SnapWave (blue) matched to the D-Flow FM output points, depicted with their ~~total~~ maximum water level value (viridis scale), to add the simulated wave setup to the simulated tide and surge. Panel b shows an example of the simulated total water level (blue) after adding wave setup (orange) to tide and surge (green) for the period of 12 to 17 March 2019 at station 62, which is the station closest to Beira.

S1.5 Flood map satellite comparison

The simulated factual flooding from our SFINCS model simulations is compared to the satellite-derived flood extent for TC Idai from UNOSAT (https://unosat.org/products) and CEMS (https://portal.gfm.eodc.eu/; Fig. S8). Several metrics are used to compare our simulated flooding with that derived from the satellite products, based on Eilander et al. (2023). The critical success index (C) is the ratio between the correctly classified instances and the union of both error and correct instances. The hit rate (H) is the proportion of observed flooding that is correctly estimated by the model. The false-alarm ratio (F) is the proportion of modelled flooded area that is not flooded in the observation dataset.

We find a good hit rate when comparing the estimated flooding to both satellite products (> 76%), but a poor false-alarm ratio for the CEMS comparison (60 %). The critical success index is better for the UNOSAT (68 %) than for the CEMS (40 %) comparison. Important to note is the large difference in detected flood extent between the two satellite products, highlighting the lack of "truth". We have more trust in the UNOSAT product, as there is no flooding present in Beira for the CEMS product, even though flooding is documented (e.g. ReliefWeb, 2019). For the region North East of Beira, we underpredict flooding compared to the UNOSAT product but overestimate compared to the CEMS product. This area might be difficult to observe due to the larger elevation gradient with forest transitioning to grass- and cropland (Lisboa et al., 2024).

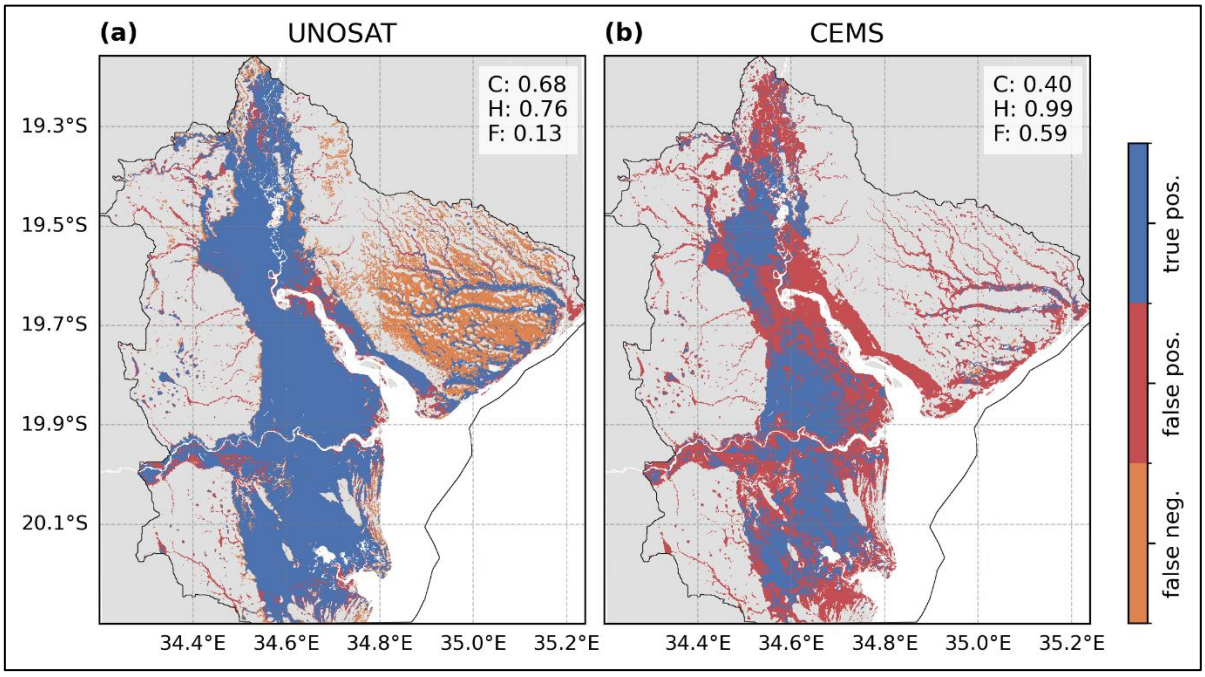

Figure S8: Our factual maximum flood depth simulations compared to satellite observed flood extent of UNOSAT (a) and CEMS (b). The agreement between the model and satellite products is expressed using the critical success index (C), hit rate (H) and false-alarm ratio (F), based on Eilander et al. (2023).

S1.6 Counterfactual forcing

For the counterfactual rainfall scenario, every rainfall value in space and time of the ERA5 reanalysis dataset for the period of the event is multiplied by $1 + \frac{CF_{rain}}{100\,\%}$ ~~0.92~~ to remove the plausible climate trend ~~8%~~ (where CF_{rain} is -4 %, -8 % or -16 %) of increased rainfall due to climate change from the factual data.

For the counterfactual wind scenario, the maximum sustained wind speed (U_{max}) along the track is adjusted using the counterfactual wind value (CF_{wind}) of -1 %, -5 % or -10 %, following the methodology of Mester et al. (2023):

$$U_{\max\_CF} = U_{max} * 1 + \frac{1}{CF_{wind}}; \qquad \text{(S1)}$$

Also the pressure is adjusted accordingly, where the minimum pressure (P_{min}) along the track is increased with the product of the inverse of the counterfactual wind value (CF_{wind}) and the pressure difference between P_{min} and the environmental pressure (P_{env}, Eq. S2). The new wind and pressure values are used to create counterfactual wind and pressure fields for Idai.

$$P_{min\_CF} = P_{min} + -1 * \frac{1}{CF_{wind}} * (P_{env} - P_{min}) \qquad \text{(S2)}$$

For the counterfactual SLR scenario, the SLR is removed from the tidal boundary conditions and initial water level of D-Flow FM using the Python package dfm_tools for pre- and postprocessing of model in- and output files (Veenstra, 2025). The SLR

at all stations Five stations are selected along the coast of Mozambique, within the D-Flow FM domain are averaged, resulting in a SLR removal of -10 cm for the medium counterfactual scenario. We adjust the medium value by ± 5 cm the low and high counterfactual scenario based on (Strauss et al., 2021)The SLR of these stations is averaged. Our SLR estimate is in line with tide gauge observations from the Permanent Service for Mean Sea Level (PSMSL; Holgate et al., 2013; Permanent Service for Mean Sea Level (PSMSL), 2026) at the nearest station with sufficient data, located in Durban, South Africa (analysis not shown). As mentioned in Section 2.1.3, GEBCO v2024 is used to determine the ocean's bathymetry and thereby implicitly the sea level. The ocean depth is referenced to m.s.l., yet the temporal dimension (i.e. reference year) of this mean sea level is not defined. As the development of global bathymetry datasets started in the mid-1990 thanks to the advancement of satellite altimetry (Tozer et al., 2019), we assume that the m.s.l. measured then is the vertical datum still used today. Therefore, we analyse the mean regional SLR from the ISIMIP Hourly Coastal water levels with Counterfactual (HCC) dataset (Treu et al., 2024) for 1990 – 2000 and add the difference between then and medium SLR scenario for 2019 (4 cm; Fig. S10) to the tidal boundary and initial water level of the factual scenario. The difference between 1901 (start of the dataset) and the 1990 – 2000 mean (10 cm) is subtracted from the tidal boundary and initial water level for the different counterfactual scenarios (-1, -6, -11 cm for a SLR scenarios of -5, -10 and -15 cm, respectively), leading to a 14 cm difference between the factual and counterfactual scenario. Global bathymetry data inaccuracies can vastly surpass the size of SLR (Tozer et al., 2019) and advancements of local bathymetry data are crucial to accurately estimate the effect of SLR.

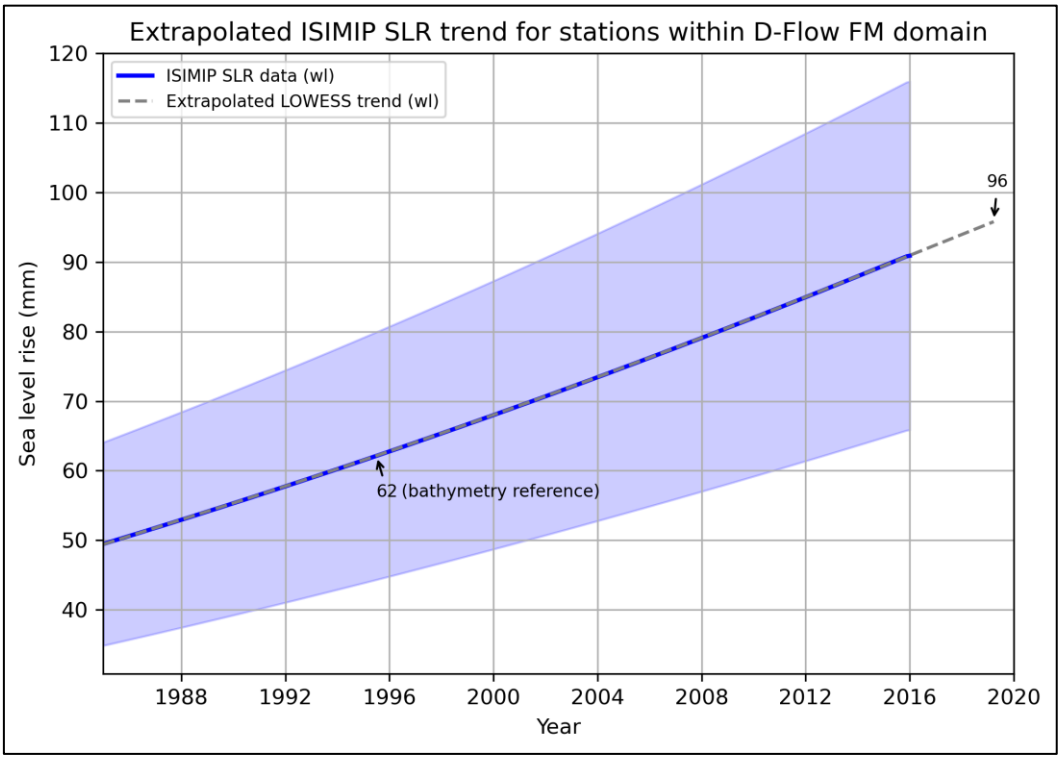

Figure S9~~10~~: The ISIMIP HCC dataset for 30 years, extrapolated from 2015 to March 2019, when Tropical Cyclone Idai occurred. We use a LOWESS-based extrapolation of the regional average SLR, calculated from stations along the Mozambique coast within the D-Flow FM domain. To calculate the implicit SLR in the GEBCO bathymetry dataset, we calculate the mean of the SLR between 1990 and 2000, annotated as bathymetry reference.

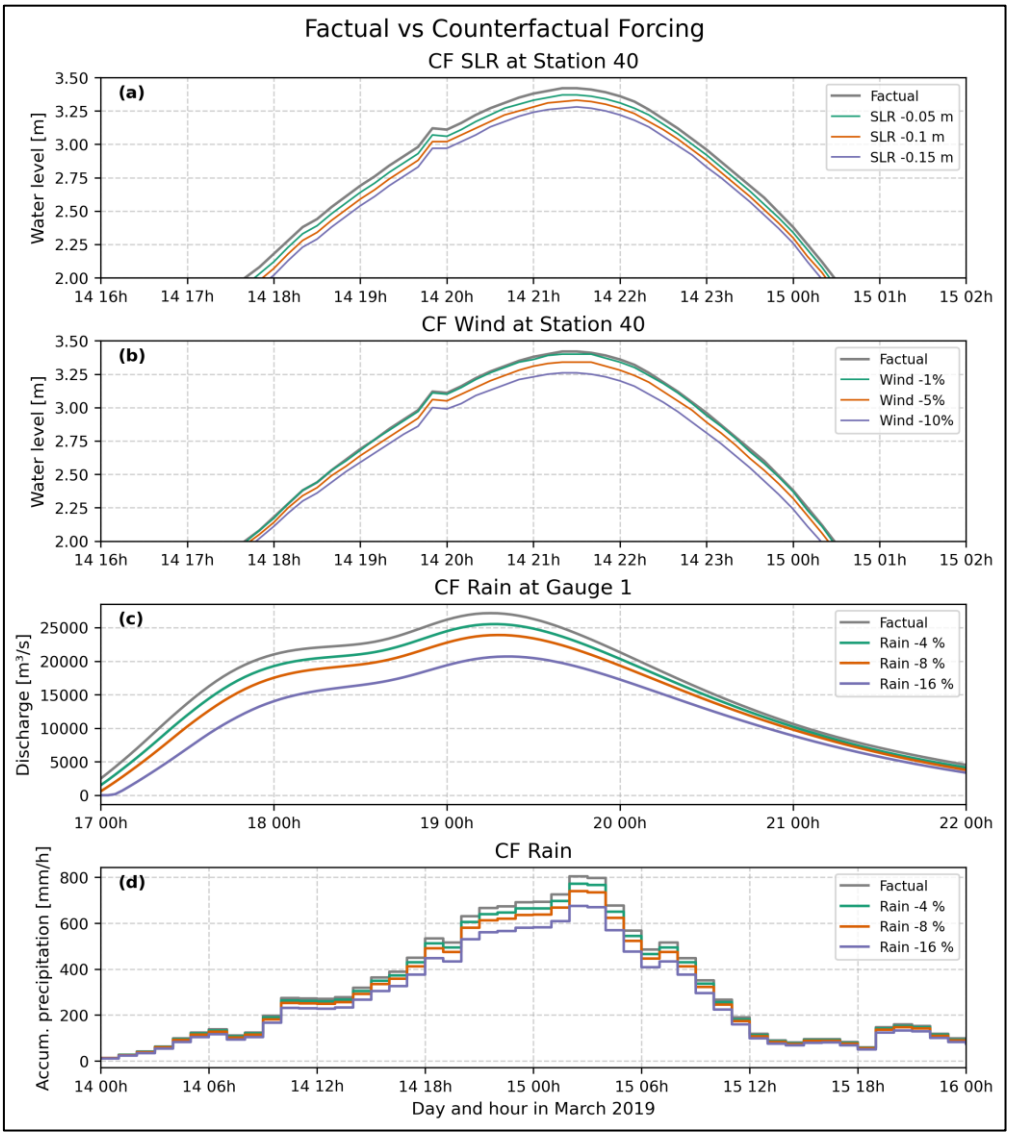

145

Figure S1~~0~~1: The factual and counterfactual (CF) timeseries data for the change in SLR and wind at a coastal water level boundary point (S40, see Fig S1~~2~~3 for location; panels a and b), the change in rain for two discharge boundary points of the Buzi (G1) and Pungwe (G2) rivers (panel c; for locations see Fig S1~~2~~3), and for change in accumulated rainfall over the SFINCS model domain (panel d). Note the use of different x axis to better capture the timing range of the factual and counterfactual flood driver peaks.

S2 Supplementary result figures

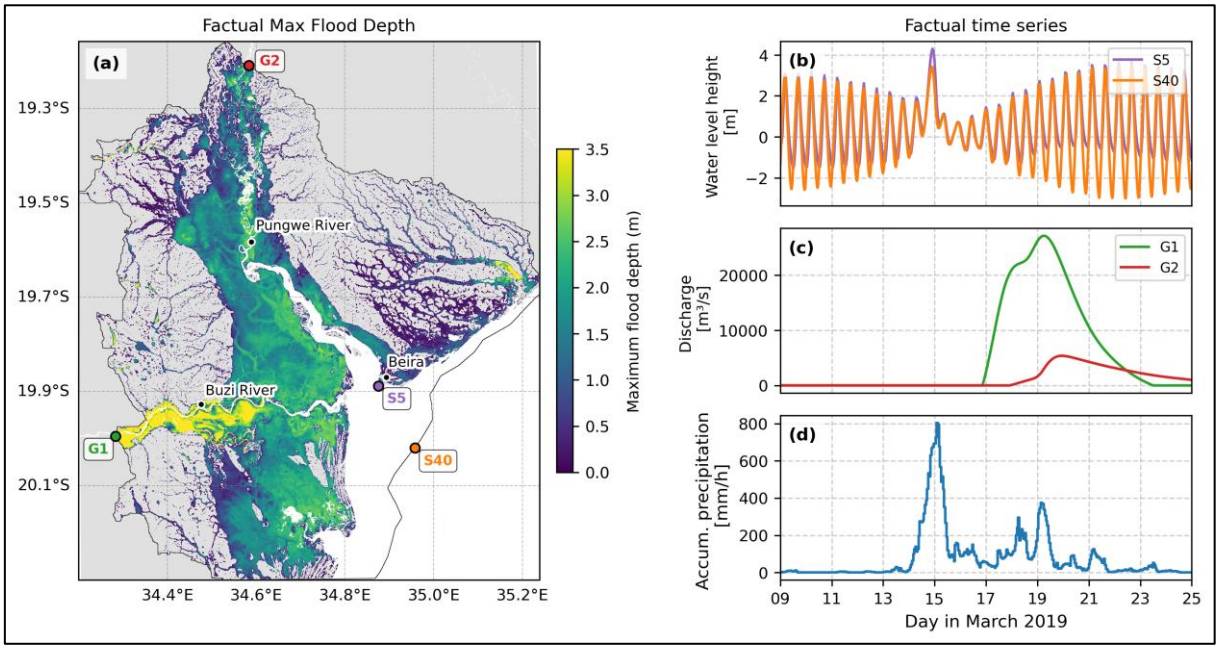

Figure S1~~1~~2: The factual simulated maximum flood depth in meters from TC Idai (a), and the factual forcing over time for coastal water levels at two stations in m (S5 and S40; b), discharge in m^3/s at the Buzi (G1) and Pungwe (G2) rivers (c), and accumulated rainfall over the SFINCS model domain in mm/h from ERA5 (d). The SFINCS model domain is shown in black in panel (a).

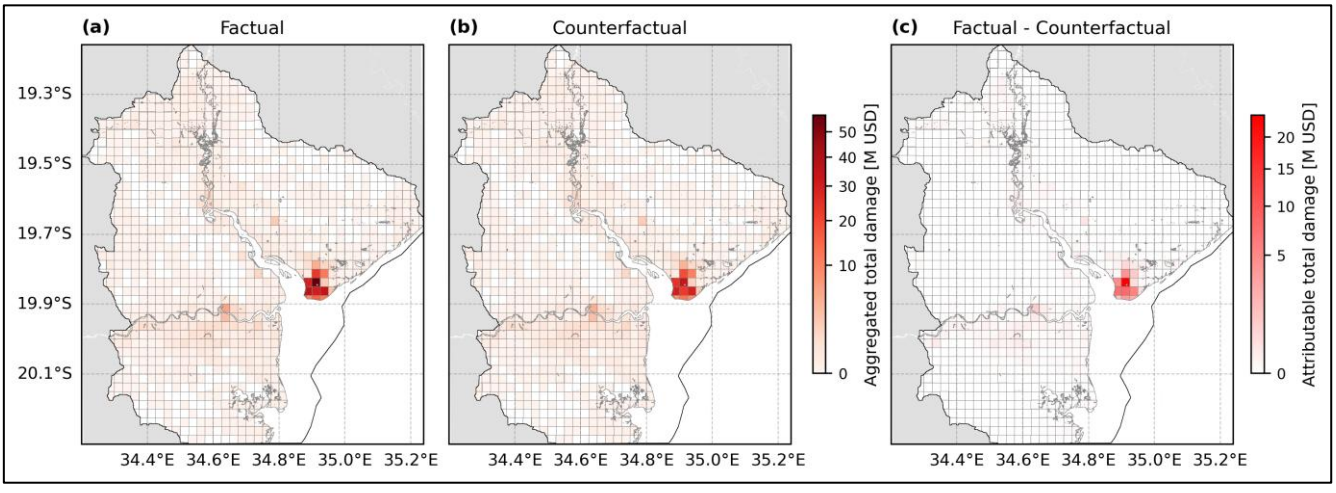

Figure S1~~2~~3: The aggregated (0.025° grid cells) total damage for the factual (a) and medium counterfactual (b) scenarios with all drivers combined, and the absolute difference attributable to climate change (c). The compound flood model (SFINCS) domain is shown in black.

References

Bocharov, G.: pyextremes (Version 2.3.3), https://github.com/georgebv/pyextremes, 2023.

Eilander, D., Couasnon, A., Leijnse, T., Ikeuchi, H., Yamazaki, D., Muis, S., Dullaart, J., Haag, A., Winsemius, H. C., and Ward, P. J.: A globally applicable framework for compound flood hazard modeling, Natural Hazards and Earth System Sciences, 23, 823–846, https://doi.org/10.5194/nhess-23-823-2023, 2023.

Grimaldi, S., Salamon, P., Disperati, J., Zsoter, E., Russo, C., Ramos, A., Carton De Wiart, C., Barnard, C., Hansford, E., Gomes, G., and Prudhomme, C.: River discharge and related forecasted data from the Global Flood Awareness System, https://doi.org/10.24381/cds.a4fdd6b9, 2023.

Holgate, S. J., Matthews, A., Woodworth, P. L., Rickards, L. J., Tamisiea, M. E., Bradshaw, E., Foden, P. R., Gordon, K. M., Jevrejeva, S., and Pugh, J.: New Data Systems and Products at the Permanent Service for Mean Sea Level, J. Coast. Res., 29, 493–504, https://doi.org/10.2112/JCOASTRES-D-12-00175.1, 2013.

Joint Research Center and Copernicus Emergency Management Service: River discharge and related forecasted data from the Global Flood Awareness System, Early Warning Data Store (EWDS), https://doi.org/10.24381/cds.a4fdd6b9, 2020.

Lisboa, S. N., Grinand, C., Betbeder, J., Montfort, F., and Blanc, L.: Disentangling the drivers of deforestation and forest degradation in the Miombo landscape: A case study from Mozambique, International Journal of Applied Earth Observation and Geoinformation, 130, 103904, https://doi.org/10.1016/j.jag.2024.103904, 2024.

Liu, Y., Wortmann, M., Hawker, L., Neal, J., Yin, J., Santos, M. S., Anderson, B., Boothroyd, R., Nicholas, A., Smith, G. S., Ashworth, P., Cloke, H., Gebrechorkos, S., Leyland, J., Zhang, B., Vahidi, E., Griffith, H., Delorme, P., McLelland, S., Parsons, D., Darby, S., and Slater, L.: Global Estimation of River Bankfull Discharge Reveals Distinct Flood Recurrences Across Different Climate Zones, https://doi.org/10.21203/RS.3.RS-5185659/V1, 2024.

Mester, B., Vogt, T., Bryant, S., Otto, C., Frieler, K., and Schewe, J.: Human displacements from Tropical Cyclone Idai attributable to climate change, Hazards Earth Syst. Sci, 23, 3467–3485, https://doi.org/10.5194/nhess-23-3467-2023, 2023.

Permanent Service for Mean Sea Level (PSMSL): Tide Gauge Data, 2026.

ReliefWeb: Mozambique: Cyclone Idai & Floods Situation Report No. 2 (as of 3 April 2019) - Mozambique | ReliefWeb, 2019.

Strauss, B. H., Orton, P. M., Bittermann, K., Buchanan, M. K., Gilford, D. M., Kopp, R. E., Kulp, S., Massey, C., Moel, H. de, and Vinogradov, S.: Economic damages from Hurricane Sandy attributable to sea level rise caused by anthropogenic climate change, Nat. Commun., 12, 2720, https://doi.org/10.1038/s41467-021-22838-1, 2021.

Tozer, B., Sandwell, D. T., Smith, W. H. F., Olson, C., Beale, J. R., and Wessel, P.: Global Bathymetry and Topography at 15 Arc Sec: SRTM15+, Earth and Space Science, 6, 1847–1864, https://doi.org/10.1029/2019EA000658, 2019.

Treu, S., Muis, S., Dangendorf, S., Wahl, T., Oelsmann, J., Heinicke, S., Frieler, K., and Mengel, M.: Reconstruction of hourly coastal water levels and counterfactuals without sea level rise for impact attribution, Earth Syst. Sci. Data, 16, 1121–1136, https://doi.org/10.5194/ESSD-16-1121-2024, 2024.

Veenstra, J.: dfm_tools: A Python package for pre- and postprocessing D-FlowFM model input and output files (v0.35.0), Zenodo, https://doi.org/10.5281/zenodo.14901200, 2025.

Zsoter, E., Harrigan, S., Barnard, C., Wetterhall, F., Ferrario, I., Mazzetti, C., Alfieri, L., Salamon, P., and Prudhomme, C.: River discharge and related forecasted data from the Global Flood Awareness System, https://doi.org/10.24381/cds.a4fdd6b9, 2021.